

AD _____

Award Number: W81XWH-FE~~FE~~ Í G

TITLE: V@ÁÜ[|^Á Á æ[ÜPÖÄ äÜF€FÄ ÁÜ[•æ^ÁÖæ &^!ÁÜ[*|^••ä }
Ö } ÁÖà[|ÉÄ ÖÄ Ì F€JÁ

PRINCIPAL INVESTIGATOR: ÖiÉÜäÖæ

CONTRACTING ORGANIZATION: V@ÁÜ, ä^!•æ Á Á æÖæ æ
Ö } ÁÖà[|ÉÄ ÖÄ Ì F€JÁ

REPORT DATE: Ü^] ç{ à^!ÖFF

TYPE OF REPORT: Annual Ü~ { { æ^

PREPARED FOR: U.S. Army Medical Research and Materiel Command
Fort Detrick, Maryland 21702-5012

DISTRIBUTION STATEMENT: Approved for public release; distribution unlimited

The views, opinions and/or findings contained in this report are those of the author(s) and should not be construed as an official Department of the Army position, policy or decision unless so designated by other documentation.

REPORT DOCUMENTATION PAGE				Form Approved OMB No. 0704-0188	
Public reporting burden for this collection of information is estimated to average 1 hour per response, including the time for reviewing instructions, searching existing data sources, gathering and maintaining the data needed, and completing and reviewing this collection of information. Send comments regarding this burden estimate or any other aspect of this collection of information, including suggestions for reducing this burden to Department of Defense, Washington Headquarters Services, Directorate for Information Operations and Reports (0704-0188), 1215 Jefferson Davis Highway, Suite 1204, Arlington, VA 22202-4302. Respondents should be aware that notwithstanding any other provision of law, no person shall be subject to any penalty for failing to comply with a collection of information if it does not display a currently valid OMB control number. PLEASE DO NOT RETURN YOUR FORM TO THE ABOVE ADDRESS.					
1. REPORT DATE (DD-MM-YYYY) 01-09-2011		2. REPORT TYPE Annual Summary		3. DATES COVERED (From - To) 1 SEP 2010 - 31 AUG 2011	
4. TITLE AND SUBTITLE The Role of microRNA miR-101 in Prostate Cancer Progression				5a. CONTRACT NUMBER	
				5b. GRANT NUMBER W81XWH-10-1-0652	
				5c. PROGRAM ELEMENT NUMBER	
6. AUTHOR(S) Dr. Qi Cao E-Mail: qciao@med.umich.edu				5d. PROJECT NUMBER	
				5e. TASK NUMBER	
				5f. WORK UNIT NUMBER	
7. PERFORMING ORGANIZATION NAME(S) AND ADDRESS(ES) The University of Michigan Ann Arbor, MI 48109				8. PERFORMING ORGANIZATION REPORT NUMBER	
9. SPONSORING / MONITORING AGENCY NAME(S) AND ADDRESS(ES) U.S. Army Medical Research and Materiel Command Fort Detrick, Maryland 21702-5012				10. SPONSOR/MONITOR'S ACRONYM(S)	
				11. SPONSOR/MONITOR'S REPORT NUMBER(S)	
12. DISTRIBUTION / AVAILABILITY STATEMENT Approved for Public Release; Distribution Unlimited					
13. SUPPLEMENTARY NOTES					
14. ABSTRACT Polycomb group (PcG) proteins are chromatin-modifying complexes that regulate epigenetic silencing and play an important role in determining cell fate. PcG proteins form two major complexes, Polycomb Repressive Complex 1 (PRC1) and Polycomb Repressive Complex 2 (PRC2). PRC2 methylates histone H3 on lysine27 (H3K27) creating a chromatin mark which stimulates PRC1 to enact gene silencing at target genes. Employing in vitro and in vivo cancer models, combined with human tumor studies, we demonstrate that PRC2 and PRC1 coordinate their function through regulation of specific microRNAs including miR-203, miR-181a,b and miR-200b,c. Increased PRC2 activity in cancer leads to repression of these microRNAs, which in turn leads to increased expression of PRC1 components. Thus, we propose that key microRNAs link PRC2 to PRC1 forming an integral regulatory axis of the epigenetic silencing machinery.					
15. SUBJECT TERMS PcG, PRC2, PRC1, miRNA, epigenetics, histone methylation					
16. SECURITY CLASSIFICATION OF:			17. LIMITATION OF ABSTRACT	18. NUMBER OF PAGES	19a. NAME OF RESPONSIBLE PERSON
a. REPORT	b. ABSTRACT	c. THIS PAGE			USAMRMC
U	U	U	UU	50	19b. TELEPHONE NUMBER (include area code)

Table of Contents

	<u>Page</u>
Introduction.....	4
Research Progress.....	7
Key Research Accomplishments.....	9
Reportable Outcomes.....	9
Conclusion.....	10
Abbreviations.....	11
References.....	12
Appendices.....	15

Introduction

Background

Prostate Cancer. Every year over 180,000 American men are diagnosed with prostate cancer [1]. Although most will receive some type of treatment, such as chemotherapy and/or radiotherapy, mortality for the 10% of patients with recurrences and or metastases is nearly 100%.

MicroRNAs and Cancer. MicroRNAs are regulatory, non-protein-coding, endogenous RNAs that have recently gained considerable attention in the scientific community. They are 18-24 nucleotides in length and are thought to regulate gene expression through translational repression by binding to a target mRNA [2-4]. Many microRNAs are defined to be either tumor suppressors or oncogenes [5-7] and play a crucial role in variety of cellular processes such as cell cycle control, apoptosis, haematopoiesis and tumorigenesis [8,9].

Recent studies indicate that selected miRNAs may play a role in human cancer pathogenesis [6,10]. The results of large-scale miRNA profiling studies, using normal and cancer tissues, suggest that a number of microRNAs are either overexpressed or downregulated in tumors [11-18]. The genes encoding mir-15 and mir-16 are located at chromosome 13q14, a region that is deleted in the majority of B-cell chronic lymphocytic leukemias (B-CLL), suggesting that mir-15 and mir-16 may possibly function as tumor suppressors. Let-7 miRNA family members are known to downregulate the oncogene RAS [19]. In contrast, several microRNAs are upregulated in cancer and may function as oncogenes. Members of the miR-17 cluster provide an oncogenic function via their upregulated expression by c-Myc, leading to effects on downstream genes that are mediators of cell cycle and apoptosis events [20]. And miR-21 promotes cell transformation by targeting PDCD4 and is overexpressed in prostate, breast, lung and colon cancers [21].

Specific expression of microRNA may be of prognostic significance, indicating that miRNAs are determinants of clinical aggressiveness [12,15,22]. Thus, **microRNA expression profiles may serve as a promising new class of cancer biomarkers.** Prostate cancer microRNA profiling studies by several groups [12,23,24] indicated that there were significant differences in the expression patterns of several microRNAs between normal and neoplastic tissues.

EZH2 and Cancer. EZH2, a protein of Polycomb Group (PcG), plays a master regulatory role in controlling important cellular process such as maintaining stem cell pluripotency [25-27], cell proliferation [28,29], early embryogenesis [30], and X chromosome inactivation [31]. EZH2 functions in a multi-protein complex called Polycomb Repressive Complex 2 (PRC2), which includes SUZ12 (Suppressor of Zeste 12) and EED (Embryonic Ectoderm Development) [32,33]. The primary activity of the EZH2 protein complex is to tri-methylate histone

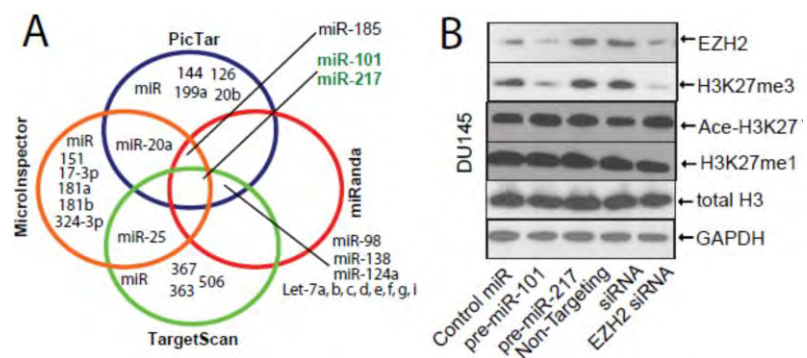


Fig 1. miR-101 regulates EZH2 expression. **(A)** Venn diagram displaying miRNAs computationally predicted to target EZH2 from softwares. **(B)** miR-101 downregulates EZH2 expression and decrease H3K27me3 levels in DU145 cells, while Ace-H3K27 and H3K27me1 levels were not altered by miR-101. GAPDH and total H3 were used for load control.

H3 lysine 27 (H3K27) at target gene promoters, leading to epigenetic silencing [34,35]. Mounting evidence suggests that EZH2 has properties consistent with those of an oncogene, as overexpression promotes cell proliferation, colony formation, and increased invasion of benign cells *in vitro* [28,29,36] and induces xenograft tumor growth *in vivo* [37]. Likewise, knock-down of EZH2 in cancer cells results in growth arrest [28,37] as well as diminished tumor growth [34] and metastasis *in vivo* [38].

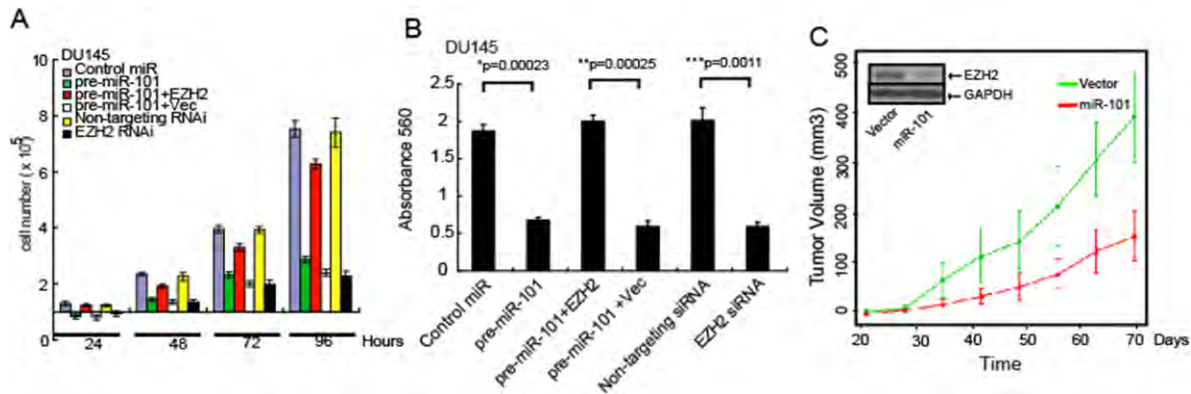


Fig 2. The role of miR-101 in regulating cell proliferation, invasion and tumor growth. **(A)** miR-101 overexpression reduces cell proliferation. Cell growth assay of DU145 cells treated with either precursor miR-101 or siRNA targeting EZH2. **(B)** miR-101 expression decreases cell invasion of DU145 cells. Cells were transfected with miR-101, EZH2-specific siRNA, control miR and non-targeting siRNA. All cells were subjected to a matrigel invasion assay. **(C)** Over-expression of miR-101 attenuates prostate tumor growth. Over-expression of miR-101 reduces DU145 tumor growth in a mouse xenograft model. Plot of mean tumor volume trajectories over time for the mice inoculated with miR-101 (red) and vector (green) expressing DU145 cells.

miR-101 represses EZH2 expression. In order to examine whether microRNAs regulate EZH2 expression during cancer progression, we used prediction software programs to nominate microRNA candidates and found that only miR-101 and miR-217 are predicted by all four of the programs we used (PicTar [39], TargetScan [40], miRanda [41], and miRInspector [42]) (**Fig.1A**). MiR-101 always ranked as the best predicted target by the four programs, though they used different algorithms. After transfecting miR-101, miR-217 and control microRNAs into the prostate cancer cell line DU145, we found that EZH2 protein expression was only repressed by miR-101, as good as by EZH2 siRNA duplex, but not by miR-217, as compared to control microRNA or siRNA duplex by immunoblot analysis (**Fig 1B**). And H3K27 tri-methylation levels were decreased by miR-101 and EZH2 siRNA duplex, while Ace-H3K27 and H3K27me1 levels were not altered.

miR-101 inhibits cancer cell potentials. To determine whether miR-101 inhibits the function of EZH2 and PRC2, we evaluated cell proliferation and invasion following transfection of miRNA precursors. **As predicted, miR-101 overexpression significantly attenuated prostate cancer cells DU145 proliferation and invasion, and co-expression of EZH2 (without endogenous 3'UTR) rescued the miR-101 mediated inhibition of cell growth and invasion (Fig 2A, B).** Furthermore, *in vivo*, DU145 cells stably overexpressing miR-101 grew markedly slower than the vector control xenograft ($P=0.0001$), (**Fig 2C**). All of these findings demonstrated that miR-101 was a tumor suppressor and inhibited these cancer cell specific properties.

miR-101 expression is inversely correlated to EZH2 expression in cancer progression. When we examined the miR-101 expression in human tissues, we observed that **miR-101 and EZH2 expression were inversely correlated during prostate cancer progression (Fig 3A)**. miR-101 expression was significantly decreased in metastatic prostate cancer relative to clinically localized disease or benign adjacent prostate tissue, while EZH2 was significantly upregulated in metastatic prostate cancer relative to clinically localized disease or benign adjacent prostate tissue ($P < 0.0001$). This was consistent with the functional connection between miR-101 and EZH2. Based on genomic PCR, 2 of 16 clinically localized prostate cancers and 17 of 33 metastatic prostate cancers exhibited loss of the miR-101-1 locus (**Fig. 3B**). To formally demonstrate that genomic loss of miR-101 loci was somatic in nature, we identified 9 metastatic prostate cancers that exhibited loss of miR-101-1 and obtained DNA from matched normal tissue. As expected, 8 of 9 cases exhibited a marked decrease in relative levels of miR-101-1 copy number in cancer when compared to matched normal tissue (**Fig. 3C**). In addition, our meta-analysis of the majority of publicly available microRNA expression datasets suggested that **miR-101 is significantly under-expressed in prostate, breast, ovarian, lung and colon cancers [14,15,22]**.

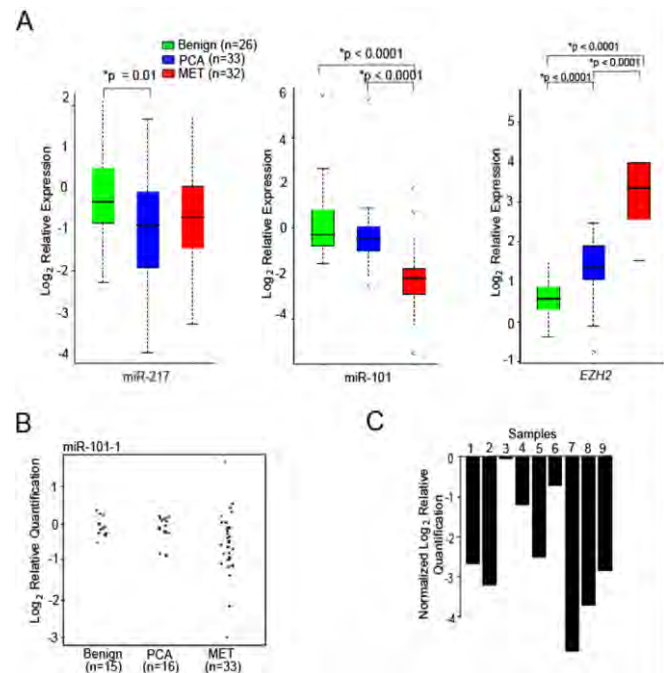


Fig. 3. Genomic loss of the miR-101 locus may explain overexpression of EZH2 in solid tumors. **(A)** miR-101 transcript levels are inversely correlated with EZH2 expression in prostate cancer progression. **(B)** Genomic PCR of miR-101-1. Vertical axes represent log (base 2) relative quantification values; dashed lines are shown at the deletion threshold of $\log_2(0.7) \approx -0.51$. For clarity, points have been horizontally displaced within each sample class. **(C)** Evidence that the miR-101-1 locus is somatically lost in tumors samples relative to matched normal samples. Nine metastatic prostate cancers were chosen that have copy number loss in the miR-101-1 locus, and matched normal tissue were analyzed for comparison. Bar heights represent differences in \log_2 (RQ) values between metastatic and matched normal tissues.

Research progress:

Specific Aim 1: To characterize miR-101 as a biomarker of metastatic prostate cancer, and the role of miR-101 in prostate cancer progression.

By microRNA profiling, we identified that miR-101 target EZH2 could repress over 100 miRNAs. Among these PRC2 protein EZH2-regulated miRNAs, we found that miR-181b,c, miR-200b,c and miR-203 could repress PRC1 proteins BMI1 and RING2, therefore decrease their substrate ubiquityl-H2A-K119 levels (Fig. 4).

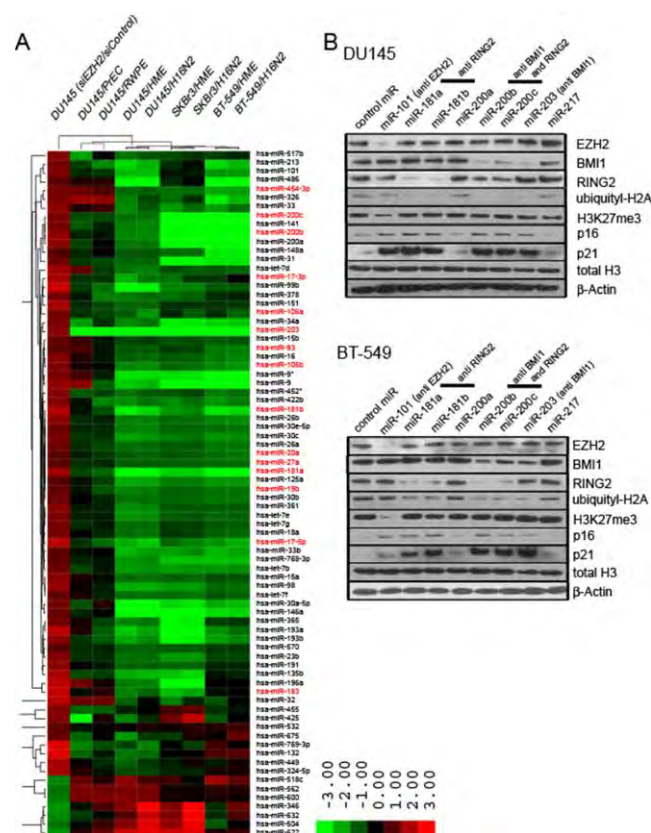


Fig. 4. PRC2-regulated miRNAs repress PRC1 proteins BMI1 and RING2.

(A) miRNA profiling of DU145 prostate cancer cells in which EZH2 was knocked-down compared to DU145 cancer cells relative to benign cells HME, PrEC, RWPE and H16N2. Shades of red represent increased gene expression while shades of green represent decreased expression. (B) Overexpression of indicated miRs in DU145 and BT-549 cells and expression of PRC components and PRC1 target histone mark and genes by immunoblot analysis. β-actin was used as loading control.

Further, we performed miRNA qPCR and confirmed that miR-101 and EZH2 siRNA really regulate these miRNAs by repressing EZH2 expression (Fig. 5)

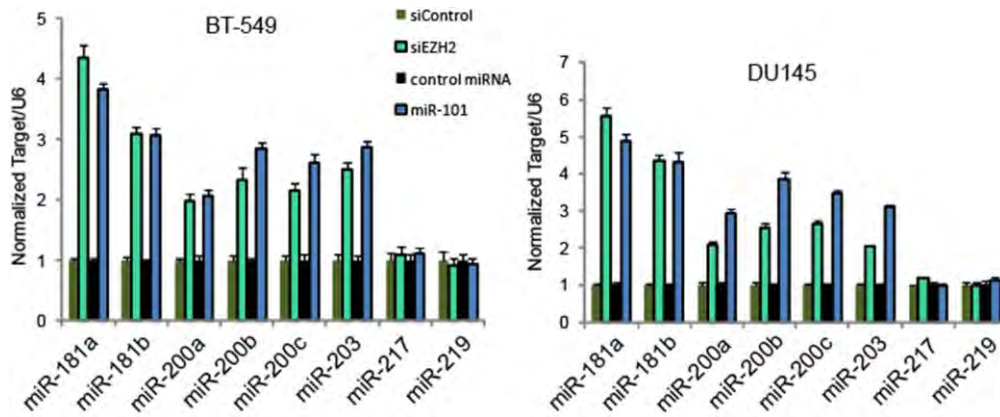


Fig. 5. miR-101 and EZH2 siRNA increased miR-181b,c miR-200a,b,c and miR-203 expression in BT-549 and DU145 cells, but not the control miRNAs miR-217 or miR-219.

Most importantly, miR-101 target EZH2 is negatively correlated with miR-101, miR-181b,c, miR-200b,c and miR-203 during prostate cancer progression (Fig. 6A) and proposed a model of coordinated regulation of PRC complexes in cancer (Fig. 6B).

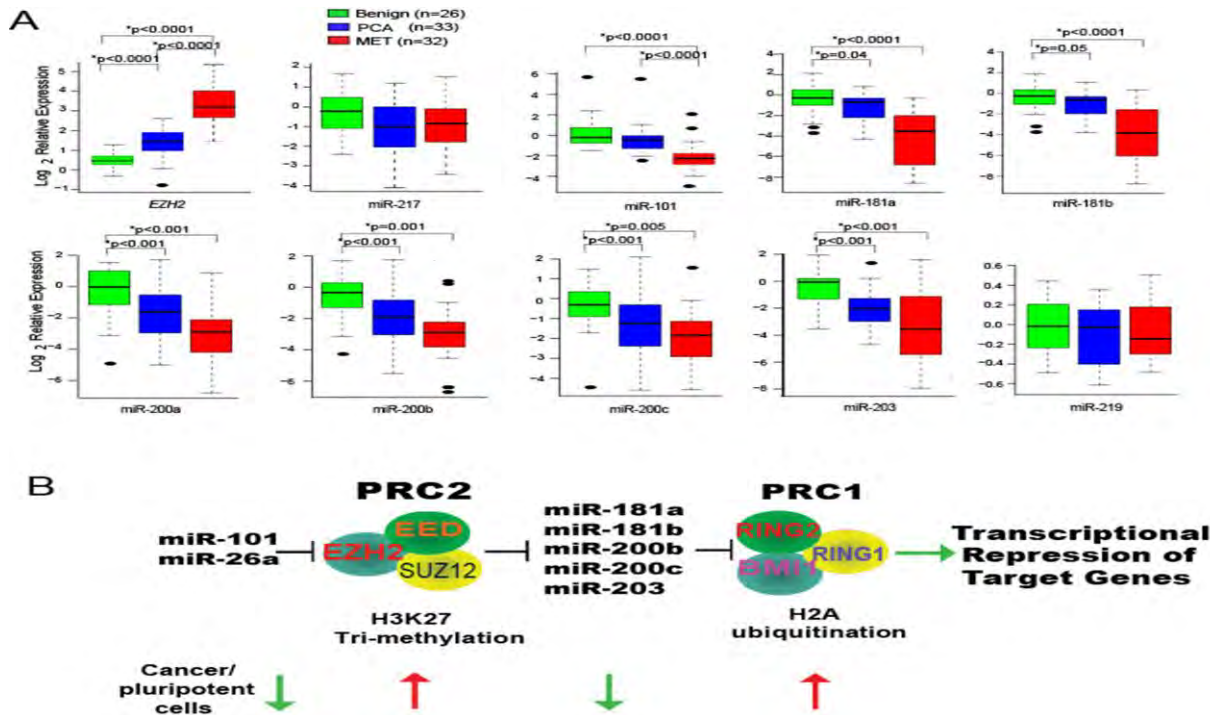


Fig. 6. Coordinated expression of PcG proteins and PRC regulatory miRNAs in prostate cancer progression. (A) Expression of indicated miRs as assessed by q-PCR in benign prostate, clinically localized prostate cancer and metastatic prostate cancer tissues. (B) A proposed model role for microRNAs in regulating PRCs. Specifically, PRC2 is molecularly linked to PRC1 via a set of regulatory miRs.

Specific Aim 2: To identify the mechanisms by which miR-101 is dysregulated in prostate cancer.

Our preliminary data showed that, in some of our prostate cancer samples, miR-101 was underexpressed but miR-101 genomic loci were not deleted. To investigate whether the upstream DNA from miR-101 is methylated, we employed pyro-sequencing technology using the prostate tissue specimens including benign, PCA and metastatic prostate cancer samples. We are in the process of preparing the libraries and going to perform the assays and analyze the result.

To investigate whether miR-101 target EZH2 3'UTR regions are mutated in metastatic prostate cancers, we employ the next generation sequencing powered by Solexa technology to sequence the cohort of prostate cancer tissue specimens. We are in the process of analyzing the sequencing data.

Key Research and Training Accomplishments:

- ❖ We identified miRNAs that are negatively regulated by PRC2 protein, EZH2.
- ❖ EZH2-regulated miRNAs in turn regulate PRC1 proteins, BMI1 and RING2.
- ❖ miRNAs and PRC protein levels are inversely correlated in prostate cancer.
- ❖ PRC1 and PRC2 activities are coordinately regulated *via* miRNAs.

REPORTABLE OUTCOMES:

Manuscript Published:

- 1) **Cao Q**, Mani RS, Ateeq B, Dhanasekaran SM, Asangani IA, Prensner JR, Kim JH, Brenner JC, Jing X, Cao X, Wang R, Li Y, Dahiya A, Wang L, Pandhi M, Lonigro RJ, Wu Y-M, Tomlins SA, Palanisamy N, Qin Z, Yu J, Maher CA, Varambally S, Chinnaiyan AM. Coordinated regulation of Polycomb group complexes through microRNAs in cancer. *Cancer Cell*. 2011 Aug 16;20(2):187-99.
- 2) Prensner JR, Iyer MK, Balbin OA, Dhanasekaran SM, **Cao Q**, Brenner JC, Laxman B, Asangani IA, Grasso C, Kominsky HD, Cao X, Jing X, Wang X, Siddiqui J, Wei JT, Robinson D, Iyer HK, Palanisamy N, Maher CA, Chinnaiyan AM. Transcriptome Sequencing Identifies PCAT-1, a Novel lincRNA Implicated in Prostate Cancer Progression. *Nat. Biotechnol*. 2011 Jul 31;29(8):742-9. doi: 10.1038/nbt.1914.

- 3) Ateeq B, Tomlins, SA, Laxman B, Asangani IA, **Cao Q**, Cao X, Yong L, Wang X, Feng FY, Pienta KJ, Varambally S, Chinnaiyan AM. Therapeutic targeting of SPINK1-positive prostate cancer. *Sci. Transl. Med.* 2011 3: 72ra17 (2011). PMID: 21368222.

Oral and Poster Presentations:

- 1) **Cao Q.**, An onco-protein axis linking polycomb repressive complex 2 and polycomb repressive complex 1 through miRNAs in cancer. American Association for Cancer Research (AACR) 102nd Annual Meeting, Orlando, FL. April 2-6, 2011 (**Oral presentation**)
- 2) Cao Q., et al., Coordinated regulation of Polycomb group complexes through microRNAs in cancer. Multi-Institutional Prostate SPORC retreat (Poster presentation), Fort Lauderdale, FL., Mar 21-23, 2011

Award:

2011 American Association for Cancer Research 102nd Annual Meeting AACR-Aflac Scholar-in-Training Award

Conclusion:

Our previous studies showed that microRNA miR-101 represses histone methyltransferase EZH2 at transcript and protein levels. And miR-101 expression levels were decreased during prostate cancer progression and negatively correlated with EZH2. In addition, we demonstrated that genomic loci encoding miR-101 were deleted in metastatic prostate and the genomic loss of miR-101 leads to EZH2 overexpression in cancer.

Based on the aims of this proposal, we performed miRNA profiling and identified additional miR-101 downstream targets BMI1 and RING2 through EZH2-regulated miRNAs miR-181a,b miR-200b,c and miR-203. Importantly, we identified these miRNAs including miR-101 are inversely correlated with PRC proteins EZH2, BMI1 and RING2 during prostate cancer progression and discovered the coordinated regulation between PRC2 and PRC1 through miRNAs. Furthermore, we are investigating the DNA methylation in miR-101 regions and EZH2 3'UTR mutations in cancer.

ABBREVIATIONS

PCA: prostate cancer

miRNA: microRNA

EZH2: enhancer of zeste homolog 2

BMI1: B lymphoma Mo-MLV insertion region 1 homolog

PRC: Polycomb Repressive Complex

References

1. Jemal, A., Murray, T., Samuels, A., Ghafoor, A., Ward, E. and Thun, M.J. (2003) Cancer statistics, 2003. *CA Cancer J Clin*, 53, 5-26.
2. Lim, L.P., Glasner, M.E., Yekta, S., Burge, C.B. and Bartel, D.P. (2003) Vertebrate microRNA genes. *Science*, 299, 1540.
3. Chen, C.Z. and Lodish, H.F. (2005) MicroRNAs as regulators of mammalian hematopoiesis. *Semin Immunol*, 17, 155-65.
4. Sevignani, C., Calin, G.A., Siracusa, L.D. and Croce, C.M. (2006) Mammalian microRNAs: a small world for fine-tuning gene expression. *Mamm Genome*, 17, 189-202.
5. Mysliwiec, M.R., Chen, J., Powers, P.A., Bartley, C.R., Schneider, M.D. and Lee, Y. (2006) Generation of a conditional null allele of jumonji. *Genesis*, 44, 407-11.
6. Zhang, B., Pan, X., Cobb, G.P. and Anderson, T.A. (2006) microRNAs as oncogenes and tumor suppressors. *Dev Biol*.
7. Calin, G.A. and Croce, C.M. (2006) MicroRNA signatures in human cancers. *Nat Rev Cancer*, 6, 857-66.
8. Hwang, H.W. and Mendell, J.T. (2006) MicroRNAs in cell proliferation, cell death, and tumorigenesis. *Br J Cancer*, 94, 776-80.
9. Thomson, J.M., Newman, M., Parker, J.S., Morin-Kensicki, E.M., Wright, T. and Hammond, S.M. (2006) Extensive post-transcriptional regulation of microRNAs and its implications for cancer. *Genes Dev*, 20, 2202-7.
10. Calin, G.A., Dumitru, C.D., Shimizu, M., Bichi, R., Zupo, S., Noch, E., Aldler, H., Rattan, S., Keating, M., Rai, K., Rassenti, L., Kipps, T., Negrini, M., Bullrich, F. and Croce, C.M. (2002) Frequent deletions and down-regulation of micro- RNA genes miR15 and miR16 at 13q14 in chronic lymphocytic leukemia. *Proc Natl Acad Sci U S A*, 99, 15524-9.
11. Alvarez-Garcia, I. and Miska, E.A. (2005) MicroRNA functions in animal development and human disease. *Development*, 132, 4653-62.
12. Volinia, S., Calin, G.A., Liu, C.G., Ambs, S., Cimmino, A., Petrocca, F., Visone, R., Iorio, M., Roldo, C., Ferracin, M., Prueitt, R.L., Yanaihara, N., Lanza, G., Scarpa, A., Vecchione, A., Negrini, M., Harris, C.C. and Croce, C.M. (2006) A microRNA expression signature of human solid tumors defines cancer gene targets. *Proc Natl Acad Sci U S A*, 103, 2257-61.
13. Cummins, J.M., He, Y., Leary, R.J., Pagliarini, R., Diaz, L.A., Jr., Sjoblom, T., Barad, O., Bentwich, Z., Szafranska, A.E., Labourier, E., Raymond, C.K., Roberts, B.S., Juhl, H., Kinzler, K.W., Vogelstein, B. and Velculescu, V.E. (2006) The colorectal microRNAome. *Proc Natl Acad Sci U S A*, 103, 3687-92.
14. Yanaihara, N., Caplen, N., Bowman, E., Seike, M., Kumamoto, K., Yi, M., Stephens, R.M., Okamoto, A., Yokota, J., Tanaka, T., Calin, G.A., Liu, C.G., Croce, C.M. and Harris, C.C. (2006) Unique microRNA molecular profiles in lung cancer diagnosis and prognosis. *Cancer Cell*, 9, 189-98.
15. Iorio, M.V., Ferracin, M., Liu, C.G., Veronese, A., Spizzo, R., Sabbioni, S., Magri, E., Pedriali, M., Fabbri, M., Campiglio, M., Menard, S., Palazzo, J.P., Rosenberg, A., Musiani, P., Volinia, S., Nenci, I., Calin, G.A., Querzoli, P., Negrini, M. and Croce, C.M. (2005) MicroRNA gene expression deregulation in human breast cancer. *Cancer Res*, 65, 7065-70.
16. Calin, G.A., Liu, C.G., Sevignani, C., Ferracin, M., Felli, N., Dumitru, C.D., Shimizu, M., Cimmino, A., Zupo, S., Dono, M., Dell'Aquila, M.L., Alder, H., Rassenti, L., Kipps, T.J., Bullrich, F., Negrini, M. and Croce, C.M. (2004) MicroRNA profiling reveals distinct signatures in B cell chronic lymphocytic leukemias. *Proc Natl Acad Sci U S A*, 101, 11755-60.
17. Calin, G.A., Ferracin, M., Cimmino, A., Di Leva, G., Shimizu, M., Wojcik, S.E., Iorio, M.V., Visone, R., Sever, N.I., Fabbri, M., Iuliano, R., Palumbo, T., Pichiorri, F., Roldo, C., Garzon, R., Sevignani, C., Rassenti, L., Alder, H., Volinia, S., Liu, C.G., Kipps, T.J., Negrini, M. and Croce, C.M. (2005) A MicroRNA

signature associated with prognosis and progression in chronic lymphocytic leukemia. *N Engl J Med*, 353, 1793-801.

18. Pallante, P., Visone, R., Ferracin, M., Ferraro, A., Berlingieri, M.T., Troncone, G., Chiappetta, G., Liu, C.G., Santoro, M., Negrini, M., Croce, C.M. and Fusco, A. (2006) MicroRNA deregulation in human thyroid papillary carcinomas. *Endocr Relat Cancer*, 13, 497-508.
19. Johnson, S.M., Grosshans, H., Shingara, J., Byrom, M., Jarvis, R., Cheng, A., Labourier, E., Reinert, K.L., Brown, D. and Slack, F.J. (2005) RAS is regulated by the let-7 microRNA family. *Cell*, 120, 635-47.
20. O'Donnell, K.A., Wentzel, E.A., Zeller, K.I., Dang, C.V. and Mendell, J.T. (2005) c-Myc-regulated microRNAs modulate E2F1 expression. *Nature*, 435, 839-43.
21. Lu, Z., Liu, M., Stribinskis, V., Klinge, C.M., Ramos, K.S., Colburn, N.H. and Li, Y. (2008) MicroRNA-21 promotes cell transformation by targeting the programmed cell death 4 gene. *Oncogene*, 27, 4373-9.
22. Lu, J., Getz, G., Miska, E.A., Alvarez-Saavedra, E., Lamb, J., Peck, D., Sweet-Cordero, A., Ebert, B.L., Mak, R.H., Ferrando, A.A., Downing, J.R., Jacks, T., Horvitz, H.R. and Golub, T.R. (2005) MicroRNA expression profiles classify human cancers. *Nature*, 435, 834-8.
23. Ozen, M., Creighton, C.J., Ozdemir, M. and Ittmann, M. (2008) Widespread deregulation of microRNA expression in human prostate cancer. *Oncogene*, 27, 1788-93.
24. Porkka, K.P., Pfeiffer, M.J., Waltering, K.K., Vessella, R.L., Tammela, T.L. and Visakorpi, T. (2007) MicroRNA expression profiling in prostate cancer. *Cancer Res*, 67, 6130-5.
25. Boyer, L.A., Plath, K., Zeitlinger, J., Brambrink, T., Medeiros, L.A., Lee, T.I., Levine, S.S., Wernig, M., Tajonar, A., Ray, M.K., Bell, G.W., Otte, A.P., Vidal, M., Gifford, D.K., Young, R.A. and Jaenisch, R. (2006) Polycomb complexes repress developmental regulators in murine embryonic stem cells. *Nature*, 441, 349-53.
26. Lee, T.I., Jenner, R.G., Boyer, L.A., Guenther, M.G., Levine, S.S., Kumar, R.M., Chevalier, B., Johnstone, S.E., Cole, M.F., Isono, K., Koseki, H., Fuchikami, T., Abe, K., Murray, H.L., Zucker, J.P., Yuan, B., Bell, G.W., Herbolsheimer, E., Hannett, N.M., Sun, K., Odom, D.T., Otte, A.P., Volkert, T.L., Bartel, D.P., Melton, D.A., Gifford, D.K., Jaenisch, R. and Young, R.A. (2006) Control of developmental regulators by Polycomb in human embryonic stem cells. *Cell*, 125, 301-13.
27. Sher, F., Rossler, R., Brouwer, N., Balasubramanian, V., Boddeke, E. and Copray, S. (2008) Differentiation of Neural Stem Cells into Oligodendrocytes: Involvement of the Polycomb Group Protein Ezh2. *Stem Cells*.
28. Varambally, S., Dhanasekaran, S.M., Zhou, M., Barrette, T.R., Kumar-Sinha, C., Sanda, M.G., Ghosh, D., Pienta, K.J., Sewalt, R.G., Otte, A.P., Rubin, M.A. and Chinnaiyan, A.M. (2002) The polycomb group protein EZH2 is involved in progression of prostate cancer. *Nature*, 419, 624-9.
29. Bracken, A.P., Pasini, D., Capra, M., Prosperini, E., Colli, E. and Helin, K. (2003) EZH2 is downstream of the pRB-E2F pathway, essential for proliferation and amplified in cancer. *Embo J*, 22, 5323-35.
30. Erhardt, S., Su, I.H., Schneider, R., Barton, S., Bannister, A.J., Perez-Burgos, L., Jenuwein, T., Kouzarides, T., Tarakhovsky, A. and Surani, M.A. (2003) Consequences of the depletion of zygotic and embryonic enhancer of zeste 2 during preimplantation mouse development. *Development*, 130, 4235-48.
31. Plath, K., Fang, J., Mlynarczyk-Evans, S.K., Cao, R., Worringer, K.A., Wang, H., de la Cruz, C.C., Otte, A.P., Panning, B. and Zhang, Y. (2003) Role of histone H3 lysine 27 methylation in X inactivation. *Science*, 300, 131-5.
32. Cao, R., Wang, L., Wang, H., Xia, L., Erdjument-Bromage, H., Tempst, P., Jones, R.S. and Zhang, Y. (2002) Role of histone H3 lysine 27 methylation in Polycomb-group silencing. *Science*, 298, 1039-43.
33. Kuzmichev, A., Nishioka, K., Erdjument-Bromage, H., Tempst, P. and Reinberg, D. (2002) Histone methyltransferase activity associated with a human multiprotein complex containing the Enhancer of Zeste protein. *Genes Dev*, 16, 2893-905.
34. Yu, J., Cao, Q., Mehra, R., Laxman, B., Yu, J., Tomlins, S.A., Creighton, C.J., Dhanasekaran, S.M., Shen, R., Chen, G., Morris, D.S., Marquez, V.E., Shah, R.B., Ghosh, D., Varambally, S. and Chinnaiyan, A.M.

- (2007) Integrative genomics analysis reveals silencing of beta-adrenergic signaling by polycomb in prostate cancer. *Cancer Cell*, 12, 419-31.
35. Cao, Q., Yu, J., Dhanasekaran, S.M., Kim, J.H., Mani, R.S., Tomlins, S.A., Mehra, R., Laxman, B., X., C., Yu, J., Kleer, C.G., Varambally, S. and Chinnaiyan, A.M. (2008) Repression of E-cadherin by the Polycomb Group Protein EZH2 in Cancer. *Oncogene*.
 36. Kleer, C.G., Cao, Q., Varambally, S., Shen, R., Ota, I., Tomlins, S.A., Ghosh, D., Sewalt, R.G., Otte, A.P., Hayes, D.F., Sabel, M.S., Livant, D., Weiss, S.J., Rubin, M.A. and Chinnaiyan, A.M. (2003) EZH2 is a marker of aggressive breast cancer and promotes neoplastic transformation of breast epithelial cells. *Proc Natl Acad Sci U S A*, 100, 11606-11.
 37. Croonquist, P.A. and Van Ness, B. (2005) The polycomb group protein enhancer of zeste homolog 2 (EZH 2) is an oncogene that influences myeloma cell growth and the mutant ras phenotype. *Oncogene*, 24, 6269-80.
 38. Takeshita, F., Minakuchi, Y., Nagahara, S., Honma, K., Sasaki, H., Hirai, K., Teratani, T., Namatame, N., Yamamoto, Y., Hanai, K., Kato, T., Sano, A. and Ochiya, T. (2005) Efficient delivery of small interfering RNA to bone-metastatic tumors by using atelocollagen in vivo. *Proc Natl Acad Sci U S A*, 102, 12177-82.
 39. Krek, A., Grun, D., Poy, M.N., Wolf, R., Rosenberg, L., Epstein, E.J., MacMenamin, P., da Piedade, I., Gunsalus, K.C., Stoffel, M. and Rajewsky, N. (2005) Combinatorial microRNA target predictions. *Nat Genet*, 37, 495-500.
 40. Lewis, B.P., Shih, I.H., Jones-Rhoades, M.W., Bartel, D.P. and Burge, C.B. (2003) Prediction of mammalian microRNA targets. *Cell*, 115, 787-98.
 41. John, B., Enright, A.J., Aravin, A., Tuschl, T., Sander, C. and Marks, D.S. (2004) Human MicroRNA targets. *PLoS Biol*, 2, e363.
 42. Rusinov, V., Baev, V., Minkov, I.N. and Tabler, M. (2005) MicroInspector: a web tool for detection of miRNA binding sites in an RNA sequence. *Nucleic Acids Res*, 33, W696-700.

APPENDICES

PDFs of articles

- 1) **Cao Q**, Mani RS, Ateeq B, Dhanasekaran SM, Asangani IA, Prensner JR, Kim JH, Brenner JC, Jing X, Cao X, Wang R, Li Y, Dahiya A, Wang L, Pandhi M, Lonigro RJ, Wu Y-M, Tomlins SA, Palanisamy N, Qin Z, Yu J, Maher CA, Varambally S, Chinnaiyan AM. Coordinated regulation of Polycomb group complexes through microRNAs in cancer. *Cancer Cell*. 2011 Aug 16;20(2):187-99.
- 2) Prensner JR, Iyer MK, Balbin OA, Dhanasekaran SM, **Cao Q**, Brenner JC, Laxman B, Asangani IA, Grasso C, Kominsky HD, Cao X, Jing X, Wang X, Siddiqui J, Wei JT, Robinson D, Iyer HK, Palanisamy N, Maher CA, Chinnaiyan AM. Transcriptome Sequencing Identifies PCAT-1, a Novel lincRNA Implicated in Prostate Cancer Progression. *Nat. Biotechnol*. 2011 Jul 31;29(8):742-9. doi: 10.1038/nbt.1914.
- 3) Ateeq B, Tomlins, SA, Laxman B, Asangani IA, **Cao Q**, Cao X, Yong L, Wang X, Feng FY, Pienta KJ, Varambally S, Chinnaiyan AM. Therapeutic targeting of SPINK1-positive prostate cancer. *Sci. Transl. Med*. 2011 3: 72ra17 (2011). PMID: 21368222.

Curriculum Vitae of PI

Coordinated Regulation of Polycomb Group Complexes through microRNAs in Cancer

Qi Cao,^{1,2} Ram-Shankar Mani,^{1,2} Bushra Ateeq,^{1,2} Saravana M. Dhanasekaran,^{1,2} Irfan A. Asangani,^{1,2} John R. Prensner,^{1,2} Jung H. Kim,^{1,2} J. Chad Brenner,^{1,2} Xiaojun Jing,^{1,2} Xuhong Cao,^{1,3} Rui Wang,^{1,2} Yong Li,^{1,2} Arun Dahiya,¹ Lei Wang,^{1,2} Mithil Pandhi,¹ Robert J. Lonigro,^{1,2} Yi-Mi Wu,^{1,2} Scott A. Tomlins,^{1,2} Nallasivam Palanisamy,^{1,2,6} Zhaohui Qin,⁷ Jindan Yu,^{1,2,9} Christopher A. Maher,^{1,2,4} Sooryanarayana Varambally,^{1,2,6,8} and Arul M. Chinnaiyan^{1,2,3,5,6,8,*}

¹Michigan Center for Translational Pathology

²Department of Pathology, University of Michigan

³Howard Hughes Medical Institute, University of Michigan Medical School

⁴Center for Computational Medicine and Bioinformatics

⁵Department of Urology, University of Michigan

⁶Comprehensive Cancer Center, University of Michigan Medical School
Ann Arbor, MI 48109, USA

⁷Department of Biostatistics and Bioinformatics, Center for Comprehensive Informatics, Emory University, Atlanta, GA 30329, USA

⁸These authors contributed equally to this work

⁹Present address: Division of Hematology/Oncology, Northwestern University, Robert H. Lurie Comprehensive Cancer Center, Chicago, IL 60611, USA

*Correspondence: arul@umich.edu

DOI 10.1016/j.ccr.2011.06.016

SUMMARY

Polycomb Repressive Complexes (PRC1 and PRC2)-mediated epigenetic regulation is critical for maintaining cellular homeostasis. Members of Polycomb Group (PcG) proteins including EZH2, a PRC2 component, are upregulated in various cancer types, implicating their role in tumorigenesis. Here, we have identified several microRNAs (miRNAs) that are repressed by EZH2. These miRNAs, in turn, regulate the expression of PRC1 proteins BMI1 and RING2. We found that ectopic overexpression of EZH2-regulated miRNAs attenuated cancer cell growth and invasiveness, and abrogated cancer stem cell properties. Importantly, expression analysis revealed an inverse correlation between miRNA and PRC protein levels in cell culture and prostate cancer tissues. Taken together, our data have uncovered a coordinate regulation of PRC1 and PRC2 activities that is mediated by miRNAs.

INTRODUCTION

Polycomb group (PcG) proteins are evolutionarily conserved regulators of gene silencing important in metazoan development (Surface et al., 2010), stem cell pluripotency (Pereira et al., 2010), and X chromosome inactivation (Cao et al., 2002; Margueron and Reinberg, 2011). PcG proteins form multiprotein repressive complexes called PRCs. Both PRC1 and PRC2 play a critical role in the maintenance of normal and cancer stem cell populations (Ezhkova et al., 2009; Lukacs et al., 2010; Pietersen et al., 2008). Dysregulation of PcG proteins can contribute to

a number of human diseases, most notably, cancer (Bracken and Helin, 2009; Margueron and Reinberg, 2011).

Key components of the human PRC2 include the histone methyltransferase Enhancer of Zeste Homolog 2 (EZH2), and its binding partners, Embryonic Ectoderm Development (EED) and Suppressor of Zeste 12 (SUZ12), which function as a multi-subunit complex that trimethylates histone H3K27. PRC2 is thought to be recruited to target genomic loci by long noncoding RNAs (ncRNAs) such as HOTAIR (Gupta et al., 2010; Kaneko et al., 2010; Rinn et al., 2007). EZH2, which is the enzymatic component of PRC2, is elevated in aggressive forms of prostate

Significance

Polycomb group (PcG) proteins are chromatin-modifying complexes that regulate epigenetic silencing and play an important role in determining cell fate. PcG proteins form two major complexes, Polycomb Repressive Complex 1 (PRC1) and Polycomb Repressive Complex 2 (PRC2). PRC2 methylates histone H3 on lysine27 (H3K27), a chromatin mark that stimulates PRC1 to enact gene silencing at target genes. Employing in vitro and in vivo cancer models and human tumor studies, we demonstrate that PRC2 and PRC1 coordinate their functions through regulation of specific microRNAs. Increased PRC2 activity in cancer leads to repression of these microRNAs, and subsequent increase of PRC1 components. Thus, we propose that key microRNAs link PRC2 to PRC1 forming an integral regulatory axis of the epigenetic silencing machinery.

and breast cancer (Kleer et al., 2003; Varambally et al., 2002), as well as multiple other solid tumors (Matsukawa et al., 2006; Sudo et al., 2005). Loss of microRNA (miRNA)-101, has been shown to be one mechanism that leads to elevated EZH2 and PRC2 activity in tumors (Cao et al., 2010; Chiang et al., 2010; Friedman et al., 2009; Varambally et al., 2008; Wang et al., 2010). Also, miR-26a was reported to target EZH2 in cancer and myogenesis (Lu et al., 2011; Wong and Tellam, 2008). Accumulating evidence suggests that increased activity of PRC2 is oncogenic as measured by cell proliferation (Bracken et al., 2003; Varambally et al., 2002), cell invasion (Cao et al., 2008; Kleer et al., 2003), anchorage-independent growth (Bracken et al., 2003; Kleer et al., 2003), maintenance of tumor-initiating cells, tumor xenograft growth (Yu et al., 2007b), and metastasis in vivo (Min et al., 2010).

A key collaborator of PRC2 in epigenetic silencing is human PRC1, which comprises B lymphoma Mo-MLV insertion region 1 (BMI1), RING1 (also known as RING1A or RNF1) and RING2 (also known as RING1B or RNF2), and functions as a multiprotein complex to ubiquitinate histone H2A at lysine 119 (uH2A) (Cao et al., 2005; Wang et al., 2004). The prevailing hypothesis is that PRC2-mediated trimethylation of H3K27 recruits PRC1 to gene loci, which enacts chromatin condensation and epigenetic silencing of target genes (Bracken and Helin, 2009). Like PRC2 component EZH2, BMI1 and RING2 have been shown to be elevated in a number of tumor types (Glinsky et al., 2005; Sánchez-Beato et al., 2006) and regulate self-renewal of embryonic stem cells and cancer stem cells (Galmozzi et al., 2006; Valk-Lingbeek et al., 2004). The mechanism of how PRC2 and PRC1 coordinate their functions is still unclear. In this study, we sought to explore the regulatory axis between PRCs and whether miRNAs mediate the synergy between the two complexes.

RESULTS

PcG Proteins Are Regulated by miRNAs

Previously, it has been reported that EZH2, the methyltransferase subunit of the PRC2 complex, is repressed by miR-101 (Friedman et al., 2009; Varambally et al., 2008) and miR-26a (Lu et al., 2011; Wong and Tellam, 2008). We hypothesized that PcG proteins (comprising the mammalian PRC complexes) may in general be regulated by miRNAs. To test this hypothesis, we knocked down Dicer, a key protein required for miRNA processing, by employing Dicer-specific siRNA duplexes. By immunoblot analysis, we found that PRC2 proteins EZH2, EED, and SUZ12, and PRC1 proteins BMI1 and RING2 were increased significantly by three different Dicer siRNA duplexes (Figure 1A; see Figure S1A available online). These experiments support the general notion that miRNAs function to repress PcG expression.

Identification of EZH2-Regulated miRNAs

To explore miRNAs regulated by PRC2 globally, we knocked down EZH2 in DU145 prostate cancer cells with a validated siRNA targeting EZH2 and monitored miRNA expression with Illumina BeadChips. In parallel, we compared these miRNA profiles with DU145 cells relative to four benign epithelial cell lines of either prostate (PrEC and RWPE) or breast (H16N2 and HME) origin. We primarily observed miRNAs that were

decreased in cancer cells relative to benign that are targets of repression by EZH2, and thus PRC2. We found 63 miRNAs that were downregulated in DU145 cells compared with the normal cell lines, and inhibition of EZH2 by knockdown restored expression of these miRNAs (Figure 1B; Table S1). Similarly, the expression levels of these 63 miRNAs were downregulated in breast cancer cells BT-549 and SKBr3 compared with breast benign epithelial cells H16N2 and HME (Figure 1B; Table S1). Using miRNA target analysis (www.targetscan.org), we identified 14 miRNAs as top candidates with the following properties: (1) upregulated by EZH2 knockdown in DU145 cancer cells which express high levels of PRC2; (2) higher in benign cell lines compared with DU145 cells, and (3) predicted to bind to the 3' untranslated region (UTR) of target PRC1 components based on TargetScan (Figure 1C). Thirteen of the 14 miRNAs meeting these criterion fell into several known miRNAs clusters and families, including miR-200b and miR-200c in the miR-200 family, which has previously been reported to repress BMI1 (Shimono et al., 2009; Wellner et al., 2009). Of the 14 miRNAs, only miR-203, which is also known to target BMI1 (Wellner et al., 2009), does not belong to any known cluster or family (Figure S1B).

EZH2-Regulated microRNAs Inhibit Expression of PRC1 Proteins BMI1 and RING2

To pinpoint the specific miRNAs that target PRC1 (out of the 14 that were nominated by computational approaches) (Figure 1C), we overexpressed each of them in BT-549 and DU145 cancer cell lines and monitored EZH2, BMI1, and RING2 protein expression (Figure 2A; Figure S2A). Of these, miR-181a, b decreased RING2 protein levels, miR-203 decreased BMI1 protein levels while miR-200b, c decreased both BMI1 and RING2 (Figure 2A). Attenuation of these PRC1 members resulted in decreased global ubiquityl-H2A, a known PRC1 substrate and mark of gene repression. Furthermore, PRC1 targets including p16INK4A (Jacobs et al., 1999a) and p21 (Waf1/Cip) (Fasano et al., 2007) were derepressed (Figure 2A). Several of the miRNAs computationally predicted to inhibit PRC1 failed to do so by overexpression including miR-17, miR-19b, and others (Figure S2A). Similar to protein levels, real-time qPCR showed miR-181a, b and miR-200b, c decreased RING2 transcript levels and miR-200b, c and miR-203 decreased BMI1 transcript levels in BT-549 cells (Figure 2B). As expected, overexpressing miR-200b or miR-203 decreased BMI1 occupancy on known PRC1 target gene p16, p19 (Jacobs et al., 1999b), p21, and HoxC13 (Cao et al., 2005) regions (Figure S2B).

To further corroborate our miRNA overexpression studies, we also extinguished expression of miRNAs using antagomiRs (Krützfeldt et al., 2005). Consistent with our predictions, antagomiR-200b, antagomiR-200c, and antagomiR-203 increased BMI1 protein levels, while antagomiR-181a, antagomiR-181b, antagomiR-200b, and antagomiR-200c increased RING2 protein levels in H16N2 cells (Figure 2C).

To evaluate whether these miRNAs directly bind to the 3' UTR of BMI1 or RING2, we cloned the predicted binding sites of the wild-type or mutant 3' UTR into a luciferase reporter system and cotransfected them with miRNA expression vectors into BT-549 cells (Figure 2D; Figures S2C–S2F). As expected, inhibition of luciferase activity was observed in cells transfected with constructs containing wild-type binding sites but not the mutant

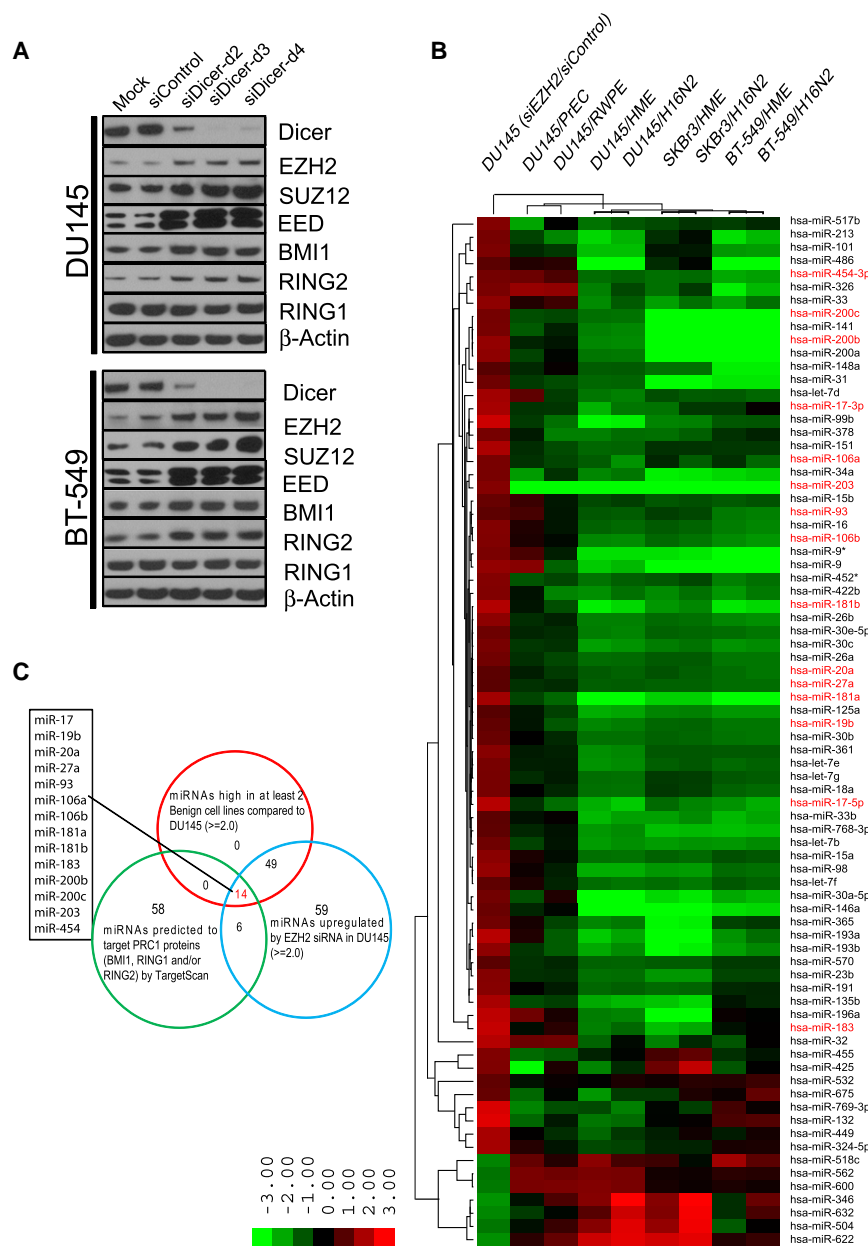


Figure 1. PcG Proteins Are Regulated by miRNAs

(A) Knockdown of Dicer in DU145 and BT-549 cells by three different Dicer-specific duplexes and PcG protein expression was assessed.

(B) miRNA profiling of DU145 prostate cancer cells in which EZH2 was knocked down compared with DU145 cancer cells relative to benign cells HME, PrEC, RWPE, and H16N2. Shades of red represent increased gene expression while shades of green represent decreased expression.

(C) A Venn diagram depicting 14 miRNAs that were upregulated by EZH2 knockdown, had high endogenous levels in normal cells, and were predicted to target PRC1 proteins. See also Figure S1 and Table S1.

Further, we observed similar expression changes in these microRNAs upon stable overexpression of miR-101 or EZH2 shRNA in DU145 and SKBr3 cells (Figure S3A). Also we observed that miR-101 was increased in DU145 cells in which EZH2 was stably knocked down, suggesting the existence of feedback regulation between EZH2 and miR-101. In contrast, overexpression of EZH2, but not EZH2ΔSET (which is missing its catalytic SET domain), decreased miR-181a, miR-181b, miR-200a, miR-200b, miR-200c, and miR-203 levels in H16N2 cells (Figure S3B).

Next, we treated DU145 cells with the global histone methylation inhibitor, deazaneplanocin A (DZNep), that depletes PRC2 and thus attenuates H3K27me3 (Tan et al., 2007). Interestingly, DZNep treatment led to derepression of the putative PRC2-targeted miRNAs including miR-181a,b, miR-200a,b,c, and miR-203 (Figure 3B). This effect was both concentration and incubation time dependent. Control microRNAs, miR-217, miR-219, and miR-21 were not affected by DZNep treatment.

constructs. The RING2 3' UTR reporters were downregulated by miR-181a, miR-181b, miR-200b, and miR-200c while the BMI1 3' UTR reporters were downregulated by miR-200b, miR-200c, and miR-203 (Figure 2D).

We next determined whether the miRNAs that regulate PRC1 were directly regulated by PRC2 in BT-549 and DU145 cells. Cells were transfected with either a validated EZH2 siRNA or miR-101 (both of which target and downregulate the PRC2), and expression levels of target miRNAs were measured by real-time PCR. miR-181a, miR-181b, miR-200a, miR-200b, miR-200c, and miR-203 expression levels were increased in EZH2 siRNA or miR-101-transfected cells. Expression of miRNAs miR-217 and miR-219, two control microRNAs not predicted to be regulated by EZH2, were not altered (Figure 3A).

In addition to DZNep, we evaluated other chemical inhibitors of epigenetic pathways. As HDAC activity is essential for EZH2 function (Cao et al., 2008; Kleer et al., 2003), and EZH2 directly or indirectly facilitates DNA methylation (Viré et al., 2006), we predicted that treatment with the HDAC inhibitor suberoylanilide hydroxamic acid (SAHA) and/or the DNA methylation inhibitor 5-aza-2'-deoxycytidine (5-aza-dC) would inhibit EZH2-mediated epigenetic modifications, leading to an increase in miRNA expression. Treatment of BT-549 and DU145 cells with 5-aza-dC or SAHA alone or in combination, resulted in a marked increase in miR-181a,b, miR-200a,b,c, and miR-203 expression, suggesting epigenetic regulation of these microRNAs (Figure 3C).

Importantly, when we overexpressed EZH2 by adenovirus in DZNep or SAHA and 5-aza-dC-treated DU145 cells, EZH2 could

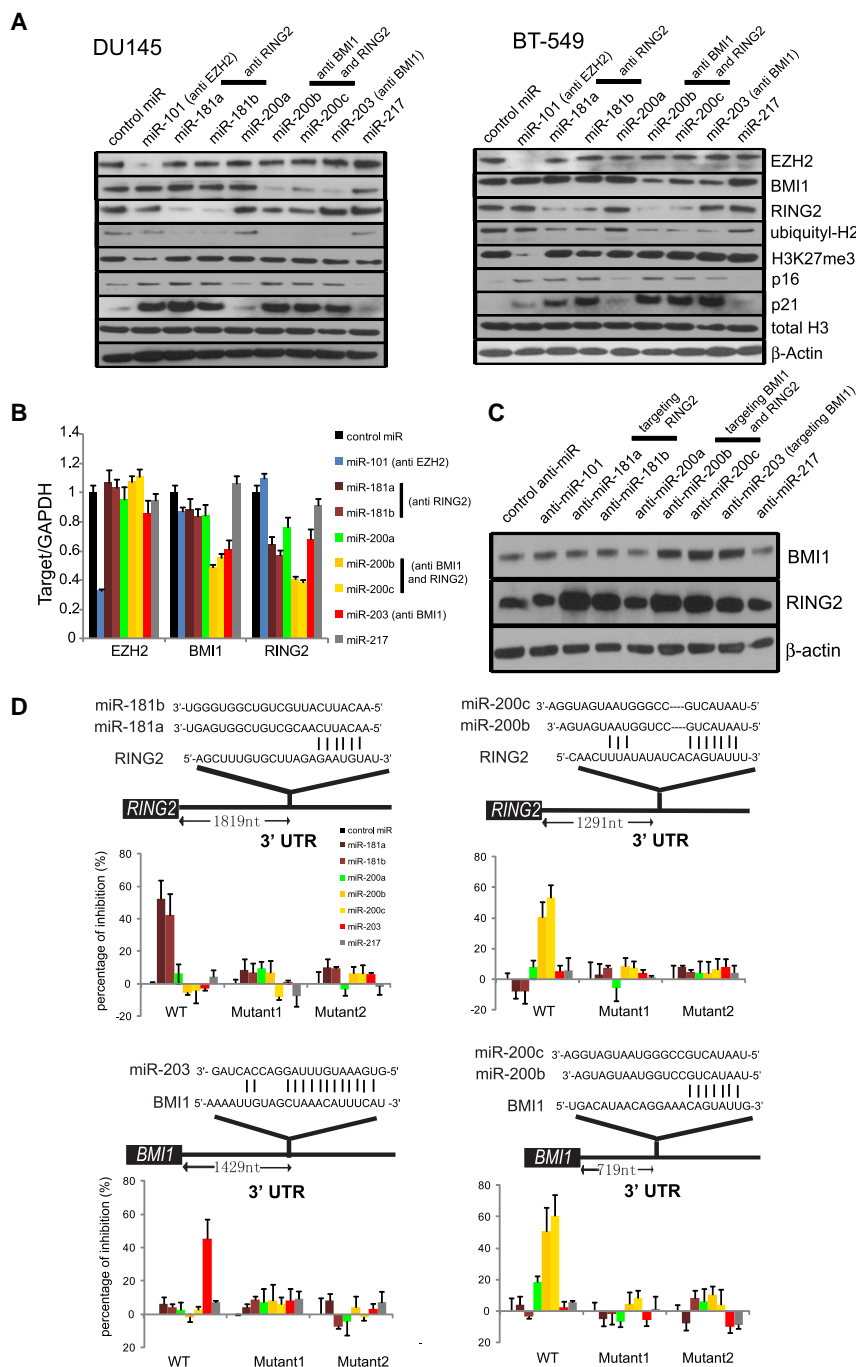


Figure 2. PRC2-Regulated miRNAs Repress PRC1 Proteins BMI1 and RING2

(A) Overexpression of indicated miRs in DU145 and BT-549 cells and expression of PRC components, PRC2 histone mark H3K27me3, PRC1 target histone mark ubiquitinyl-H2A and indicated genes by immunoblot analysis. β-actin and total H3 were used as loading controls.

(B) As in (A), except transcript level was assessed in BT-549 by qPCR.

(C) Transfection of indicated antagomiRs (anti-miR) in H16N2 cells and immunoblot analysis for BMI1 and RING2. β-actin was used as a loading control.

(D) TargetScan analysis depicting potential binding sites for EZH2-regulated miRNAs in the 3' UTR of BMI1 and RING2. Luciferase reporter assays with wild-type or mutant 3' UTR constructs of BMI1 or RING2 demonstrate that miR-181a, miR-181b, miR-200b, miR-200c, and miR-203 repress BMI1 and/or RING2 activity.

All bar graphs are shown with ± SEM. See also Figure S2.

that a negative feedback system between PRC2-regulated miRNAs and PRC1 may exist. Furthermore, an EZH2-specific siRNA (Figure S3F) or treatment with 5-aza-dC and SAHA, either alone or in combination (Figure 3D), markedly decreased the H3K27me3 occupancy in these regions.

EZH2-Regulated miRNAs Attenuate Growth, Invasiveness, and Self-Renewal of Cancer Cells

Because EZH2 has been shown to repress several tumor suppressor genes (Cao et al., 2008; Chen et al., 2005; Fujii et al., 2008; Min et al., 2010; Yu et al., 2007b, 2010), we postulated that the EZH2-regulated microRNAs also functioned as tumor suppressors. Consistent with this hypothesis, overexpression of either miR-181a, miR-181b, miR-200a, miR-200b, miR-200c, or miR-203 markedly attenuated BT-549 and DU145 cell proliferation to levels similar to that of cells transfected with EZH2 siRNA, or cells overexpressing miR-101 (Figure 4A

completely abolish DZNep-mediated miRNA upregulation (Figure S3C), and partially decreased SAHA and 5-aza-dC-mediated miRNA upregulation (Figure S3D) presumably because SAHA and 5-aza-dC also inhibited HDAC and DNMT activities.

To confirm that EZH2 regulates these microRNAs by epigenetic repression, we performed chromatin immunoprecipitation (ChIP) assays with anti-H3K27me3, EZH2 and BMI1 antibodies in BT-549 cells. Interestingly, H3K27me3 and EZH2 occupied the PRC2-regulated miRNAs regions as expected. In addition, BMI1 also occupied these regions (Figure S3E), suggesting

*p < 0.001, **p < 0.01; Figure S4A). Likewise, overexpression of either miR-181a, miR-181b, miR-200a, miR-200b, miR-200c, or miR-203 inhibited the in vitro invasive potential of BT-549 and DU145 cells through modified Boyden chambers coated with Matrigel (Figure 4B, *p < 0.005, **p < 0.02). However, overexpressing EZH2-repressed miRNAs had no effect on the invasiveness of RWPE-UBE2L3-KRAS and RWPE-SLC45A3-BRAF stable cells, in which fusion proteins UBE2L3-KRAS (Wang et al., 2011) and SLC45A3-BRAF (Bonci et al., 2008; Palanisamy et al., 2010) confer neoplastic properties to RWPE cells

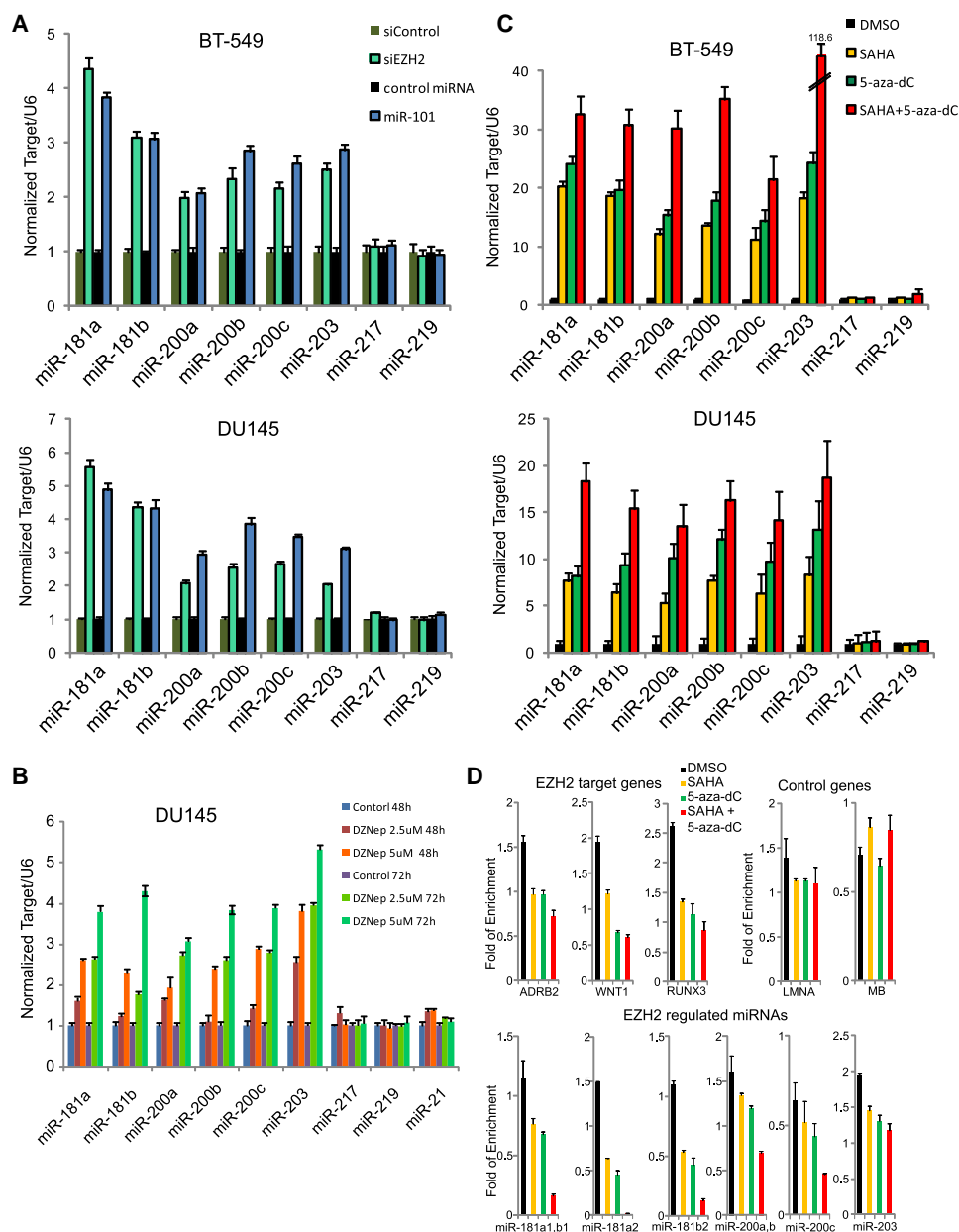


Figure 3. PRC2 Silences Multiple miRNAs by Epigenetic Mechanisms

(A) Taqman miRNA qPCR analysis of indicated miRs in BT-549 and DU145 cells in which EZH2 was knocked down using siRNA or miR-101 (a microRNA which targets EZH2). Quantitative microRNA levels were normalized against U6.

(B) As in (A), except DZNep at two different doses and time points was incubated with DU145 cells.

(C) As in (A), except SAHA and/or 5-aza-dC was used in BT-549 and DU145 cells.

(D) ChIP-qPCR analysis of H3K27me3 at indicated genes and microRNAs in BT-549 cells treated with SAHA and/or 5-aza-dC.

All bar graphs are shown with \pm SEM. See also Figure S3.

(Figure S4B), suggesting that EZH2-repressed miRNAs miR-181a,b, miR-200b,c, and miR-203 may inhibit cell invasion through acting on PRC1 proteins. However, EZH2-repressed miRNAs still decreased RWPE-UBE2L3-KRAS and RWPE-SLC45A3-BRAF proliferation (Figure S4C), consistent with a critical role of PcG proteins in cell growth.

To investigate whether miR-181a, miR-181b, miR-200a, miR-200b, miR-200c, or miR-203 inhibit anchorage-independent

growth, we performed soft agar colony formation assays. Similar to miR-101 and EZH2 knockdown controls, overexpression of miR-181a, miR-181b, miR-200a, miR-200b, miR-200c, and miR-203 markedly suppressed DU145 colony formation (Figure 4C, $*p < 0.001$, $**p < 0.01$). Next, we evaluated the ability of DU145 to form prostatospheres in sphere-promoting cell media. This assay serves as a surrogate measure of stem cell-like phenotypes, and cells that are able to form spheres have

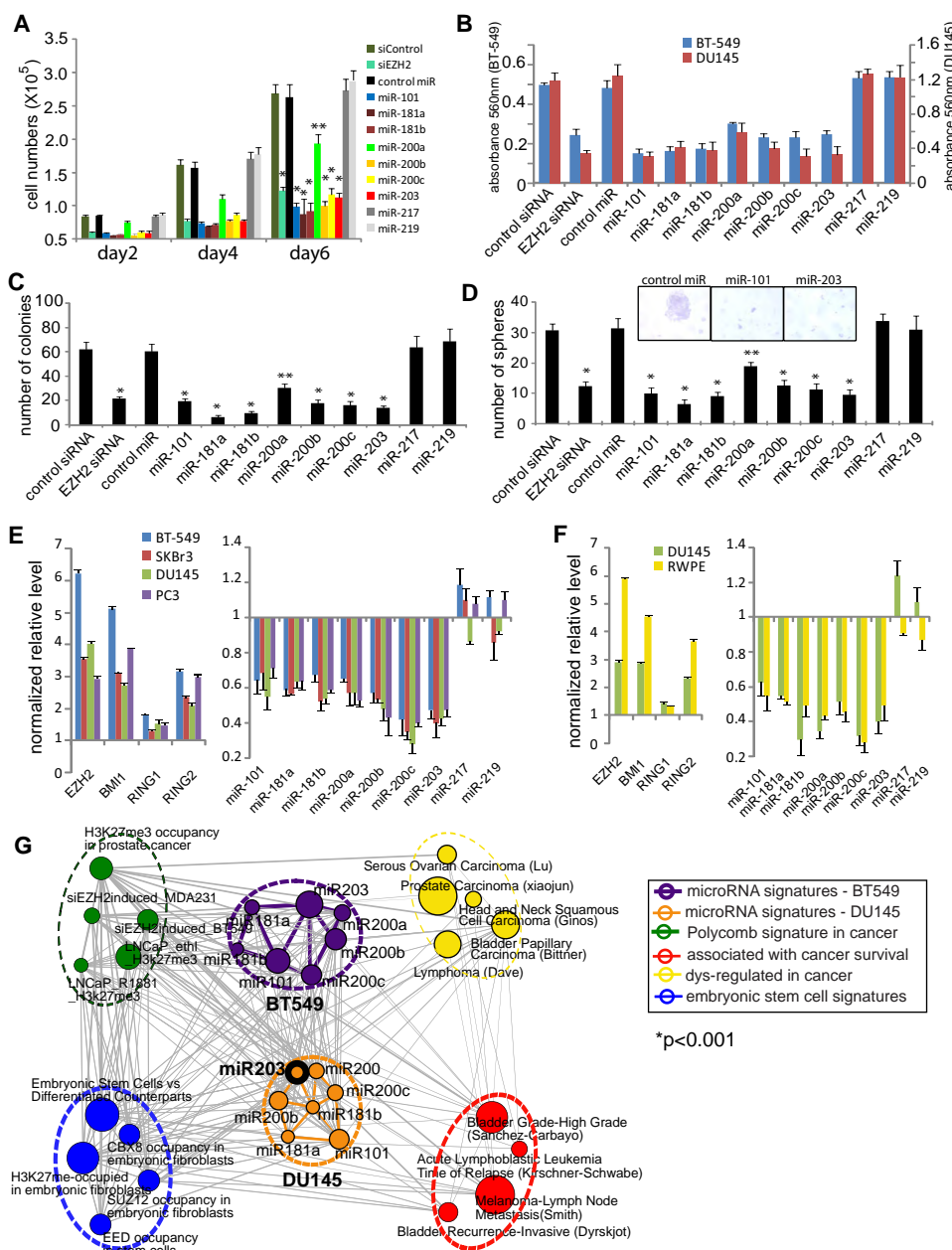


Figure 4. PRC2-Mediated Regulation of microRNAs Potentiates the Cancer Cell Phenotype

(A) Overexpression of PRC2-regulated miRNAs, but not control miR-217 or miR-219, inhibited BT-549 cell proliferation. EZH2 siRNA and miR-101 overexpression were positive controls and miR-217 and miR-219 overexpression were negative controls. * $p < 0.001$, ** $p < 0.01$. (Student's t test).

(B) Overexpression of PRC2-regulated miRNAs decreased BT-549 and DU145 cell invasion in vitro. * $p < 0.01$. (Student's t test).

(C) Overexpression of PRC2-regulated miRNAs suppressed DU145 anchorage-independent growth in soft agar. * $p < 0.01$. (Student's t test).

(D) Overexpression of EZH2-regulated miRNAs decreased prostatosphere formation by DU145 cells. * $p < 0.01$. (Student's t test). Representative images of prostatospheres (scale bar: 100 μ m) were shown in the inset.

(E) qPCR analysis demonstrating EZH2, BMI1 and RING2 transcript levels were higher in spheres compared with monolayer culture, while miR-101, miR-181a,b, miR-200a,b,c, and miR-203, but not miR-217 or miR-219, were lower in spheres compared with monolayers. Expression level of each gene was normalized to GAPDH or U6 and normalized to corresponding monolayer cultured cell line.

(F) qPCR analysis showing EZH2, BMI1 and RING2 levels were higher in sorted CD24-/CD44+ DU145 and RWPE cells compared with the unsorted population, while miR-101, miR-181a,b, miR-200a,b,c, and miR-203, but not miR-217 or miR-219, were lower in CD24-/CD44+ DU145 and RWPE cells compared with an unsorted population.

(G) Genes regulated by EZH2-repressed miRNAs cluster into multiple functional concepts. BT-549 and DU145 cells were transfected with EZH2-repressed miRNAs followed by gene expression profiling and Molecular Concepts analysis. Each node represents a molecular concept or set of biologically related genes. miR-101, miR-181a, miR-181b, miR-200a, miR-200b, miR-200c, and miR-203 (miRNA signatures, purple for BT-549, orange for DU145) were enriched

enhanced stem cell characteristics (Lawson et al., 2007). We found that miR-181a, miR-181b, miR-200a, miR-200b, miR-200c, and miR-203 overexpression, as well as miR-101 overexpression and EZH2 siRNA controls, significantly inhibited the ability of DU145 cells to form spheres in this assay (Figure 4D, * $p < 0.001$, ** $p < 0.01$). Intriguingly, several genes implicated in pluripotency and cellular reprogramming by induced pluripotency, such as Klf4, Sox2, and c-Myc, were markedly downregulated by miR-200b, miR-200c, and miR-203, and marginally decreased by miR-101, miR-181a, miR-181b, and miR-200a expression, but not by miR-217 or miR-219 controls (Figure S4D). Relative to the human embryonic stem cell H7, BT-549 and DU145 cancer cells have comparable expression levels of iPS factors and PcG proteins (Figure S4E).

Next, we measured expression levels of EZH2, BMI1, RING2, and key microRNAs relevant to this study in spheres and monolayers. In BT-549, SKBr3, DU145, and PC3 cells, we observed that EZH2, BMI1, and RING2 levels were higher in spheres than in monolayers; conversely miR-101, miR-181a, miR-181b, miR-200a, miR-200b, miR-200c, and miR-203 levels were lower in spheres than in monolayers (Figure 4E). Using DU145 and RWPE parental cell lines, we employed flow cytometry to isolate cells with high expression of the CD44 surface antigen and low expression of the CD24 surface antigen (CD24-/CD44+), a cell population enriched for stem cell-like phenotypes (Hurt et al., 2008). We measured EZH2, BMI1, RING2, and miRNA levels in CD24-/CD44+ cells compared with total, unsorted cells. We observed that EZH2, BMI1, and RING2 levels were increased in CD24-/CD44+ cells, but miR-101, miR-181a, miR-181b, miR-200a, miR-200b, miR-200c, and miR-203 expression were decreased in this cell population (Figure 4F). Taken together, the data provide compelling evidence for the coordinated regulation of PRC2, PRC1, and miRNAs in the maintenance of a differentiated cellular state and inhibition of stem cell-like phenotypes.

In order to understand the functional biology of the miRNAs identified in this study, we sought to identify global gene expression patterns and molecular pathways to which they might contribute. We conducted gene expression microarray analyses of DU145 and BT-549 cells transfected with control miRNA, miR-101, miR-181a, miR-181b, miR-200a, miR-200b, miR-200c, or miR-203. As shown in Table S2 and Table S3, EZH2-repressed miRNAs targeted many predicted genes. When we analyzed the miRNA-regulated genes using Molecular Concepts Maps (MCM) (Tomlins et al., 2007b), as expected, molecular concepts associated with these miRNAs were highly overlapping, showing a high correlation to gene sets representing multiple cancers, metastatic cancer processes, cancer survival, Polycomb Group targets, and stem cell-related genes (Figure 4G; Table S4).

In order to further examine the molecular link between PRC1 and PRC2 activities, we generated DU145 cells stably overexpressing miR-200b and miR-203 (Figure S5A) and monitored levels of BMI1 and RING2. BMI1 and RING2 were decreased in miR-200b stable cells while only BMI1 was decreased in miR-203 stable cells. In addition, uH2A, the histone modification mediated by PRC1, was similarly decreased in both miR-200b-

and miR-203-expressing cells. Interestingly, BMI1, RING2, and uH2A, as well as EZH2 and H3K27me3, were decreased in miR-101 stable expressing DU145 cells (Figure 5A) suggesting that prolonged knockdown of PRC2 components leads to suppression of PRC1. Using cell count and Boyden chamber invasion assays, we found that similar to miR-101, miR-200b and miR-203 stably expressing cells grew more slowly and were less invasive than vector-transfected cells (Figures 5B and 5C). Intriguingly, coexpression of BMI1 or EZH2 (control) without the 3' UTR both restored the proliferation and invasion properties of DU145 cells despite the presence of miR-101, miR-200b, or miR-203 (Figures 5B and 5C). Importantly, murine xenograft experiments demonstrated that DU145 cells with stable knockdown of PRC1 proteins BMI1 or RING2 (Figure S5B), or expressing miR-181b (Figure S5C), miR-200b, or miR-203 grew more slowly than the vector control in vivo ($p = 0.0001$, Figures 5D and 5E).

EZH2-Regulated miRNAs Inversely Correlate with PRC Protein Levels in Prostate Cancer

Since miR-101, miR-181a, miR-181b, miR-200a, miR-200b, miR-200c, and miR-203 appear to play an important role in cancer progression, we next measured the endogenous expression levels of these miRNAs by qPCR analysis of a cohort of benign prostate, localized, and metastatic prostate cancers in which we had measured miR-101, miR-217, and EZH2 levels previously (Varambally et al., 2008). As expected, miR-181a, miR-181b, miR-200a, miR-200b, miR-200c, and miR-203 levels were lowest in metastatic prostate cancer tissues, and highest in benign prostate tissues (Figure 6A). In addition, immunoblot analyses showed that BMI1, RING2, and uH2A, as well as EZH2, but not RING1, were increased in metastatic prostate cancer compared with benign tissues and localized cancer samples (Figure 6B; Figure S6A). EZH2 levels were highly correlated with BMI1, RING2, and H2A protein levels (Figure S6B), further supporting a molecular link between PRC1 and PRC2 expression and activities during cancer progression. As expected, ChIP assays showed that H3K27me3-marked chromatin occupied the miR-203 upstream region in metastatic prostate cancer, but not in localized prostate cancer (PCA) (Figure S6C). Similarly, DNA methylation of the miR-203 genomic region was observed in localized and metastatic prostate cancer but not benign prostate tissue (Figure 6C). Taken together, these data suggest that EZH2-mediated epigenetic repression of miR-181a, miR-181b, miR-200b, miR-200c, and miR-203 results in an upregulation of PRC1 proteins BMI1 and RING2 and histone code ubiquityl-H2A in advanced prostate cancer.

DISCUSSION

This study unravels the intricacies in the regulation of the polycomb protein complexes mediated by various miRNAs, and substantiates the essential role played by PRC in cancer. We demonstrated that increased PRC2 activity results in repression of numerous miRNAs that are known to be important in the

for concepts related to cancer (yellow), cancer survival (red), stem cell likeness (blue), and function of polycomb group (green). All bar graphs are shown with \pm SEM.

See also Figure S4, and Table S2, Table S3, and Table S4.

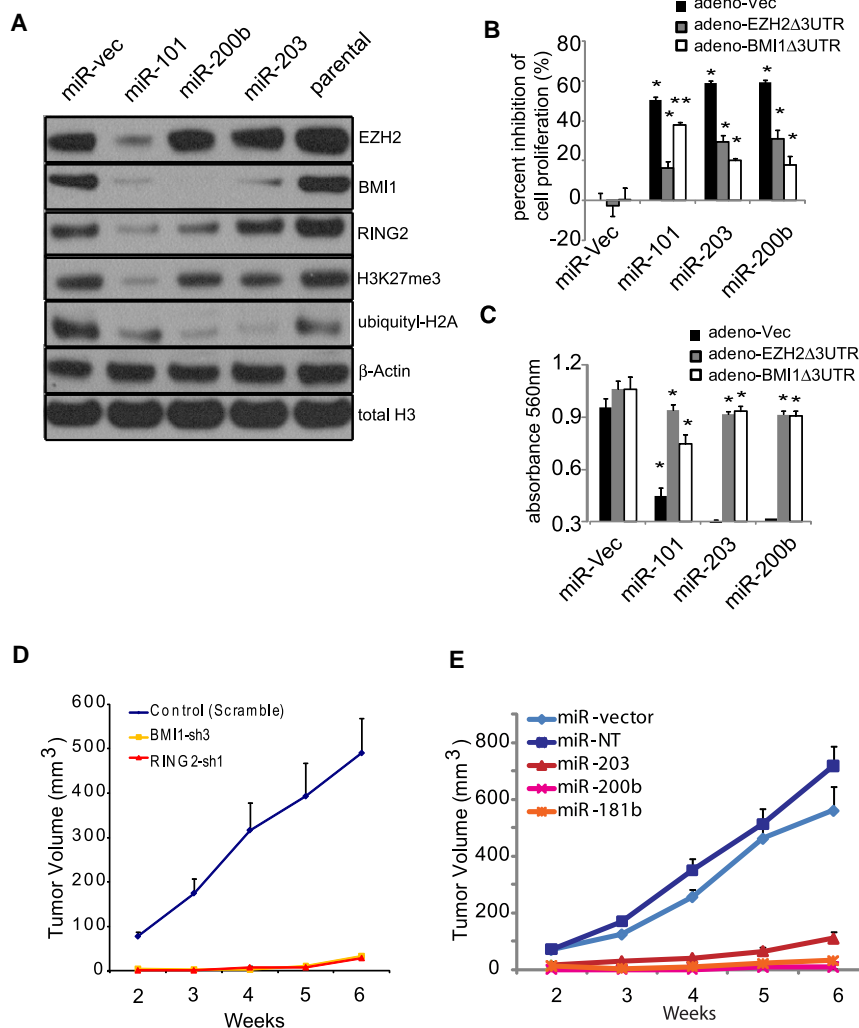


Figure 5. PRC2-Repressed miRNAs Inhibit Tumor Growth

(A) DU145 cells stably overexpressing miR-101, miR-200b, and miR-203 demonstrated repression of EZH2, BMI1, or RING2, as well as decreased H3K27me3 and ubiquitinyl-H2A (uH2A) levels.

(B and C) Coexpression of EZH2Δ3'UTR or BMI1Δ3'UTR rescued cell proliferation (B), and invasiveness (C) of DU145 cells stably overexpressing miR-101, miR-203, or miR-200b.

(D) Stably knocking down BMI1 or RING2 by BMI1-specific shRNA (BMI1-sh3) or RING2-specific shRNA (RING2-sh1) decreased DU145 tumor growth in mice. N = 8 for DU145 control (scramble), BMI1-sh3, and RING2-sh1, respectively, were used for the xenograft.

(E) Stable overexpression of miR-181b, miR-200b, or miR-203 decreased DU145 tumor growth in mice. DU145 miR-vector (N = 9), miR-NT (non-targeting) (N = 8), miR-181b (N = 8), miR-200b (N = 8), or miR-203 (N = 7) were used for the xenograft experiment. DU145 stable pools were injected subcutaneously.

All bar graphs are shown with ± SEM. See also Figure S5.

maintenance of stem cell-like phenotypes in cancer cells. We show that PRC2 epigenetically represses miR-181a, miR-181b, miR-200b, miR-200c, and miR-203 expression by facilitating H3K27me3 trimethylation at these loci, and that exogenous overexpression of miR-181a, miR-181b, miR-200b, miR-200c, and miR-203 inhibits a cancer phenotype in vitro. Furthermore, miR-181b, miR-200b, and miR-203 overexpression suppressed prostate tumor formation and growth in mouse xenografts. Recently, several groups have also reported roles for miR-200b, miR-200c, and miR-203 in controlling stem cell differentiation (Yi et al., 2008), epithelial-to-mesenchymal transition (EMT) (Park et al., 2008; Wellner et al., 2009), and cancer progression (Faber et al., 2008; Shimono et al., 2009).

Here, we demonstrated that PRC1 proteins BMI1 and RING2 are direct targets of miR-181a, miR-181b, miR-200b, miR-200c, and miR-203 in breast and prostate cancer. Furthermore, we observed a significant negative correlation between PRC2 expression and miR-181a, miR-181b, miR-200b, miR-200c, and miR-203, as well as a strong positive correlation between EZH2, BMI1, and RING2 protein levels. Intriguingly, earlier studies suggested a discrepancy between BMI1 protein and

miR-203 function as tumor suppressors during prostate cancer progression.

Interestingly, several recent studies have reported similar microRNA-protein regulatory networks that play critical roles in cancer. In one study, the *RAS* proto-oncogene was shown to be coordinately regulated by the *let-7* family of miRs (Johnson et al., 2005). Likewise, the miR-15a-miR-16-1 cluster, located on chr13q14, was proposed to serve as a tumor suppressor in prostate tissue by regulating levels of cancer-related genes such as *BCL2*, *CCND1*, and *WNT3A* (Bonci et al., 2008). Recently, Poliseno et al. (2010) reported a proto-oncogenic miRNA-dependent network in prostate cancer progression in which the miR-106b~25 cluster regulates *PTEN* expression and cooperates with *MCM7* in cellular transformation. These studies, along with our present study, strongly suggest that dysregulation of miRNA and target protein networks may contribute to cancer development.

Here, we propose a model for a coordinated PRC2-PRC1 oncoprotein axis, and epigenetic link between H3K27me3 and ubiquitinyl-H2A, mediated by PRC2-regulated miRNAs (Figure 7). Recently, Iliopoulos et al. (2010) reported that miR-200b

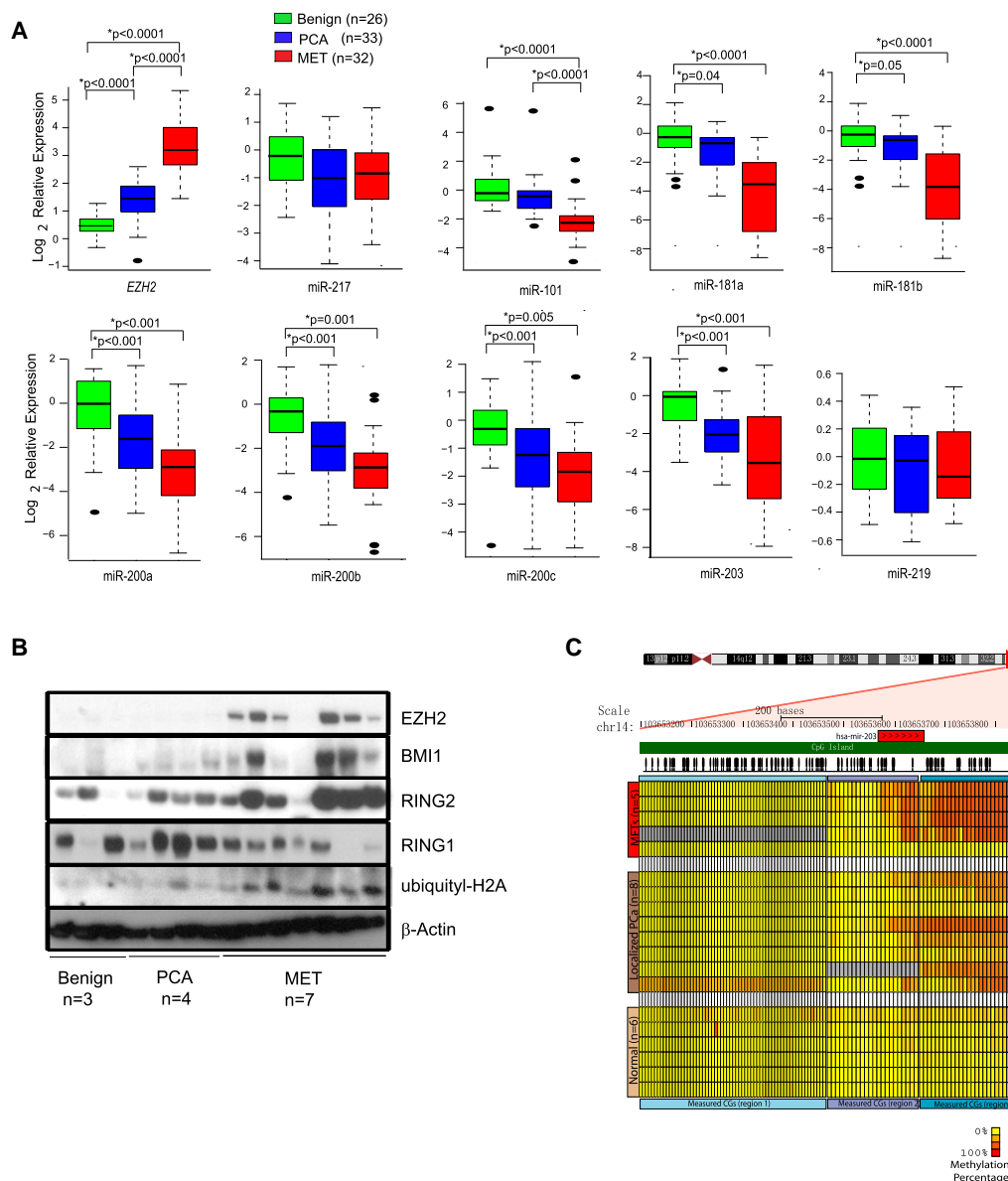


Figure 6. Coordinated Expression of PcG Proteins and PRC Regulatory miRNAs in Prostate Cancer Progression

(A) Expression of indicated miRs as assessed by q-PCR in benign prostate, clinically localized prostate cancer and metastatic prostate cancer tissues. Data for EZH2, miR-217, and miR-101 were reported previously ([Varambally et al., 2008](#)) and displayed here for comparison (Student's t test).

(B) Bisulfite sequencing analysis of the miR-203 genomic region revealed cancer-specific DNA methylation in a region proximal to miR-203 in prostate cancer tissues.

All bar graphs are shown with \pm SEM. See also [Figure S6](#).

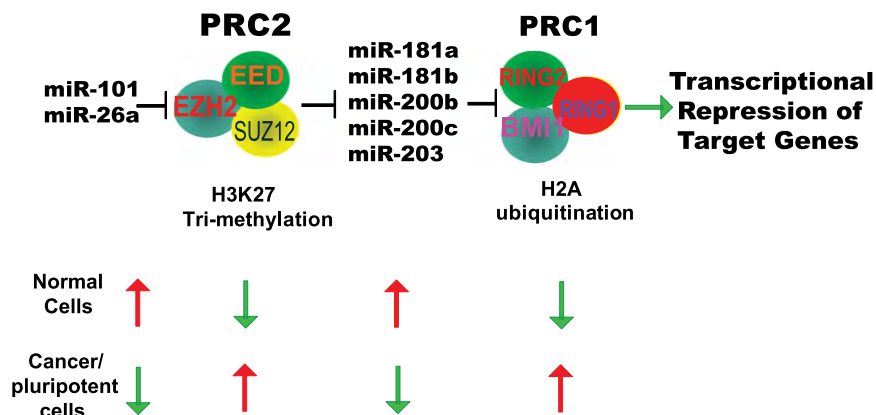
regulates PRC2 protein SUZ12 in a manner similar to that of miR-101, lending further support for microRNA-mediated PRC activity during cancer progression. These findings offer multiple targets for therapeutic interventions in the treatment of aggressive cancers (Garzon et al., 2010).

EXPERIMENTAL PROCEDURES

Cell Lines

Breast cancer cell line BT-549 was grown in RPMI 1640 (Invitrogen, Carlsbad, CA) with 0.023 IU/ml insulin and 10% FBS (Invitrogen) in 5% CO₂ cell culture

incubator; breast cancer cell line SKBR3 was grown in RPMI 1640 (Invitrogen) with 10% FBS (Invitrogen) in 5% CO₂ cell culture incubator; and prostate cancer cell line DU145 was grown in MEM with 10% FBS in 5% CO₂ cell culture incubator. Immortalized breast cell lines HME and H16N2 were grown in F-12 Nutrient Mixture with 5 µg/ml Insulin (Sigma, St. Louis, MO), 1 µg/ml Hydrocortisone (Sigma), 10 ng/ml EGF (Invitrogen), 5 mM Ethanolamine (Sigma), 5 µg/ml Transferrin (Sigma), 10 nM Triiodo Thyronine (Sigma), 50 nM Sodium Selenite (Sigma), 10 mM HEPES (Invitrogen) and 50 unit/ml Penstrep (Invitrogen), 10% CO₂. The PREC (Lonza, Conshohocken, PA) and RWPE (ATCC, Manassas, VA) cells were grown in their respective medium as specified by the suppliers. miR-181b, miR-200b, and miR-203 overexpression constructs were obtained from Openbiosystems (Huntsville, AL).



Lentiviruses were generated by the University of Michigan Vector Core. BMI1, RING2 and control shRNA lentivirus were obtained from Sigma. Prostate cancer cell line DU145 was infected with lentiviruses expressing BMI1 shRNA, RING2 shRNA, miR-181b, miR-200b, and miR-203 or controls only, and stable cell lines were generated by selection with 300 µg/ml puromycin (Invitrogen).

Benign and Tumor Tissues

In this study, we utilized tissues from clinically localized prostate cancer patients who underwent radical prostatectomy as a primary therapy between 2004 and 2006 at the University of Michigan Hospital. Samples were also used from androgen-independent metastatic prostate cancer patients from a rapid autopsy program described previously (Tomlins et al., 2005, 2007a). The detailed clinical and pathological data are maintained in a secure relational database. This study was approved by the Institutional Review Board at the University of Michigan Medical School. Informed consent was also obtained from all subjects through the Institutional Review Board at the University of Michigan Medical School. Both radical prostatectomy series and the rapid autopsy program are part of the University of Michigan Prostate Cancer Specialized Program of Research Excellence Tissue Core.

Illumina microRNA Profiling

Total RNA (500 ng) from each sample was labeled and hybridized on the Human v2 microRNA Expression BeadChips (Illumina, San Diego, CA) according to the manufacturers recommendations. BeadChips were scanned with the Illumina iScan Reader. Data were then average median normalized before generating differential expression values between treated and control samples.

microRNA Transfection, AntagomiR Transfection, and Small RNA Interference

Knockdown of EZH2 or Dicer was accomplished by RNA interference using siRNA duplexes (Dharmacon, Lafayette, CO) as previously described (Varmally et al., 2002). Precursors of respective microRNAs, antagomiRs and negative controls were purchased from Ambion (Austin, TX). Transfections were performed with oligofectamine (Invitrogen). EZH2 siRNA duplexes sequences, (duplex 1: GAGGTTTCAGACGAGCTGAT; duplex 2: AGACTCT GAATGCA GTTGC).

miR Reporter Luciferase Assays

The 50 bp of wild-type or mutant 3' UTR of BMI1 and RING2 containing the predicted miR-181a,b, miR-200b,c or miR-203 binding sites (as described in Figures S2C–S2F) were cloned into the pMIR-REPORT miRNA Expression Reporter Vector (Ambion). BT-549 cells were transfected with miRNAs or controls and then cotransfected with wild-type 3' UTR-luc or mutant 3' UTR-luc, as well as pRL-TK vector as internal control for luciferase activity. After 48 hours of transfection, the cells were lysed and luciferase assays were conducted using the dual luciferase assay system (Promega, Madison, WI). Each experiment was performed in triplicate. Drug Treatment.

BT-549 and DU145 cells were treated with 5 µM 5-aza-2'-deoxycytidine (5-aza-dC) for 6 days (fresh media change containing the drug was performed

Figure 7. A Proposed Model Role for microRNAs in Regulating PRCs

Specifically, PRC2 is molecularly linked to PRC1 via a set of regulatory miRs.

every other day) and/or 1 µM suberoylanilide hydroxamic acid (SAHA) for 2 days. DU145 cells were treated with 2.5 or 5 µM deazaneplanocin A (DZNep) for 2 or 3 days followed by RNA extraction or chromatin immunoprecipitation.

Cell Proliferation Assay and Basement Membrane Matrix Invasion Assays

Invasive breast cancer cell BT-549 and prostate cancer cell DU145 were transfected with miRNAs or controls. The cell proliferation and invasion

assays were performed as described (Cao et al., 2008; Kleer et al., 2003; Varmally et al., 2008; Yu et al., 2007b).

Soft Agar Colony Formation Assays

A 50 µl base layer of agar (0.6% Agar in DMEM with 10% FBS) was allowed to solidify in a 96-well flat-bottom plate prior to the addition of a 75 µl miRNAs or control-transfected or stable DU145 cell suspension containing 4000 cells in 0.4% Agar in DMEM with 10% FBS. The cell containing layer was then solidified at 4°C for 15 min prior to the addition of 100 µl of MEM with 5% FBS. Colonies were allowed to grow for 21 days followed by counting and imaging under a light microscope.

Spheres Culture

Spheres culture was performed as described (Dontu et al., 2003; Yu et al., 2007a). Briefly, cells (1000 cells/ml) were cultured in suspension in serum-free DMEM-F12 (Invitrogen), supplemented with B27 (1:50, Invitrogen), 20 ng/ml EGF (BD Biosciences), 0.4% bovine serum albumin (Sigma), and 4 µg/ml insulin (Sigma). To propagate spheres in vitro, spheres were collected by gentle centrifugation, dissociated to single cells as described (Dontu et al., 2003; Yu et al., 2007a), and then cultured to generate prostatospheres of the next generation. Spheres larger than 50 µm were counted.

Gene Expression Profiling

Expression profiling was performed using the Agilent Whole Human Genome Oligo Microarray (Santa Clara, CA) according to the manufacturer's protocol. BT-549 and DU145 cells were transfected with miRNAs or negative control for precursor microRNA. Over- and underexpressed signatures were generated by filtering to include only features with significant differential expression (Log ratio, $p < .01$) in all hybridizations and 2-fold average over- or under-expression (Log ratio). Gene expression data are deposited into GEO (GSE26996).

Gene Set Enrichment Analysis

Molecular Concept Map (MCM) analysis was performed using gene list of putative targets to search for all concepts available in the Oncomine database as previously described (Yu et al., 2007c). Representative concepts with significant enrichment ($p < 0.001$) were displayed as a network (Figure 4G; Table S4).

Prostate Tumor Xenograft Model

All procedures involving mice were approved by the University Committee on Use and Care of Animals (UCUCA) at the University of Michigan and conform to their relevant regulatory standards. Five-week-old male nude athymic BALB/c nu/nu mice (Charles River Laboratory, Wilmington, MA) were used for examining tumorigenicity. To evaluate the role of BMI1 and RING2 knockdown, or miR-181b, miR-200b, and miR-203 overexpression in tumor formation, the DU145 stably overexpressing BMI1 shRNA, RING2 shRNA, scramble shRNA, miR-181b, miR-200b, miR-203, nontargeting miR or vector control cells were propagated and 5×10^6 cells were inoculated subcutaneously into the dorsal flank of mice ($n = 7$ for miR-203, $n = 9$ for vector control, and $n = 8$ for Scramble, BMI1-sh3, RING2-sh1, miR-181b, miR-200b, and miR-NT,

respectively). Tumor size was measured every week, and tumor volumes were estimated using the formula $(\pi/6)(L \times W^2)$, where L = length of tumor and W = width.

Bisulfite Modification and Methylation-Specific PCR of miR-203 in Prostate Tissues

Bisulfite conversion was carried out using EZ DNA methylation gold kit (Zymo Research Corporation, Orange, CA) according to manufacturer's instructions. Purified DNA (2 μ l) was used as template for PCRs with primers (Integrated DNA Technologies Inc., San Diego, CA) and synthesized according to bisulfite converted DNA sequences for the regions of interest using the Meth-primer software (Li and Dahiya, 2002). The PCR product was gel purified and cloned into pCR4 TOPO TA sequencing vector (Invitrogen, Carlsbad, CA). Plasmid DNA isolated from ten colonies from each sample was sequenced by conventional Sanger Sequencing (University of Michigan DNA Sequencing Core). The "BIQ Analyzer" (Bock et al., 2005) online tool was used to calculate the methylation percentage and to generate the bar graphs.

ACCESSION NUMBERS

Coordinates have been deposited in Gene Expression Omnibus database with accession code GSE26996.

SUPPLEMENTAL INFORMATION

Supplemental Information includes six figures, four tables, and Supplemental Experimental Procedures and can be found with this article online at doi:10.1016/j.ccr.2011.06.016.

ACKNOWLEDGMENTS

We thank Xia Jiang, Javed Siddiqui, Wei Yan, Bo Han, Khalid Suleman, Rohit Mehra, Rupal Shastri, and Joy E. Tsai for technical assistance, Victor E. Marquez for providing DZNep, Michigan Center for hES Cell Research for H7 RNA and qPCR, the University of Michigan Vector Core for generating adenovirus and lentivirus, Kenneth J. Pienta, Xiaosong Wang, and Shanker Kalyana-Sundaram for discussions, and Jyoti Athanikar and Karen Giles for critically reading the manuscript and submission documents. This work is supported in part by the Early Detection Research Network UO1 CA111275, Prostate SPORE P50CA69568 and P50CA090386, and National Institutes of Health (R01CA132874, R01CA157845). A.M.C. is supported by the Doris Duke Charitable Foundation Clinical Scientist Award, Burroughs Wellcome Foundation Award in Clinical Translational Research, the Prostate Cancer Foundation (PCF) and the Howard Hughes Medical Institute. A.M.C. is an American Cancer Society Research Professor. Q.C., J.R.P., and J.C.B. are supported by U.S. Department of Defense (PC094725 to Q.C.; PC094290 to J.R.P.; BC083217 to J.C.B.); R.-S.M., S.A.T., and C.A.M. are supported by Young Investigator Awards from the PCF; B.A. is supported by the Genentech Foundation Postdoctoral Fellowship and Young Investigator Award from the Expedition Inspiration Fund for Breast Cancer Research. N.P. is supported by the University of Michigan Prostate Cancer SPORE Career Development award. Z.Q. is supported by National Institutes of Health (7R01HG005119-02). J.Y. is supported by U.S. Department of Defense (PC080665) and National Institutes of Health (5R00CA129565); S.V. is supported by National Institutes of Health (R01CA157845) and Prostate Cancer SPORE Career Development award. Q.C. and A.M.C. designed the experiments. Q.C., R.-S.M., B.A., S.M.D., I.A.A., J.R.P., J.H.K., J.C.B., X.J., X.C., R.W., Y.L., A.D., L.W., M.P., Y.-M.W., S.A.T., N.P., J.Y., and S.V. performed the experimental work. R.J.L., Z.Q., and C.A.M. performed statistical analysis on miRNA and gene expression data. Q.C. and A.M.C. wrote the paper. All authors discussed the results and commented on the manuscript.

Received: January 31, 2011

Revised: May 18, 2011

Accepted: June 17, 2011

Published: August 15, 2011

REFERENCES

- Bock, C., Reither, S., Mikeska, T., Paulsen, M., Walter, J., and Lengauer, T. (2005). BiQ Analyzer: visualization and quality control for DNA methylation data from bisulfite sequencing. *Bioinformatics* 21, 4067–4068.
- Bonci, D., Coppola, V., Musumeci, M., Addario, A., Giuffrida, R., Memeo, L., D'Urso, L., Pagliuca, A., Biffoni, M., Labbaye, C., et al. (2008). The miR-15a-miR-16-1 cluster controls prostate cancer by targeting multiple oncogenic activities. *Nat. Med.* 14, 1271–1277.
- Bracken, A.P., and Helin, K. (2009). Polycomb group proteins: navigators of lineage pathways led astray in cancer. *Nature Rev.* 9, 773–784.
- Bracken, A.P., Pasini, D., Capra, M., Prosperini, E., Colli, E., and Helin, K. (2003). EZH2 is downstream of the pRB-E2F pathway, essential for proliferation and amplified in cancer. *EMBO J.* 22, 5323–5335.
- Cao, R., Wang, L., Wang, H., Xia, L., Erdjument-Bromage, H., Tempst, P., Jones, R.S., and Zhang, Y. (2002). Role of histone H3 lysine 27 methylation in Polycomb-group silencing. *Science* 298, 1039–1043.
- Cao, R., Tsukada, Y., and Zhang, Y. (2005). Role of Bmi-1 and Ring1A in H2A ubiquitylation and Hox gene silencing. *Mol. Cell* 20, 845–854.
- Cao, Q., Yu, J., Dhanasekaran, S.M., Kim, J.H., Mani, R.S., Tomlins, S.A., Mehra, R., Laxman, B., Cao, X., Yu, J., et al. (2008). Repression of E-cadherin by the polycomb group protein EZH2 in cancer. *Oncogene* 27, 7274–7284.
- Cao, P., Deng, Z., Wan, M., Huang, W., Cramer, S.D., Xu, J., Lei, M., and Sui, G. (2010). MicroRNA-101 negatively regulates Ezh2 and its expression is modulated by androgen receptor and HIF-1alpha/HIF-1beta. *Mol. Cancer* 9, 108.
- Chen, H., Tu, S.W., and Hsieh, J.T. (2005). Down-regulation of human DAB2IP gene expression mediated by polycomb Ezh2 complex and histone deacetylase in prostate cancer. *J. Biol. Chem.* 280, 22437–22444.
- Chiang, C.W., Huang, Y., Leong, K.W., Chen, L.C., Chen, H.C., Chen, S.J., and Chou, C.K. (2010). PKCalpha mediated induction of miR-101 in human hepatoma HepG2 cells. *J. Biomed. Sci.* 17, 35.
- Dontu, G., Abdallah, W.M., Foley, J.M., Jackson, K.W., Clarke, M.F., Kawamura, M.J., and Wicha, M.S. (2003). In vitro propagation and transcriptional profiling of human mammary stem/progenitor cells. *Genes Dev.* 17, 1253–1270.
- Ezhkova, E., Pasolli, H.A., Parker, J.S., Stokes, N., Su, I.H., Hannon, G., Tarakhovskiy, A., and Fuchs, E. (2009). Ezh2 orchestrates gene expression for the stepwise differentiation of tissue-specific stem cells. *Cell* 136, 1122–1135.
- Faber, J., Gregory, R.I., and Armstrong, S.A. (2008). Linking miRNA regulation to BCR-ABL expression: the next dimension. *Cancer Cell* 13, 467–469.
- Fasano, C.A., Dimos, J.T., Ivanova, N.B., Lowry, N., Lemischka, I.R., and Temple, S. (2007). shRNA knockdown of Bmi-1 reveals a critical role for p21-Rb pathway in NSC self-renewal during development. *Cell Stem Cell* 1, 87–99.
- Friedman, J.M., Liang, G., Liu, C.C., Wolff, E.M., Tsai, Y.C., Ye, W., Zhou, X., and Jones, P.A. (2009). The putative tumor suppressor microRNA-101 modulates the cancer epigenome by repressing the polycomb group protein EZH2. *Cancer Res.* 69, 2623–2629.
- Fujii, S., Ito, K., Ito, Y., and Ochiai, A. (2008). Enhancer of zeste homologue 2 (EZH2) down-regulates RUNX3 by increasing histone H3 methylation. *J. Biol. Chem.* 283, 17324–17332.
- Galmozzi, E., Facchetti, F., and La Porta, C.A. (2006). Cancer stem cells and therapeutic perspectives. *Curr. Med. Chem.* 13, 603–607.
- Garzon, R., Marcucci, G., and Croce, C.M. (2010). Targeting microRNAs in cancer: rationale, strategies and challenges. *Nat. Rev. Drug Discov.* 9, 775–789.
- Glinsky, G.V., Berezovska, O., and Glinskii, A.B. (2005). Microarray analysis identifies a death-from-cancer signature predicting therapy failure in patients with multiple types of cancer. *J. Clin. Invest.* 115, 1503–1521.
- Gupta, R.A., Shah, N., Wang, K.C., Kim, J., Horlings, H.M., Wong, D.J., Tsai, M.C., Hung, T., Argani, P., Rinn, J.L., et al. (2010). Long non-coding RNA

- HOTAIR reprograms chromatin state to promote cancer metastasis. *Nature* 464, 1071–1076.
- Hurt, E.M., Kawasaki, B.T., Klarmann, G.J., Thomas, S.B., and Farrar, W.L. (2008). CD44+ CD24(-) prostate cells are early cancer progenitor/stem cells that provide a model for patients with poor prognosis. *Br. J. Cancer* 98, 756–765.
- Iliopoulos, D., Lindahl-Allen, M., Polytharchou, C., Hirsch, H.A., Tschlis, P.N., and Struhl, K. (2010). Loss of miR-200 inhibition of Suz12 leads to polycomb-mediated repression required for the formation and maintenance of cancer stem cells. *Mol. Cell* 39, 761–772.
- Jacobs, J.J., Kieboom, K., Marino, S., DePinho, R.A., and van Lohuizen, M. (1999a). The oncogene and Polycomb-group gene *bmi-1* regulates cell proliferation and senescence through the *ink4a* locus. *Nature* 397, 164–168.
- Jacobs, J.J., Scheijen, B., Voncken, J.W., Kieboom, K., Berns, A., and van Lohuizen, M. (1999b). *Bmi-1* collaborates with *c-Myc* in tumorigenesis by inhibiting *c-Myc*-induced apoptosis via *INK4a/ARF*. *Genes Dev.* 13, 2678–2690.
- Johnson, S.M., Grosshans, H., Shingara, J., Byrom, M., Jarvis, R., Cheng, A., Labourier, E., Reinert, K.L., Brown, D., and Slack, F.J. (2005). RAS is regulated by the *let-7* microRNA family. *Cell* 120, 635–647.
- Kaneko, S., Li, G., Son, J., Xu, C.F., Margueron, R., Neubert, T.A., and Reinberg, D. (2010). Phosphorylation of the PRC2 component *Ezh2* is cell cycle-regulated and up-regulates its binding to ncRNA. *Genes Dev.* 24, 2615–2620.
- Kleer, C.G., Cao, Q., Varambally, S., Shen, R., Ota, I., Tomlins, S.A., Ghosh, D., Sewalt, R.G., Otte, A.P., Hayes, D.F., et al. (2003). *EZH2* is a marker of aggressive breast cancer and promotes neoplastic transformation of breast epithelial cells. *Proc. Natl. Acad. Sci. USA* 100, 11606–11611.
- Krützfeldt, J., Rajewsky, N., Braich, R., Rajeev, K.G., Tuschl, T., Manoharan, M., and Stoffel, M. (2005). Silencing of microRNAs in vivo with “antagomirs”. *Nature* 438, 685–689.
- Lawson, D.A., Xin, L., Lukacs, R.U., Cheng, D., and Witte, O.N. (2007). Isolation and functional characterization of murine prostate stem cells. *Proc. Natl. Acad. Sci. USA* 104, 181–186.
- Li, L.C., and Dahiya, R. (2002). MethPrimer: designing primers for methylation PCRs. *Bioinformatics* 18, 1427–1431.
- Lu, J., He, M.L., Wang, L., Chen, Y., Liu, X., Dong, Q., Chen, Y.C., Peng, Y., Yao, K.T., Kung, H.F., and Li, X.P. (2011). *miR-26a* inhibits cell growth and tumorigenesis of nasopharyngeal carcinoma through repression of *EZH2*. *Cancer Res.* 71, 225–233.
- Lukacs, R.U., Memarzadeh, S., Wu, H., and Witte, O.N. (2010). *Bmi-1* is a crucial regulator of prostate stem cell self-renewal and malignant transformation. *Cell Stem Cell* 7, 682–693.
- Margueron, R., and Reinberg, D. (2011). The Polycomb complex PRC2 and its mark in life. *Nature* 469, 343–349.
- Matsukawa, Y., Semba, S., Kato, H., Ito, A., Yanagihara, K., and Yokozaki, H. (2006). Expression of the enhancer of zeste homolog 2 is correlated with poor prognosis in human gastric cancer. *Cancer Sci.* 97, 484–491.
- Min, J., Zaslavsky, A., Fedele, G., McLaughlin, S.K., Reczek, E.E., De Raedt, T., Guney, I., Strohlich, D.E., Macconail, L.E., Beroukhim, R., et al. (2010). An oncogene-tumor suppressor cascade drives metastatic prostate cancer by coordinately activating Ras and nuclear factor- κ B. *Nat. Med.* 16, 286–294.
- Palanisamy, N., Ateeq, B., Kalyana-Sundaram, S., Pflueger, D., Ramnarayanan, K., Shankar, S., Han, B., Cao, Q., Cao, X., Suleman, K., et al. (2010). Rearrangements of the RAF kinase pathway in prostate cancer, gastric cancer and melanoma. *Nat. Med.* 16, 793–798.
- Park, S.M., Gaur, A.B., Lengyel, E., and Peter, M.E. (2008). The *miR-200* family determines the epithelial phenotype of cancer cells by targeting the *E-cadherin* repressors *ZEB1* and *ZEB2*. *Genes Dev.* 22, 894–907.
- Pereira, C.F., Piccolo, F.M., Tsubouchi, T., Sauer, S., Ryan, N.K., Bruno, L., Landeira, D., Santos, J., Banito, A., Gil, J., et al. (2010). ESCs require PRC2 to direct the successful reprogramming of differentiated cells toward pluripotency. *Cell Stem Cell* 6, 547–556.
- Pietersen, A.M., Evers, B., Prasad, A.A., Tanger, E., Cornelissen-Steijger, P., Jonkers, J., and van Lohuizen, M. (2008). *Bmi1* regulates stem cells and proliferation and differentiation of committed cells in mammary epithelium. *Curr. Biol.* 18, 1094–1099.
- Poliseno, L., Salmena, L., Riccardi, L., Fornari, A., Song, M.S., Hobbs, R.M., Sportoletti, P., Varmeh, S., Egia, A., Fedele, G., et al. (2010). Identification of the *miR-106b~25* microRNA cluster as a proto-oncogenic *PTEN*-targeting intron that cooperates with its host gene *MCM7* in transformation. *Sci. Signal.* 3, ra29.
- Rinn, J.L., Kertesz, M., Wang, J.K., Squazzo, S.L., Xu, X., Bruggmann, S.A., Goodnough, L.H., Helms, J.A., Farnham, P.J., Segal, E., and Chang, H.Y. (2007). Functional demarcation of active and silent chromatin domains in human *HOX* loci by noncoding RNAs. *Cell* 129, 1311–1323.
- Sánchez-Beato, M., Sánchez, E., González-Carrero, J., Morente, M., Díez, A., Sánchez-Verde, L., Martín, M.C., Cigudosa, J.C., Vidal, M., and Piris, M.A. (2006). Variability in the expression of polycomb proteins in different normal and tumoral tissues. A pilot study using tissue microarrays. *Mod. Pathol.* 19, 684–694.
- Shimono, Y., Zabala, M., Cho, R.W., Lobo, N., Dalerba, P., Qian, D., Diehn, M., Liu, H., Panula, S.P., Chiao, E., et al. (2009). Downregulation of *miRNA-200c* links breast cancer stem cells with normal stem cells. *Cell* 138, 592–603.
- Sudo, T., Utsunomiya, T., Mimori, K., Nagahara, H., Ogawa, K., Inoue, H., Wakiyama, S., Fujita, H., Shirouzu, K., and Mori, M. (2005). Clinicopathological significance of *EZH2* mRNA expression in patients with hepatocellular carcinoma. *Br. J. Cancer* 92, 1754–1758.
- Surface, L.E., Thornton, S.R., and Boyer, L.A. (2010). Polycomb group proteins set the stage for early lineage commitment. *Cell Stem Cell* 7, 288–298.
- Tan, J., Yang, X., Zhuang, L., Jiang, X., Chen, W., Lee, P.L., Karuturi, R.K., Tan, P.B., Liu, E.T., and Yu, Q. (2007). Pharmacologic disruption of Polycomb-repressive complex 2-mediated gene repression selectively induces apoptosis in cancer cells. *Genes Dev.* 21, 1050–1063.
- Tomlins, S.A., Rhodes, D.R., Perner, S., Dhanasekaran, S.M., Mehra, R., Sun, X.W., Varambally, S., Cao, X., Tchinda, J., Kuefer, R., et al. (2005). Recurrent fusion of *TMPRSS2* and *ETS* transcription factor genes in prostate cancer. *Science* 310, 644–648.
- Tomlins, S.A., Laxman, B., Dhanasekaran, S.M., Helgeson, B.E., Cao, X., Morris, D.S., Menon, A., Jing, X., Cao, Q., Han, B., et al. (2007a). Distinct classes of chromosomal rearrangements create oncogenic *ETS* gene fusions in prostate cancer. *Nature* 448, 595–599.
- Tomlins, S.A., Mehra, R., Rhodes, D.R., Cao, X., Wang, L., Dhanasekaran, S.M., Kalyana-Sundaram, S., Wei, J.T., Rubin, M.A., Pienta, K.J., et al. (2007b). Integrative molecular concept modeling of prostate cancer progression. *Nat. Genet.* 39, 41–51.
- Valk-Lingbeek, M.E., Bruggeman, S.W., and van Lohuizen, M. (2004). Stem cells and cancer; the polycomb connection. *Cell* 118, 409–418.
- Varambally, S., Dhanasekaran, S.M., Zhou, M., Barrette, T.R., Kumar-Sinha, C., Sanda, M.G., Ghosh, D., Pienta, K.J., Sewalt, R.G., Otte, A.P., et al. (2002). The polycomb group protein *EZH2* is involved in progression of prostate cancer. *Nature* 419, 624–629.
- Varambally, S., Yu, J., Laxman, B., Rhodes, D.R., Mehra, R., Tomlins, S.A., Shah, R.B., Chandran, U., Monzon, F.A., Becich, M.J., et al. (2005). Integrative genomic and proteomic analysis of prostate cancer reveals signatures of metastatic progression. *Cancer Cell* 8, 393–406.
- Varambally, S., Cao, Q., Mani, R.S., Shankar, S., Wang, X., Ateeq, B., Laxman, B., Cao, X., Jing, X., Ramnarayanan, K., et al. (2008). Genomic loss of *microRNA-101* leads to overexpression of histone methyltransferase *EZH2* in cancer. *Science* 322, 1695–1699.
- Viré, E., Brenner, C., Deplus, R., Blanchon, L., Fraga, M., Didelot, C., Morey, L., Van Eynde, A., Bernard, D., Vanderwinden, J.M., et al. (2006). The Polycomb group protein *EZH2* directly controls DNA methylation. *Nature* 439, 871–874.
- Wang, H., Wang, L., Erdjument-Bromage, H., Vidal, M., Tempst, P., Jones, R.S., and Zhang, Y. (2004). Role of histone H2A ubiquitination in Polycomb silencing. *Nature* 431, 873–878.

Wang, H.J., Ruan, H.J., He, X.J., Ma, Y.Y., Jiang, X.T., Xia, Y.J., Ye, Z.Y., and Tao, H.Q. (2010). MicroRNA-101 is down-regulated in gastric cancer and involved in cell migration and invasion. *Eur. J. Cancer* 46, 2295–2303.

Wang, X.-S., Shanka, S., Dhanasekaran, S.M., Ateeq, B., Sasaki, A.T., Jing, X., Robinson, D., Cao, Q., Prensner, J.R., Yocum, A.K., et al. (2011). Characterization of KRAS rearrangements in metastatic prostate cancer. *Cancer Discovery* 1. Published online April 3, 2011. 10.1158/2159-8274.CD-10-0022.

Wellner, U., Schubert, J., Burk, U.C., Schmalhofer, O., Zhu, F., Sonntag, A., Waldvogel, B., Vannier, C., Darling, D., zur Hausen, A., et al. (2009). The EMT-activator ZEB1 promotes tumorigenicity by repressing stemness-inhibiting microRNAs. *Nat. Cell Biol.* 11, 1487–1495.

Wong, C.F., and Tellam, R.L. (2008). MicroRNA-26a targets the histone methyltransferase Enhancer of Zeste homolog 2 during myogenesis. *J. Biol. Chem.* 283, 9836–9843.

Yi, R., Poy, M.N., Stoffel, M., and Fuchs, E. (2008). A skin microRNA promotes differentiation by repressing “stemness”. *Nature* 452, 225–229.

Yu, F., Yao, H., Zhu, P., Zhang, X., Pan, Q., Gong, C., Huang, Y., Hu, X., Su, F., Lieberman, J., and Song, E. (2007a). let-7 regulates self renewal and tumorigenicity of breast cancer cells. *Cell* 131, 1109–1123.

Yu, J., Cao, Q., Mehra, R., Laxman, B., Yu, J., Tomlins, S.A., Creighton, C.J., Dhanasekaran, S.M., Shen, R., Chen, G., et al. (2007b). Integrative genomics analysis reveals silencing of beta-adrenergic signaling by polycomb in prostate cancer. *Cancer Cell* 12, 419–431.

Yu, J., Yu, J., Rhodes, D.R., Tomlins, S.A., Cao, X., Chen, G., Mehra, R., Wang, X., Ghosh, D., Shah, R.B., et al. (2007c). A polycomb repression signature in metastatic prostate cancer predicts cancer outcome. *Cancer Res.* 67, 10657–10663.

Yu, J., Cao, Q., Yu, J., Wu, L., Dallol, A., Li, J., Chen, G., Grasso, C., Cao, X., Lonigro, R.J., et al. (2010). The neuronal repellent SLIT2 is a target for repression by EZH2 in prostate cancer. *Oncogene* 29, 5370–5380.

Transcriptome sequencing across a prostate cancer cohort identifies *PCAT-1*, an unannotated lincRNA implicated in disease progression

John R Prensner^{1,8}, Matthew K Iyer^{1,8}, O Alejandro Balbin¹, Saravana M Dhanasekaran^{1,2}, Qi Cao¹, J Chad Brenner¹, Bharathi Laxman³, Irfan A Asangani¹, Catherine S Grasso¹, Hal D Kominsky¹, Xuhong Cao¹, Xiaojun Jing¹, Xiaoju Wang¹, Javed Siddiqui¹, John T Wei⁴, Daniel Robinson¹, Hari K Iyer⁵, Nallasivam Palanisamy^{1,2,6}, Christopher A Maher^{1,2} & Arul M Chinnaiyan^{1,2,4,6,7}

Noncoding RNAs (ncRNAs) are emerging as key molecules in human cancer, with the potential to serve as novel markers of disease and to reveal uncharacterized aspects of tumor biology. Here we discover 121 unannotated prostate cancer-associated ncRNA transcripts (PCATs) by *ab initio* assembly of high-throughput sequencing of polyA⁺ RNA (RNA-Seq) from a cohort of 102 prostate tissues and cell lines. We characterized one ncRNA, *PCAT-1*, as a prostate-specific regulator of cell proliferation and show that it is a target of the Polycomb Repressive Complex 2 (PRC2). We further found that patterns of *PCAT-1* and PRC2 expression stratified patient tissues into molecular subtypes distinguished by expression signatures of *PCAT-1*-repressed target genes. Taken together, our findings suggest that *PCAT-1* is a transcriptional repressor implicated in a subset of prostate cancer patients. These findings establish the utility of RNA-Seq to identify disease-associated ncRNAs that may improve the stratification of cancer subtypes.

Recently, RNA-Seq has provided a method to delineate the entire set of transcriptional aberrations in a disease, including novel transcripts not measured by conventional analyses^{1–5}. To facilitate interpretation of sequence read data, existing computational methods typically process individual samples using either short read gapped alignment followed by *ab initio* reconstruction^{2,3} or *de novo* assembly of read sequences followed by sequence alignment^{4,5}. These methods provide a powerful framework to uncover uncharacterized RNA species, including antisense transcripts, short RNAs <250 bp or long intergenic ncRNAs (lincRNAs) >250 bp.

Although still largely unexplored, ncRNAs, particularly lincRNAs, have emerged as a new aspect of biology, with evidence suggesting that they are frequently cell-type specific, contribute important functions to numerous systems^{6,7} and may interact with known cancer genes such as *EZH2* (ref. 8). Indeed, several well-described examples, such as *HOTAIR*^{8,9} and *ANRIL*^{10,11}, indicate that ncRNAs may be essential actors in cancer biology, typically facilitating epigenetic gene repression through chromatin-modifying complexes^{12,13}. Moreover, ncRNA expression may confer clinical information about disease outcomes and have utility as diagnostic tests^{9,14}. The characterization of RNA species, their functions and their clinical applicability is therefore a major area of biological and clinical importance.

Here, we describe a comprehensive analysis of lincRNAs in 102 prostate cancer tissue samples and cell lines by RNA-Seq. We apply

ab initio computational approaches to delineate the annotated and unannotated transcripts in this disease, and we find 121 ncRNAs, termed PCATs, whose expression patterns distinguish benign, localized cancer and metastatic cancer samples. Notably, we discover *PCAT-1*, a previously undescribed prostate cancer ncRNA that demonstrates either repression by PRC2 or an active role in promoting cell proliferation through transcriptional regulation of target genes. To our knowledge, our findings describe the first comprehensive study of lincRNAs in prostate cancer, provide a computational framework for large-scale RNA-Seq analyses and describe *PCAT-1* as a prostate cancer ncRNA functionally implicated in disease progression.

RESULTS

RNA-Seq analysis of the prostate cancer transcriptome

Over two decades of research have generated a genetic model of prostate cancer based on numerous neoplastic events, such as loss of the *PTEN*¹⁵ tumor suppressor gene and gain of oncogenic ETS family transcription factor gene fusions^{16–18} in large subsets of prostate cancer patients. As some patients lack these genetic aberrations, we hypothesized that prostate cancer similarly harbored disease-associated ncRNAs that characterized specific molecular subtypes.

To pursue this hypothesis, we applied transcriptome sequencing on a cohort of 102 prostate tissues and cell lines—20 benign adjacent prostates (benign), 47 localized prostate cancers (PCA), 14 metastatic

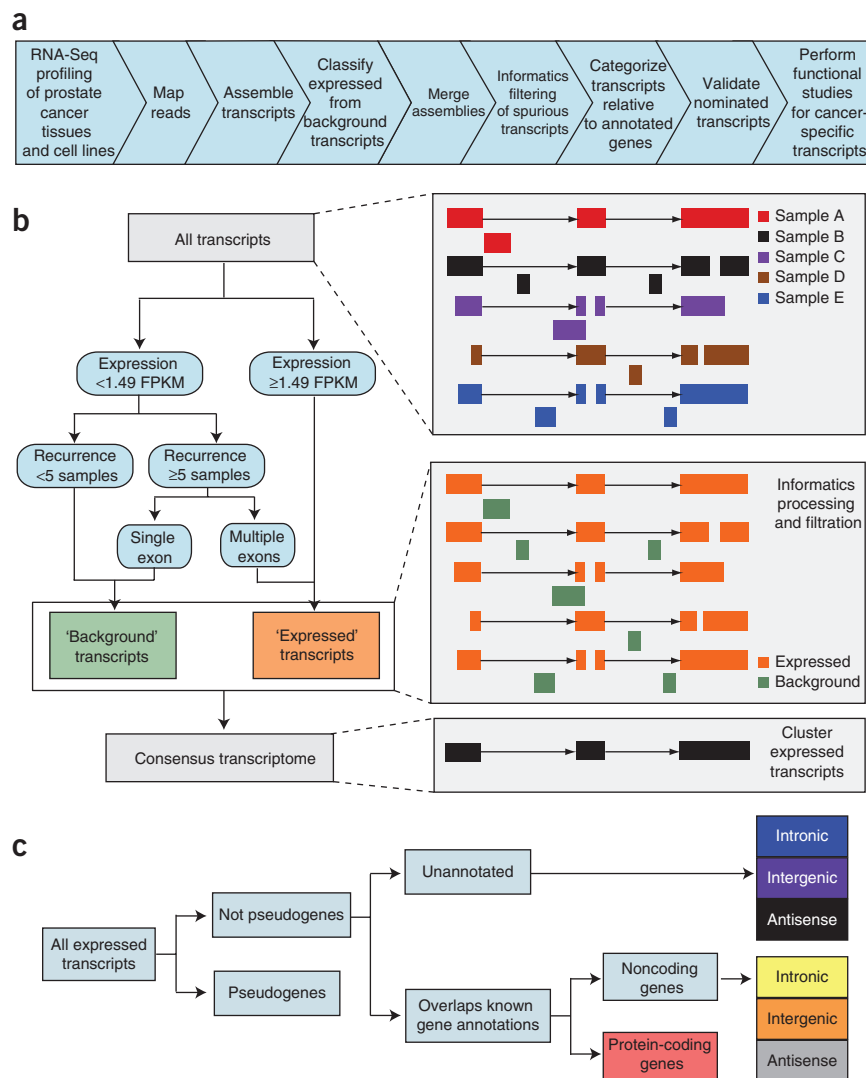
¹Michigan Center for Translational Pathology, University of Michigan Medical School, Ann Arbor, Michigan, USA. ²Department of Pathology, University of Michigan Medical School, Ann Arbor, Michigan, USA. ³Department of Medicine, University of Chicago, Chicago, Illinois, USA. ⁴Department of Urology, University of Michigan Medical School, Ann Arbor, Michigan, USA. ⁵Department of Statistics, Colorado State University, Fort Collins, Colorado, USA. ⁶Comprehensive Cancer Center, University of Michigan Medical School, Ann Arbor, Michigan, USA. ⁷Howard Hughes Medical Institute, University of Michigan Medical School, Ann Arbor, Michigan, USA. ⁸These authors contributed equally to this work. Correspondence should be addressed to A.M.C. (arul@umich.edu).

Received 11 January; accepted 10 June; published online 31 July 2011; doi:10.1038/nbt.1914



Figure 1 Analysis of transcriptome data for the detection of unannotated transcripts.

(a) Schematic overview of the methodology employed in this study. (b) Graphical representation of the bioinformatics filters used to merge individual transcriptome libraries into a single consensus transcriptome. The merged consensus transcriptome was generated by compiling all individual transcriptome libraries and using individual decision tree classifiers for each chromosome to define high-confidence 'expressed' transcripts and low-confidence 'background' transcripts, which were discarded. The example decision tree on the left was trained on transcripts on chromosome 1. The graphics on the right illustrate the application of the informatics filtration pipeline to sample assembled transcripts. (c) After informatic processing and filtration of the sequencing data, transcripts were categorized to identify unannotated ncRNAs. Transcribed pseudogenes were isolated, and the remaining transcripts were categorized based on overlap with an aggregated set of known gene annotations into annotated protein coding, noncoding and unannotated. Both annotated and unannotated ncRNA transcripts were then separated into intronic, intergenic and antisense categories based on their relationship to protein-coding genes.



tumors and 21 prostate cell lines. From a total of 1.723 billion sequence fragments from 201 lanes of sequencing (108 paired-end and 93 single reads on the Illumina Genome Analyzer and Genome Analyzer II), we performed short-read gapped alignment¹⁹ and recovered 1.41 billion mapped reads, with a median of 14.7 million mapped reads per sample (Supplementary Table 1). We used the Cufflinks *ab initio* assembly approach³ to produce, for each sample, the most probable set of putative transcripts that served as the RNA templates for the sequence fragments in that sample (Fig. 1a and Supplementary Figs. 1 and 2).

As expected from a large tumor tissue cohort, individual transcript assemblies may have sources of noise, such as artifacts of the sequence alignment process, unspliced intronic pre-mRNA and genomic DNA contamination. To exclude these from our analyses, we trained a decision tree to classify transcripts as expressed versus background on the basis of transcript length, number of exons, recurrence in multiple samples and other structural characteristics (Fig. 1b, left, and Supplementary Methods). The classifier demonstrated a sensitivity of 70.8% and specificity of 88.3% when trained using transcripts that overlapped genes in the AceView database²⁰, including 11.7% of unannotated transcripts that were classified as expressed (Fig. 1b right). We then clustered the expressed transcripts into a consensus transcriptome and applied additional heuristic filters to further refine the assembly (Supplementary Methods). The final *ab initio* transcriptome assembly yielded 35,415 distinct transcriptional loci (Supplementary Table 2 and Supplementary Methods).

Discovery of prostate cancer noncoding RNAs

We compared the assembled prostate cancer transcriptome to the UCSC, Ensembl, RefSeq, Vega and ENCODE gene databases to identify and categorize transcripts (Fig. 1c). The majority of the transcripts

(77.3%) corresponded to annotated protein coding genes (72.1%) and noncoding RNAs (5.2%), but a substantial percentage (19.8%) lacked any overlap and were designated unannotated (Fig. 2a). These included partially intronic antisense (2.44%), totally intronic (12.1%) and intergenic transcripts (5.25%), consistent with previous reports of unannotated transcription^{21–23}. Because of the added complexity of characterizing antisense or partially intronic transcripts without strand-specific RNA-Seq libraries, we focused on totally intronic and intergenic transcripts.

Global characterization of unannotated intronic and intergenic transcripts demonstrated that they were more highly expressed (Fig. 2b), had greater overlap with expressed sequence tags (ESTs) (Supplementary Fig. 3) and displayed a clear but subtle increase in conservation over randomly permuted controls (intergenic transcripts $P = 2.7 \times 10^{-4} \pm 0.0002$ for $0.4 < \omega < 0.8$; intronic transcripts $P = 2.6 \times 10^{-5} \pm 0.0017$ for $0 < \omega < 0.4$, Fisher's exact test, Fig. 2c). By contrast, unannotated transcripts scored lower than protein-coding genes for these metrics, which corroborates data in previous reports^{2,24}. Notably, a small subset of unannotated intronic transcripts showed a profound degree of conservation (Fig. 2c, inset). Finally, analysis of coding potential revealed that only 5 of 6,144 transcripts harbored a high-quality open reading frame (ORF), indicating that the vast majority of these transcripts represent ncRNAs (Supplementary Fig. 4).

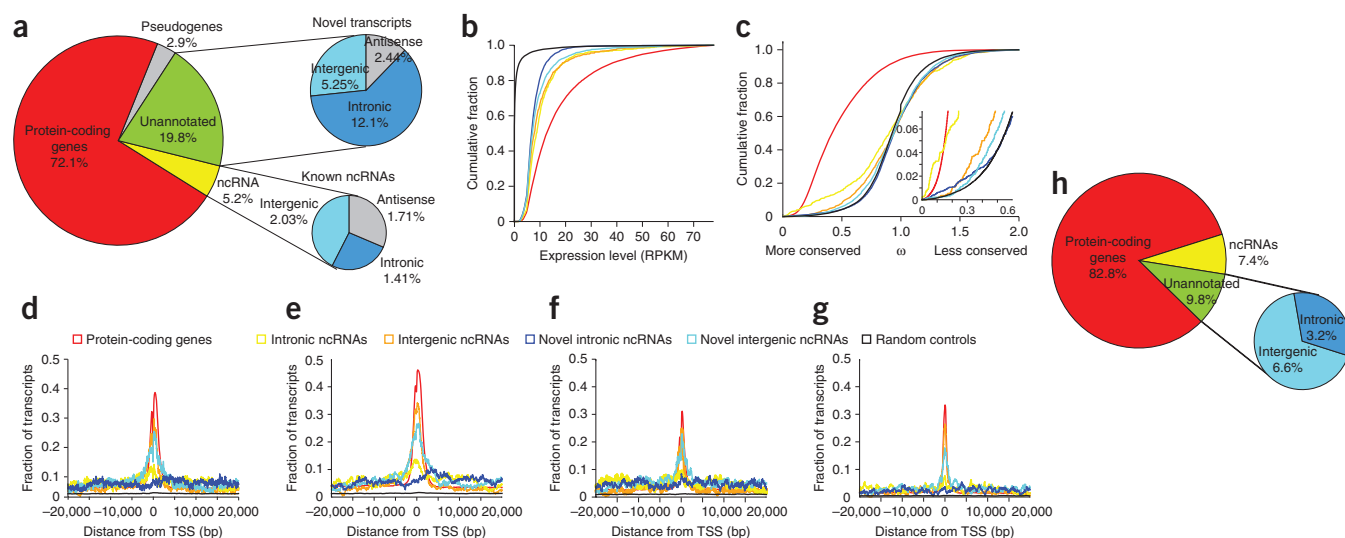


Figure 2 Prostate cancer transcriptome sequencing reveals dysregulation of unannotated transcripts. **(a)** Global overview of transcription in prostate cancer. The pie chart on the left displays transcript distribution in prostate cancer. The pie charts on the right display unannotated (upper) or annotated (lower) ncRNAs categorized as sense transcripts (intergenic and intronic) and antisense transcripts, respectively. **(b)** Line graph showing that unannotated transcripts are more highly expressed (reads per kilobase of transcript per million mapped reads; RPKM) than control regions. Negative control intervals were generated by randomly permuting the genomic positions of the transcripts. **(c)** Conservation analysis comparing unannotated transcripts to known genes and intronic controls shows a subtle degree of purifying selection among unannotated transcripts. The inset on the right shows an enlarged view. **(d–g)** Intersection plots displaying the fraction of unannotated transcripts enriched for H3K4me2 (**d**), H3K4me3 (**e**), acetyl-H3 (**f**) or RNA polymerase II (**g**) at their transcriptional start site (TSS) using ChIP-Seq and RNA-Seq data for the VCaP prostate cancer cell line. The legend applies to plots in **b–g**. **(h)** A pie chart displaying the distribution of differentially expressed transcripts in prostate cancer (FDR < 0.01).

To determine whether our unannotated transcripts were supported by histone modifications defining active transcriptional units, we used published prostate cancer chromatin immunoprecipitation (ChIP)-Seq data for two prostate cell lines²⁵, VCaP and LNCaP (Supplementary Table 3). After filtering our data set for transcribed repetitive elements known to display alternative patterns of histone modifications²⁶, we observed a strong enrichment for histone modifications characterizing transcriptional start sites (TSSs) and active transcription, including H3K4me2, H3K4me3, acetyl-H3 and RNA polymerase II (Fig. 2d–g), but not H3K4me1, which characterizes enhancer regions²⁷ (Supplementary Figs. 5 and 6). Notably, intergenic ncRNAs showed greater enrichment compared to intronic ncRNAs in these analyses (Fig. 2d–g).

To elucidate global changes in transcript abundance in prostate cancer, we analyzed differential expression for all transcripts. We found 836 genes differentially expressed between benign samples and localized tumors (false-discovery rate (FDR) < 0.01), with annotated protein-coding and ncRNA genes constituting 82.8% and 7.4% of differentially expressed genes, respectively, including known prostate cancer biomarkers such *AMACR*²⁸, *HPN*²⁹ and *PCA3* (ref. 14) (Fig. 2h, Supplementary Fig. 2 and Supplementary Table 4). Finally, 9.8% of differentially expressed genes corresponded to unannotated ncRNAs, including 3.2% within gene introns and 6.6% in intergenic regions.

Characterization of PCATs

As ncRNAs may contribute to human disease^{6–9}, we identified aberrantly expressed uncharacterized ncRNAs in prostate cancer. We found a total of 1,859 unannotated lincRNAs throughout the human genome. Overall, these intergenic RNAs resided approximately halfway between two protein coding genes (Supplementary Fig. 7), and over one-third (34.1%) were ≥ 10 kb from the nearest protein-coding

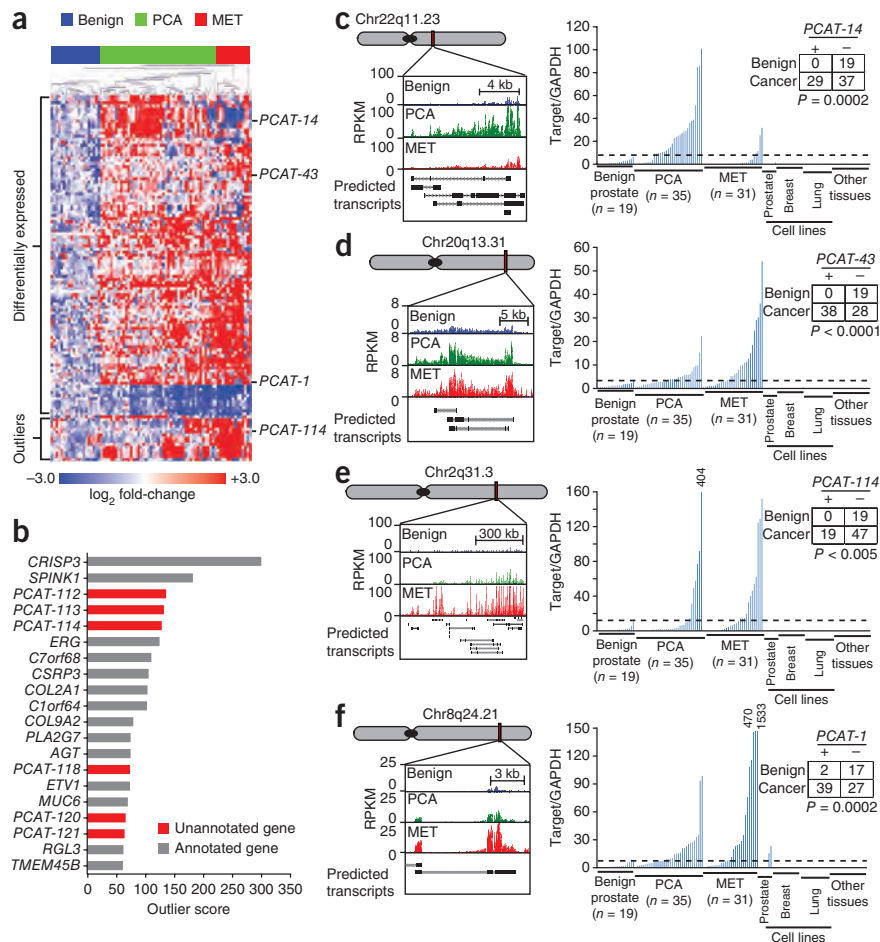
gene, which is consistent with previous reports³⁰ and supports the independence of intergenic ncRNAs genes. For example, visualizing the Chr15q arm using the Circos program (<http://circos.ca/>) illustrated genomic positions of 89 unannotated intergenic transcripts, including one differentially expressed gene centromeric to *TLE3* (Supplementary Fig. 8).

A focused analysis of the 1,859 unannotated intergenic RNAs yielded 106 that were differentially expressed in localized tumors (FDR < 0.05, Fig. 3a). A cancer outlier expression analysis (Supplementary Methods) similarly nominated numerous unannotated ncRNA outliers (Fig. 3b) as well as known prostate cancer outliers, such as *ERG*¹⁸, *ETV1* (refs. 17,18), *SPINK1* (ref. 31) and *CRISP3* (ref. 32). Merging these results produced a set of 121 unannotated transcripts that accurately discriminated benign, localized tumor and metastatic prostate samples by unsupervised clustering (Fig. 3a). Indeed, clustering analyses using unannotated ncRNA outliers also suggested disease subtypes (Supplementary Fig. 9). These 121 unannotated transcripts were ranked and named as PCATs according to their fold-change in localized tumor versus benign tissue (Supplementary Tables 5–7).

Validation of novel ncRNAs

To gain confidence in our transcript nominations, we validated multiple unannotated transcripts *in vitro* by reverse transcription PCR (RT-PCR) and quantitative real-time PCR (qPCR) (Supplementary Fig. 10). qPCR for four transcripts (*PCAT-114*, *PCAT-14*, *PCAT-43* and *PCAT-1*) on two independent cohorts of prostate tissues confirmed predicted cancer-specific expression patterns (Fig. 3c–f and Supplementary Fig. 11). Notably, all four are prostate-specific, with minimal expression seen by qPCR in breast ($n = 14$) or lung cancer ($n = 16$) cell lines or in 19 normal tissue types (Supplementary Table 8). This is further supported by expression analysis of these transcripts in

Figure 3 Unannotated intergenic transcripts differentiate prostate cancer and benign prostate samples. **(a)** Unsupervised clustering analyses of differentially expressed or outlier unannotated intergenic transcripts clusters benign samples, localized tumors and metastatic cancers. Expression is plotted as log₂ fold-change relative to the median of the benign samples. The four transcripts detailed in this study are indicated on the side. **(b)** Cancer outlier expression analysis for the prostate cancer transcriptome ranks unannotated transcripts prominently. **(c–f)** qPCR on an independent cohort of prostate and nonprostate samples (benign (*n* = 19), PCA (*n* = 35), metastatic (MET) (*n* = 31), prostate cell lines (*n* = 7), breast cell lines (*n* = 14), lung cell lines (*n* = 16), other normal samples (*n* = 19); **Supplementary Table 8**) measures expression levels of four nominated ncRNAs—*PCAT-14* (**c**), *PCAT-43* (**d**), *PCAT-114* (**e**), *PCAT-1* (**f**)—and upregulated in prostate cancer. Inset tables on the right quantify 'positive' and 'negative' expressing samples using the cut-off value (shown as a black dashed lines). Statistical significance was determined using a Fisher's exact test. qPCR analysis was performed by normalizing to *GAPDH* and the median expression of the benign samples.



our RNA-Seq compendium of 13 tumor types, representing 325 samples (**Supplementary Fig. 12**). This tissue specificity was not necessarily due to regulation by androgen receptor signaling, as only *PCAT-14* expression was induced when androgen responsive VCaP and LNCaP cells were treated with the synthetic androgen R1881, consistent with previous data from this locus¹⁷ (**Supplementary Fig. 13**). *PCAT-1* and *PCAT-14* also showed cancer-specific upregulation when tested on a panel of matched tumor-normal pair samples (**Supplementary Fig. 14**).

Of note, *PCAT-114*, which ranks as the fifth best outlier, just ahead of *ERG* (**Fig. 3b** and **Supplementary Table 7**), appears as part of a large, >500 kb locus of expression in a gene desert in Chr2q31. We termed this region 'second chromosome locus associated with prostate-1' (SchLAP1) (**Supplementary Fig. 15**). Careful analysis of the SchLAP1 locus revealed both discrete transcripts and intronic transcription, highlighting this region as an intriguing aspect of the prostate cancer transcriptome.

PCAT-1, an unannotated prostate cancer lincRNA

To explore several transcripts more closely, we carried out 5' and 3' rapid amplification of cDNA ends (RACE) for *PCAT-1* and *PCAT-14*. Interestingly, the *PCAT-14* locus contained components of viral ORFs from the HERV-K endogenous retrovirus family (**Supplementary Fig. 16**), whereas *PCAT-1* incorporates portions of a mariner family transposase^{33,34}, an *Alu* and a viral long terminal repeat promoter region (**Fig. 4a** and **Supplementary Fig. 17**). Whereas *PCAT-14* was upregulated in localized prostate cancer but largely absent in metastases (**Fig. 3c**), *PCAT-1* was strikingly upregulated in a subset of metastatic and high-grade localized (Gleason score ≥ 7) cancers (**Fig. 3f** and **Supplementary Fig. 11**). Because of this notable profile, we hypothesized that *PCAT-1* may have coordinated expression with the oncoprotein *EZH2*, a core PRC2 protein that is upregulated in solid

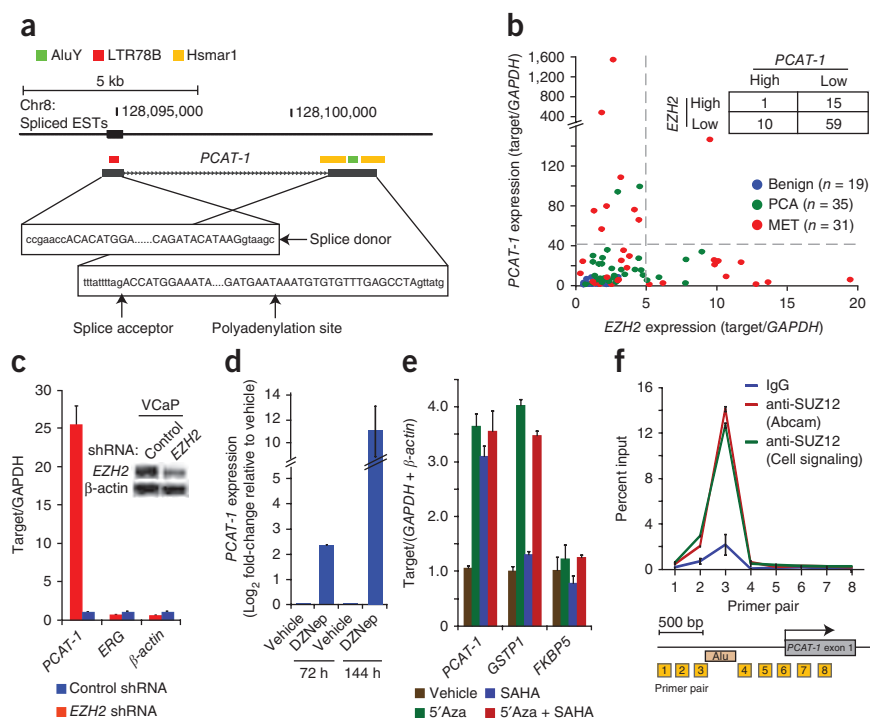
tumors and contributes to a metastatic phenotype^{35,36}. Surprisingly, we found that *PCAT-1* and *EZH2* expression were nearly mutually exclusive (**Fig. 4b**), with only one patient showing outlier expression of both. This suggests that outlier *PCAT-1* and *EZH2* expression may define two subsets of high-grade disease.

PCAT-1 is located in the chromosome 8q24 gene desert ~725 kb upstream of the *c-MYC* oncogene. To confirm that *PCAT-1* is a noncoding gene, we cloned the full-length *PCAT-1* transcript and performed *in vitro* translational assays, which were negative as expected (**Supplementary Fig. 18**). Next, because Chr8q24 is known to harbor prostate cancer-associated single nucleotide polymorphisms (SNPs) and to exhibit frequent chromosomal amplification^{37–42}, we evaluated whether the relationship between *EZH2* and *PCAT-1* was specific or generalized. To address this, we measured expression levels of *c-MYC* and *NCOA2*, two proposed targets of Chr8q amplification^{39,42}, by qPCR. Neither *c-MYC* nor *NCOA2* levels showed striking expression relationships to *PCAT-1*, *EZH2* or each other (**Supplementary Fig. 19**). Likewise, *PCAT-1* outlier expression was not dependent on Chr8q24 amplification, as highly expressing localized tumors often did not have 8q24 amplification and high copy number gain of 8q24 was not sufficient to upregulate *PCAT-1* (**Supplementary Figs. 20 and 21**).

PCAT-1 function and regulation

Despite reports showing that upregulation of the ncRNA *HOTAIR* participates in PRC2 function in breast cancer⁹, we do not observe strong expression of this ncRNA in prostate (**Supplementary Fig. 22**), suggesting that other ncRNAs may be important in this cancer. To determine the mechanism for the expression profiles of *PCAT-1* and

Figure 4 *PCAT-1* is a marker of aggressive cancer and a PRC2-repressed ncRNA. (a) The genomic location of *PCAT-1* determined by 5' and 3' RACE, with DNA sequence features indicated by the colored boxes. (b) qPCR for *PCAT-1* (y axis) and *EZH2* (x axis) on a cohort of benign ($n = 19$), localized tumor ($n = 35$) and metastatic cancer ($n = 31$) samples. The inset table quantifies patient subsets demarcated by the gray dashed lines. (c) Knockdown of *EZH2* in VCaP resulted in upregulation of *PCAT-1*. Data were normalized to *GAPDH* and represented as fold-change. *ERG* and *B-actin* serve as negative controls. The inset western blot indicates *EZH2* knockdown. (d) Treatment of VCaP cells with 0.1 μ M of the *EZH2* inhibitor DZNep or vehicle control (DMSO) shows increased expression of *PCAT-1* transcript after *EZH2* inhibition. (e) *PCAT-1* expression is increased upon treatment of VCaP cells with the demethylating agent 5'azacytidine (5'Aza), the histone deacetylase inhibitor SAHA or a combination of both. qPCR data were normalized to the average of (*GAPDH* + β -actin) and represented as fold-change. *GSTP1* and *FKBP5* are positive and negative controls, respectively. (f) ChIP assays for SUZ12 demonstrated direct binding of SUZ12 to the *PCAT-1* promoter. Primer locations are indicated (boxed numbers) in the *PCAT-1* schematic.



EZH2, we inhibited *EZH2* activity in VCaP cells, which express low-to-moderate levels of *PCAT-1*. Knockdown of *EZH2* by short hairpin (sh)RNA or pharmacologic inhibition of *EZH2* with the inhibitor 3-deazaneplanocin A (DZNep) caused a dramatic upregulation in *PCAT-1* expression levels (Fig. 4c,d), as did treatment of VCaP cells with the demethylating agent 5'azacytidine, the histone deacetylase inhibitor SAHA or both (Fig. 4e). ChIP assays also demonstrated that SUZ12, a core PRC2 protein, directly binds the *PCAT-1* promoter ~1 kb upstream of the TSS (Fig. 4f). Notably, RNA immunoprecipitation similarly showed binding of *PCAT-1* to SUZ12 protein in VCaP cells (Supplementary Fig. 23a). RNA immunoprecipitation assays followed by RNase A, RNase H or DNase I treatment either abolished, partially preserved or totally preserved this interaction, respectively (Supplementary Fig. 23b). This suggests that *PCAT-1* exists primarily as a single-stranded RNA and secondarily as a RNA/DNA hybrid.

To explore the functional role of *PCAT-1* in prostate cancer, we stably overexpressed full-length *PCAT-1* or controls in RWPE benign immortalized prostate cells. We observed a modest but consistent increase in cell proliferation when *PCAT-1* was overexpressed at physiological

levels (Fig. 5a and Supplementary Fig. 24). Next, we designed short interfering (si)RNA oligos to *PCAT-1* and performed knockdown experiments in LNCaP cells, which express higher levels of *PCAT-1* without PRC2-mediated repression (Supplementary Fig. 25). Supporting our overexpression data, knockdown of *PCAT-1* with three independent siRNA oligos resulted in a 25–50% decrease in cell proliferation in LNCaP cells (Fig. 5b), but not in control DU145 cells lacking *PCAT-1* expression (Supplementary Fig. 26) or VCaP cells, in which *PCAT-1* is expressed but repressed by PRC2 (Supplementary Fig. 27).

Gene expression profiling of LNCaP knockdown samples on cDNA microarrays indicated that *PCAT-1* modulates the transcriptional regulation of 370 genes (255 upregulated, 115 downregulated; FDR ≤ 0.01) (Supplementary Fig. 28 and Supplementary Table 9). Gene ontology analysis of the upregulated genes showed preferential enrichment for gene set concepts such as mitosis and cell cycle, whereas the downregulated genes had no concepts showing statistical significance (Fig. 5c and Supplementary Table 10). These results suggest that the function of *PCAT-1* is predominantly repressive in nature, similar to other lincRNAs. We next validated expression

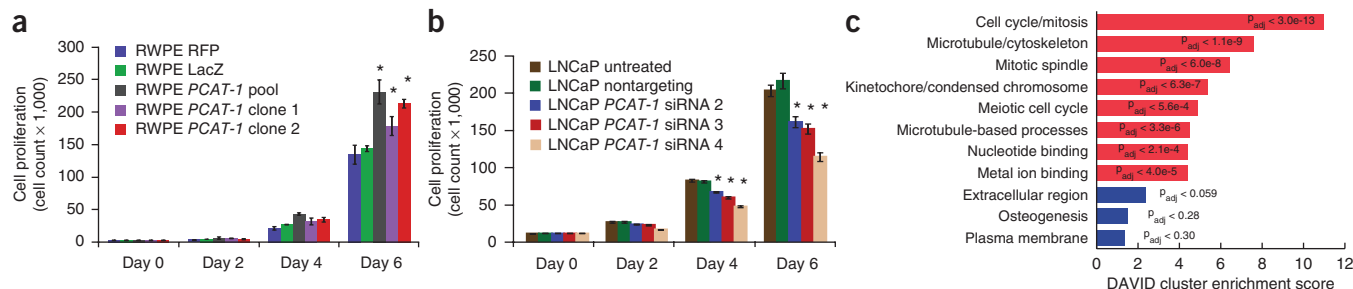


Figure 5 *PCAT-1* promotes cell proliferation. (a) Cell proliferation assays for RWPE benign immortalized prostate cells stably infected with *PCAT-1* lentivirus or RFP and LacZ control lentiviruses. An asterisk (*) indicates $P \leq 0.02$ by a two-tailed Student's t -test. (b) Cell proliferation assays in LNCaP using *PCAT-1* siRNAs. An asterisk (*) indicates $P \leq 0.005$ by a two-tailed Student's t -test. (c) Gene ontology analysis of *PCAT-1* knockdown microarray data using the DAVID program. Blue bars represent the top hits for upregulated genes. Red bars represent the top hits for downregulated genes. DAVID enrichment scores are represented with Benjamini-Hochberg-adjusted P values. All error bars in this figure are mean \pm s.e.m.

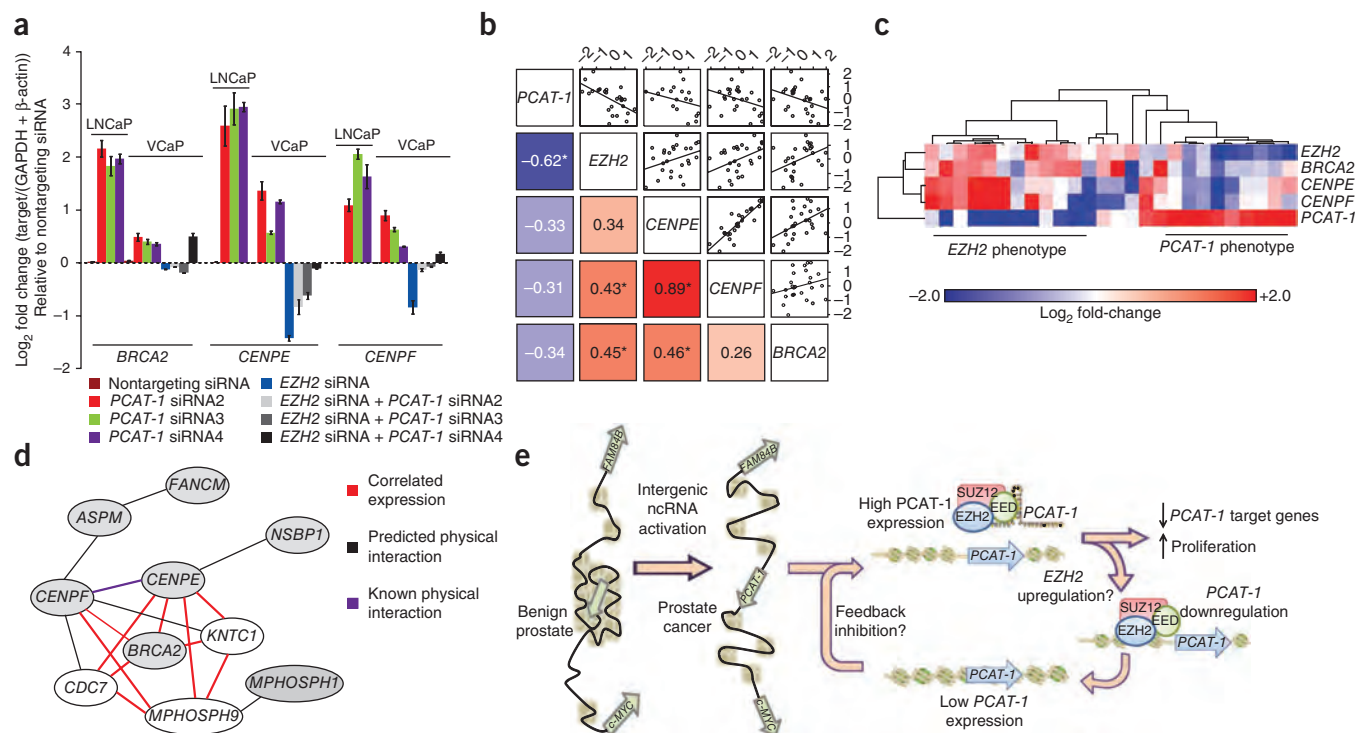


Figure 6 Prostate cancer tissues recapitulate *PCAT-1* signaling. **(a)** qPCR expression of three *PCAT-1* target genes after *PCAT-1* knockdown in VCaP and LNCaP cells, as well as following *EZH2* knockdown or dual *EZH2* and *PCAT-1* knockdown in VCaP cells. qPCR data were normalized to the average of (*GAPDH* + β -actin) and represented as fold change. Error bars represent mean \pm s.e.m. **(b)** Standardized log₂-transformed qPCR expression of a set of tumors and metastases with outlier expression of either *PCAT-1* or *EZH2*. The shaded squares in the lower left show Spearman correlation values between the indicated genes (* indicates $P < 0.05$). Blue and red indicate negative or positive correlation, respectively. The upper squares show the scatter plot matrix and fitted trend lines for the same comparisons. **(c)** A heatmap of *PCAT-1* target genes (*BRCA2*, *CENPF*, *CENPE*) in *EZH2*-outlier and *PCAT-1*-outlier patient samples (see Fig. 4b). Expression was determined by qPCR and normalized as in b. **(d)** A predicted network generated by the HefaLMP program for 7 of 20 top upregulated genes following *PCAT-1* knockdown in LNCaP cells. Gray nodes are genes found following *PCAT-1* knockdown. Red edges indicate co-expressed genes; black edges indicate predicted protein-protein interactions; and purple edges indicate verified protein-protein interactions. **(e)** A proposed schematic representing *PCAT-1* upregulation, function and relationship to PRC2.

changes in three key *PCAT-1* target genes (*BRCA2*, *CENPE* and *CENPF*) whose expression is upregulated upon *PCAT-1* knockdown (Fig. 6a) in LNCaP and VCaP cells, the latter of which appear less sensitive to *PCAT-1* knockdown likely due to lower overall expression levels of this transcript.

PCAT-1 signatures in prostate cancer

Because of the regulation of *PCAT-1* by PRC2 in VCaP cells, we hypothesized that knockdown of *EZH2* would also downregulate *PCAT-1* targets as a secondary phenomenon owing to the subsequent upregulation of *PCAT-1*. Simultaneous knockdown of *PCAT-1* and *EZH2* would thus abrogate expression changes in *PCAT-1* target genes. Carrying out this experiment in VCaP cells demonstrated that *PCAT-1* target genes were indeed downregulated by *EZH2* knockdown, and that this change was either partially or completely reversed using siRNA oligos to *PCAT-1* (Fig. 6a), lending support to the role of *PCAT-1* as a transcriptional repressor. Taken together, these results suggest that *PCAT-1* biology may exhibit two distinct modalities: one in which PRC2 represses *PCAT-1* and a second in which active *PCAT-1* promotes cell proliferation. *PCAT-1* and PRC2 may therefore characterize distinct subsets of prostate cancer.

To examine these findings, we used qPCR to measure expression of *BRCA2*, *CENPE* and *CENPF* in our cohort of tissue samples. Consistent with our model, we found that samples expressing *PCAT-1* tended to have low expression of *PCAT-1* target genes (Fig. 6b).

Moreover, comparing *EZH2*-outlier and *PCAT-1*-outlier patients (Fig. 4b), we found that two distinct phenotypes emerged. Individuals with high *EZH2* tended to have high levels of *PCAT-1* target genes, and those with high expression of *PCAT-1* itself displayed the opposite expression pattern of target genes (Fig. 6c). Network analysis of the top 20 upregulated genes after *PCAT-1* knockdown with the HefaLMP tool⁴³ further suggested that these genes form a coordinated network (Fig. 6d), corroborating our previous observations. Taken together, these results provide initial data into the composition and function of the prostate cancer ncRNA transcriptome.

DISCUSSION

To our knowledge, this study represents the largest RNA-Seq analysis to date and the first to comprehensively analyze a common epithelial cancer from a large cohort of human tissue samples. As such, our study has adapted existing computational tools intended for small-scale use³ and developed new methods to distill large numbers of transcriptome data sets into a single consensus transcriptome assembly that accurately represents disease biology (Supplementary Discussion).

Among the numerous uncharacterized ncRNA species detected by our study, we have focused on 121 PCATs, which we believe represent a set of uncharacterized ncRNAs that may have important biological functions in this disease. In this regard, these data contribute to a growing body of literature supporting the importance of unannotated ncRNA species in cellular biology and oncogenesis^{6–12},

and broadly our study confirms the utility of RNA-Seq in defining functionally important elements of the genome^{2–4}.

Of particular interest is our discovery of the prostate-specific ncRNA gene *PCAT-1*, which is markedly overexpressed in a subset of prostate cancers, particularly metastases, and may contribute to cell proliferation in these tumors. It is also notable that *PCAT-1* resides in the 8q24 ‘gene desert’ locus, in the vicinity of well-studied prostate cancer risk SNPs and the *c-MYC* oncogene, suggesting that this locus—and its frequent amplification in cancer—may be linked to additional aspects of cancer biology (**Supplementary Discussion**). In addition, the interplay between PRC2 and *PCAT-1* further suggests that this ncRNA may have an important role in prostate cancer progression (**Fig. 6e**). Other ncRNAs identified by this analysis may similarly contribute to prostate cancer as well. Furthermore, recent preclinical efforts to detect prostate cancer noninvasively through the collection of patient urine samples have shown promise for several urine-based prostate cancer biomarkers, including the ncRNA *PCA3* (refs. 44,45). Although additional studies are needed, our identification of ncRNA biomarkers for prostate cancer suggests that urine-based assays for these ncRNAs may also warrant investigation, particularly for those that may stratify patient molecular subtypes.

Our findings support an important role for tissue-specific ncRNAs in prostate cancer and suggest that cancer-specific functions of these ncRNAs may help to drive tumorigenesis. We further speculate that specific ncRNA signatures may occur universally in all disease states and that applying these methodologies to other diseases may reveal key aspects of disease biology and clinically important biomarkers.

METHODS

Methods and any associated references are available in the online version of the paper at <http://www.nature.com/naturebiotechnology/>.

Accession codes. Data from RNA-Seq experiments are deposited at the NCBI Gene Expression Omnibus as GSE25183. *PCAT-1* and *PCAT-14* nucleotide sequences are deposited at GenBank nucleotide database (nucore) as HQ605084 and HQ605085, respectively.

Note: Supplementary information is available on the Nature Biotechnology website.

ACKNOWLEDGMENTS

We thank K. Ramnarayanan and R. Morey for technical assistance with next generation sequencing. We thank R.J. Lonigro, S. Kaylana-Sundaram, T. Barrette, and M. Quist for help with sequencing data analysis, and R. Mehra, B. Han and K. Suleman for prostate tissue specimens. We thank C. Trapnell and G. Pertea for assistance with computational analyses. We thank S. Tomlins, Y.-M. Wu, S. Roychowdhury and members of the Chinnaiyan laboratory for advice and discussions. We thank R. Beroukhi for guidance. This work was supported in part by the US National Institutes of Health (NIH) Prostate Specialized Program of Research Excellence grant P50CA69568, the Early Detection Research Network grant UO1 CA111275 (to A.M.C.), the NIH R01CA132874-01A1 (to A.M.C.), the Department of Defense grant W81XWH-10-0652 and W81XWH-11-1-0337 (to A.M.C.) and the National Center for Functional Genomics supported by the Department of Defense (to A.M.C.). A.M.C. is supported by the Doris Duke Charitable Foundation Clinical Scientist Award, a Burroughs Wellcome Foundation Award in Clinical Translational Research and the Prostate Cancer Foundation. A.M.C. is an American Cancer Society Research Professor. N.P. was supported by a University of Michigan Prostate SPOR Career Development Award. C.A.M. was supported by the American Association of Cancer Research Amgen Fellowship in Clinical/Translational Research, the Canary Foundation and American Cancer Society Early Detection Postdoctoral Fellowship, and a Prostate Cancer Foundation Young Investigator Award. Q.C. was supported by a Department of Defense Postdoctoral Fellowship grant PC094725. J.R.P. was supported by the NIH Cancer Biology Training grant CA009676-18 and the Department of Defense Predoctoral Fellowship W81XWH-10-1-0551. M.K.I. was supported by the Department of Defense Predoctoral Fellowship W81XWH-11-1-0136. J.R.P. and M.K.I. are Fellows of the University of Michigan Medical Scientist Training Program.

AUTHOR CONTRIBUTIONS

M.K.I., J.R.P. and A.M.C. designed the project and directed experimental studies. M.K.I., O.A.B., C.S.G. and C.A.M. developed computational platforms and performed sequencing data analysis. M.K.I., O.A.B. and H.K.I. performed statistical analyses. J.R.P., S.M.D., J.C.B., Q.C., N.P., H.D.K., B.L., X.W., I.A.A., X.C., X.J. and D.R. performed experimental studies. J.S. and J.T.W. coordinated biospecimens. M.K.I., J.R.P. and A.M.C. interpreted data and wrote the manuscript.

COMPETING FINANCIAL INTERESTS

The authors declare competing financial interests: details accompany the full-text HTML version of the paper at <http://www.nature.com/naturebiotechnology/>.

Published online at <http://www.nature.com/naturebiotechnology/>.

Reprints and permissions information is available online at <http://www.nature.com/reprints/index.html>.

- Metzker, M.L. Sequencing technologies—the next generation. *Nat. Rev. Genet.* **11**, 31–46 (2010).
- Guttman, M. *et al.* *Ab initio* reconstruction of cell type-specific transcriptomes in mouse reveals the conserved multi-exonic structure of lincRNAs. *Nat. Biotechnol.* **28**, 503–510 (2010).
- Trapnell, C. *et al.* Transcript assembly and quantification by RNA-Seq reveals unannotated transcripts and isoform switching during cell differentiation. *Nat. Biotechnol.* **28**, 511–515 (2010).
- Robertson, G. *et al.* De novo assembly and analysis of RNA-seq data. *Nat. Methods* **7**, 909–912 (2010).
- Zerbino, D.R. & Birney, E. Velvet: algorithms for de novo short read assembly using de Bruijn graphs. *Genome Res.* **18**, 821–829 (2008).
- Huarte, M. *et al.* A large intergenic noncoding RNA induced by p53 mediates global gene repression in the p53 response. *Cell* **142**, 409–419 (2010).
- Orom, U.A. *et al.* Long noncoding RNAs with enhancer-like function in human cells. *Cell* **143**, 46–58 (2010).
- Rinn, J.L. *et al.* Functional demarcation of active and silent chromatin domains in human HOX loci by noncoding RNAs. *Cell* **129**, 1311–1323 (2007).
- Gupta, R.A. *et al.* Long non-coding RNA HOTAIR reprograms chromatin state to promote cancer metastasis. *Nature* **464**, 1071–1076 (2010).
- Pasman, E. *et al.* Characterization of a germ-line deletion, including the entire INK4/ARF locus, in a melanoma-neural system tumor family: identification of ANRIL, an antisense noncoding RNA whose expression coclusters with ARF. *Cancer Res.* **67**, 3963–3969 (2007).
- Yap, K.L. *et al.* Molecular interplay of the noncoding RNA ANRIL and methylated histone H3 lysine 27 by polycomb CBX7 in transcriptional silencing of INK4a. *Mol. Cell* **38**, 662–674 (2010).
- Tsai, M.C. *et al.* Long noncoding RNA as modular scaffold of histone modification complexes. *Science* **329**, 689–693 (2010).
- Kotake, Y. *et al.* Long non-coding RNA ANRIL is required for the PRC2 recruitment to and silencing of p15(INK4B) tumor suppressor gene. *Oncogene* **30**, 1956–1962 (2011).
- de Kok, J.B. *et al.* DD3(PCA3), a very sensitive and specific marker to detect prostate tumors. *Cancer Res.* **62**, 2695–2698 (2002).
- Li, J. *et al.* PTEN, a putative protein tyrosine phosphatase gene mutated in human brain, breast, and prostate cancer. *Science* **275**, 1943–1947 (1997).
- Prensner, J.R. & Chinnaiyan, A.M. Oncogenic gene fusions in epithelial carcinomas. *Curr. Opin. Genet. Dev.* **19**, 82–91 (2009).
- Tomlins, S.A. *et al.* Distinct classes of chromosomal rearrangements create oncogenic ETS gene fusions in prostate cancer. *Nature* **448**, 595–599 (2007).
- Tomlins, S.A. *et al.* Recurrent fusion of TMPRSS2 and ETS transcription factor genes in prostate cancer. *Science* **310**, 644–648 (2005).
- Trapnell, C., Pachter, L. & Salzberg, S.L. TopHat: discovering splice junctions with RNA-Seq. *Bioinformatics* **25**, 1105–1111 (2009).
- Thierry-Mieg, D. & Thierry-Mieg, J. AceView: a comprehensive cDNA-supported gene and transcripts annotation. *Genome Biol.* **7** (suppl. 1), S11–S14 (2006).
- Birney, E. *et al.* Identification and analysis of functional elements in 1% of the human genome by the ENCODE pilot project. *Nature* **447**, 799–816 (2007).
- The FANTOM Consortium. The transcriptional landscape of the mammalian genome. *Science* **309**, 1559–1563 (2005).
- He, Y., Vogelstein, B., Velculescu, V.E., Papadopoulos, N. & Kinzler, K.W. The antisense transcriptomes of human cells. *Science* **322**, 1855–1857 (2008).
- Guttman, M. *et al.* Chromatin signature reveals over a thousand highly conserved large non-coding RNAs in mammals. *Nature* **458**, 223–227 (2009).
- Yu, J. *et al.* An integrated network of androgen receptor, polycomb, and TMPRSS2-ERG gene fusions in prostate cancer progression. *Cancer Cell* **17**, 443–454 (2010).
- Day, D.S., Luquette, L.J., Park, P.J. & Kharchenko, P.V. Estimating enrichment of repetitive elements from high-throughput sequence data. *Genome Biol.* **11**, R69 (2010).
- Kim, T.K. *et al.* Widespread transcription at neuronal activity-regulated enhancers. *Nature* **465**, 182–187 (2010).
- Rubin, M.A. *et al.* Alpha-methylacyl coenzyme A racemase as a tissue biomarker for prostate cancer. *J. Am. Med. Assoc.* **287**, 1662–1670 (2002).

29. Dhanasekaran, S.M. *et al.* Delineation of prognostic biomarkers in prostate cancer. *Nature* **412**, 822–826 (2001).
30. van Bakel, H., Nislow, C., Blencowe, B.J. & Hughes, T.R. Most “dark matter” transcripts are associated with known genes. *PLoS Biol.* **8**, e1000371 (2010).
31. Tomlins, S.A. *et al.* The role of SPINK1 in ETS rearrangement-negative prostate cancers. *Cancer Cell* **13**, 519–528 (2008).
32. Bjartell, A.S. *et al.* Association of cysteine-rich secretory protein 3 and beta-microseminoprotein with outcome after radical prostatectomy. *Clin. Cancer Res.* **13**, 4130–4138 (2007).
33. Oosumi, T., Belknap, W.R. & Garlick, B. Mariner transposons in humans. *Nature* **378**, 672 (1995).
34. Robertson, H.M., Zuppano, K.L., Lohe, A.R. & Hartl, D.L. Reconstructing the ancient mariners of humans. *Nat. Genet.* **12**, 360–361 (1996).
35. Kleer, C.G. *et al.* EZH2 is a marker of aggressive breast cancer and promotes neoplastic transformation of breast epithelial cells. *Proc. Natl. Acad. Sci. USA* **100**, 11606–11611 (2003).
36. Varambally, S. *et al.* The polycomb group protein EZH2 is involved in progression of prostate cancer. *Nature* **419**, 624–629 (2002).
37. Ahmadiyeh, N. *et al.* 8q24 prostate, breast, and colon cancer risk loci show tissue-specific long-range interaction with MYC. *Proc. Natl. Acad. Sci. USA* **107**, 9742–9746 (2010).
38. Al Olama, A.A. *et al.* Multiple loci on 8q24 associated with prostate cancer susceptibility. *Nat. Genet.* **41**, 1058–1060 (2009).
39. Beroukhi, R. *et al.* The landscape of somatic copy-number alteration across human cancers. *Nature* **463**, 899–905 (2010).
40. Gudmundsson, J. *et al.* Genome-wide association study identifies a second prostate cancer susceptibility variant at 8q24. *Nat. Genet.* **39**, 631–637 (2007).
41. Sotelo, J. *et al.* Long-range enhancers on 8q24 regulate c-Myc. *Proc. Natl. Acad. Sci. USA* **107**, 3001–3005 (2010).
42. Taylor, B.S. *et al.* Integrative genomic profiling of human prostate cancer. *Cancer Cell* **18**, 11–22 (2010).
43. Huttenhower, C. *et al.* Exploring the human genome with functional maps. *Genome Res.* **19**, 1093–1106 (2009).
44. Laxman, B. *et al.* A first-generation multiplex biomarker analysis of urine for the early detection of prostate cancer. *Cancer Res.* **68**, 645–649 (2008).
45. Hessels, D. *et al.* DD3(PCA3)-based molecular urine analysis for the diagnosis of prostate cancer. *Eur. Urol.* **44**, 8–16 (2003).



ONLINE METHODS

Cell lines, treatments and tissues. All prostate cell lines were obtained from the American Type Culture Collection, except for PrEC (benign nonimmortalized prostate epithelial cells) and PrSMC (prostate smooth muscle cells), which were obtained from Lonza. Cell lines were maintained using standard media and conditions.

For androgen treatment experiments, LNCaP and VCaP cells were grown in androgen-depleted media for 48 h and subsequently treated with 5nM methyltrienolone (R1881, NEN Life Science Products) or an equivalent volume of ethanol for 48 h before harvesting the cells. For drug treatments, VCaP cells were treated with 20 μ M 5'-deoxyazacytidine (Sigma), 500 nM HDAC inhibitor suberoylanilide hydroxamic acid (SAHA) (Biovision), or both 5'-deoxyazacytidine and SAHA. 5'-deoxyazacytidine treatments were performed for 6 d with media and drug reapplied every 48 h. SAHA treatments were done for 48 h. DMSO treatments were done for 6 d. For DZNep treatments, DZNep was dissolved in DMSO and VCaP cells were treated with either 0.1 μ M of DZNep or vehicle control; RNA was harvested at 72 h and 144 h.

Prostate tissues were obtained from the radical prostatectomy series and Rapid Autopsy Program_ENREF_48 at the University of Michigan tissue core as part of the University of Michigan Prostate Cancer Specialized Program of Research Excellence (S.P.O.R.E.). All tissue samples were collected with informed consent under an Institutional Review Board (IRB) approved protocol at the University of Michigan.

RNA isolation, cDNA synthesis and PCR experiments. Total RNA was isolated using Trizol and an RNeasy Kit (Invitrogen) with DNase I digestion according to the manufacturer's instructions. RNA integrity was verified on an Agilent Bioanalyzer 2100 (Agilent Technologies). cDNA was synthesized from total RNA using Superscript III (Invitrogen) and random primers (Invitrogen). Quantitative Real-time PCR (qPCR) was done using Power SYBR Green Mastermix (Applied Biosystems) on an Applied Biosystems 7900HT Real-Time PCR System. (RT-PCR was done with Platinum Taq High Fidelity polymerase (Invitrogen). All oligonucleotide primers are listed in **Supplementary Table 11**. For PCR product sequencing, PCR products were resolved on a 1.5% agarose gel, and either sequenced directly or extracted using a Gel Extraction kit (Qiagen) and cloned into pcr4-TOPO vectors (Invitrogen). PCR products were bidirectionally sequenced at the University of Michigan Sequencing Core.

RNA-ligase-mediated rapid amplification of cDNA ends (RACE). 5' and 3' RACE was performed using the GeneRacer RLM-RACE kit (Invitrogen) according to the manufacturer's instructions. RACE PCR products were obtained using Platinum Taq high-fidelity polymerase (Invitrogen), the supplied GeneRacer primers, and appropriate gene-specific primers indicated in **Supplementary Table 11**.

RNA-Seq library preparation. 2 μ g total RNA was selected for polyA⁺ RNA using Sera-Mag oligo(dT) beads (Thermo Scientific), and paired-end next-generation sequencing libraries were prepared, as previously described⁴⁶, using Illumina-supplied universal adaptor oligos and PCR primers (Illumina). Samples were sequenced in a single lane on an Illumina Genome Analyzer I or Genome Analyzer II flow cell using previously described protocols⁴⁶. 36–45 mer paired-end reads were done according to the protocol provided by Illumina.

Overexpression studies. *PCAT-1* full-length transcript was cloned into the pLenti6 vector (Invitrogen) along with RFP and LacZ controls. After confirmation of the insert sequence, lentiviruses were generated at the University of Michigan Vector Core and transfected into the benign immortalized prostate cell line RWPE. RWPE cells stably expressing *PCAT-1*, RFP or LacZ were generated by selection with blasticidin (Invitrogen), and 10,000 cells were plated into 12-well plates. Cells were harvested and counted at day 2, day 4 and day 6 post-plating with a Coulter counter.

siRNA knockdown studies. Cells were plated and transfected with 20 μ M experimental siRNA oligos or nontargeting controls twice, at 12 h and 36 h post-plating. Knockdowns were performed with Oligofectamine in OptiMEM media. Knockdown efficiency was determined by qPCR. siRNA sequences (in sense format) for *PCAT-1* knockdown were as follows: siRNA 1 UUAAAGAGAUCCACAGUUAUU; siRNA 2 GCAGAAACACCAAUGGAUAUU; siRNA 3 AUACAUAAGACCAUGGAAAU; siRNA 4 GAACCUAACUGGACUUUAAUU. For *EZH2* siRNA, the following sequence was used: GAGGUUCAGACGAGCUGAUUU.

shRNA knockdown and western blot analysis. Cells were seeded at 50–60% confluency, incubated overnight, and transfected with *EZH2* or nontargeting shRNA lentiviral constructs as described in for 48 h. GFP⁺ cells were drug-selected using 1 μ g/ml puromycin. RNA and protein were harvested for PCR and western blot analysis according to standard protocols. For western blot analysis, PVDF membranes (GE Healthcare) were incubated overnight at 4 °C with either *EZH2* mouse monoclonal (1:1,000, BD Biosciences, no. 612666), or *B-actin* (Abcam, ab8226) for equal loading.

Gene expression profiling. Agilent Whole Human Genome Oligo Microarray was used for cDNA profiling of *PCAT-1* siRNA knockdown samples or nontargeting control according to standard protocols_ENREF_50. All samples were run in technical triplicates against nontargeting control siRNA. Expression array data was processed using the SAM method⁴⁷ with an FDR \leq 0.01. Up- and downregulated probes were separated and analyzed using the DAVID bioinformatics platform⁴⁸.

ChIP. Assays were done as previously described²⁵, where 4–7 μ g of the following antibodies were used: IgG (Millipore, PP64), SUZ12 (Cell Signaling, no. 3737) and SUZ12 (Abcam, ab12073). ChIP-PCR reactions were done in triplicate with SYBRGreen using 1:150th of the ChIP product per reaction.

In vitro translation. Full-length *PCAT-1*, Halo-tagged *ERG* or *GUS* positive control were cloned into the PCR2.1 entry vector (Invitrogen) and *in vitro* translational assays were done using the TnT Quick Coupled Transcription/Translation System (Promega) with 1 mM methionine and Transcend Biotin-Lysyl-tRNA (Promega) according to the manufacturer's instructions.

Bioinformatic analyses. Sequencing reads were aligned with TopHat¹⁹, and *ab initio* assembly was performed with Cufflinks³. Transcriptome libraries were merged and statistical classifiers were developed and employed to filter low-confidence transcripts. Nominated transcripts were compared to UCSC, RefSeq, Vega, Ensembl and ENCODE database, and coding potential was determined with the txCDsPredict program from UCSC. Transcript conservation was determined with the SiPhy package. Differential expression analysis was performed using SAM methodology, and outlier analysis using a modified COPA method. See the **Supplementary Methods** for details on the bioinformatics methods used.

Statistical analyses for experimental studies. All data are presented as means \pm s.e.m. All experimental assays were performed in duplicate or triplicate. Statistical analyses shown in figures represent Fisher's exact tests or two-tailed Student *t*-tests, as indicated. For details regarding the statistical methods employed during RNA-Seq and ChIP-Seq data analysis, see **Supplementary Methods**.

46. Maher, C.A. *et al.* Chimeric transcript discovery by paired-end transcriptome sequencing. *Proc. Natl. Acad. Sci. USA* **106**, 12353–12358 (2009).

47. Tusher, V.G., Tibshirani, R. & Chu, G. Significance analysis of microarrays applied to the ionizing radiation response. *Proc. Natl. Acad. Sci. USA* **98**, 5116–5121 (2001).

48. Dennis, G. Jr. *et al.* DAVID: Database for Annotation, Visualization, and Integrated Discovery. *Genome Biol.* **4**, 3 (2003).

Editor's Summary

Targeting Outside the Box

Out-of-the-box thinking is highly valued in all creative endeavors, and science is no exception. Similarly, out-of-the-cell, or extracellular, drug targets have many advantages over intracellular ones, such as easy access by small-molecule inhibitors and antibodies. Because one-third of all cases of prostate cancer—one of the most prevalent forms of the disease in men—are aggressive and fast-growing, and traditional treatments are often unhelpful and cause troublesome side effects, it is clear that some out-of-the-box thinking is required to address this therapeutic dilemma. Now, Ateeq *et al.* have identified SPINK1 (serine peptidase inhibitor, Kazal type 1) as an extracellular therapeutic target for an aggressive subset of SPINK1+ prostate cancer. SPINK1 is highly expressed in ~10% of prostate cancers, and expression has been correlated with aggressive disease. In the new work, the authors showed directly that SPINK1 contributes to the aggressive phenotype. Forced expression of recombinant SPINK1 increased prostate cancer cell proliferation and invasiveness, whereas knockdown of SPINK1 gene expression or treatment with a SPINK1-directed monoclonal antibody resulted in decreased cell division, invasiveness, and tumor growth. Moreover, SPINK1 mediated its neoplastic effects in part through interactions with the epidermal growth factor receptor (EGFR). Indeed, antibodies to both SPINK1 and EGFR blocked the growth of SPINK1+/ETS – tumors more than either antibody alone and did not affect SPINK1 – tumors. Together, these findings suggest that SPINK1 represents a new, specific, and —by virtue of its outside-of-the-box location—druggable target for a potentially lethal form of prostate cancer.

A complete electronic version of this article and other services, including high-resolution figures, can be found at:

<http://stm.sciencemag.org/content/3/72/72ra17.full.html>

Supplementary Material can be found in the online version of this article at:

<http://stm.sciencemag.org/content/suppl/2011/02/28/3.72.72ra17.DC1.html>

Related Resources for this article can be found online at:

<http://stm.sciencemag.org/content/scitransmed/3/72/72ps7.full.html>

Information about obtaining **reprints** of this article or about obtaining **permission to reproduce this article** in whole or in part can be found at:

<http://www.sciencemag.org/about/permissions.dtl>

CANCER

Therapeutic Targeting of SPINK1-Positive Prostate Cancer

Bushra Ateeq,^{1,2} Scott A. Tomlins,^{1,2} Bharathi Laxman,^{1,2} Irfan A. Asangani,^{1,2} Qi Cao,^{1,2} Xuhong Cao,^{1,3} Yong Li,^{1,2} Xiaoju Wang,^{1,2} Felix Y. Feng,^{1,4,5} Kenneth J. Pienta,^{1,5,6} Sooryanarayana Varambally,^{1,2,5} Arul M. Chinnaiyan^{1,2,3,5,7*}

Gene fusions involving ETS (erythroblastosis virus E26 transformation-specific) family transcription factors are found in ~50% of prostate cancers and as such can be used as a basis for the molecular subclassification of prostate cancer. Previously, we showed that marked overexpression of *SPINK1* (serine peptidase inhibitor, Kazal type 1), which encodes a secreted serine protease inhibitor, defines an aggressive molecular subtype of ETS fusion-negative prostate cancers (*SPINK1*⁺/*ETS*⁻, ~10% of all prostate cancers). Here, we examined the potential of SPINK1 as an extracellular therapeutic target in prostate cancer. Recombinant SPINK1 protein (rSPINK1) stimulated cell proliferation in benign RWPE as well as cancerous prostate cells. Indeed, RWPE cells treated with either rSPINK1 or conditioned medium from 22RV1 prostate cancer cells (*SPINK1*⁺/*ETS*⁻) significantly increased cell invasion and intravasation when compared with untreated cells. In contrast, knockdown of *SPINK1* in 22RV1 cells inhibited cell proliferation, cell invasion, and tumor growth in xenograft assays. 22RV1 cell proliferation, invasion, and intravasation were attenuated by a monoclonal antibody (mAb) to SPINK1 as well. We also demonstrated that SPINK1 partially mediated its neoplastic effects through interaction with the epidermal growth factor receptor (EGFR). Administration of antibodies to SPINK1 or EGFR (cetuximab) in mice bearing 22RV1 xenografts attenuated tumor growth by more than 60 and 40%, respectively, or ~75% when combined, without affecting PC3 xenograft (*SPINK1*⁻/*ETS*⁻) growth. Thus, this study suggests that SPINK1 may be a therapeutic target in a subset of patients with *SPINK1*⁺/*ETS*⁻ prostate cancer. Our results provide a rationale for both the development of humanized mAbs to SPINK1 and evaluation of EGFR inhibition in *SPINK1*⁺/*ETS*⁻ prostate cancers.

INTRODUCTION

Therapies targeted against specific molecular alterations present only in cancer cells have revolutionized the treatment of several cancers. For example, targeting ERBB2, which is amplified in ~20% of breast cancers, with the humanized monoclonal antibody (mAb) trastuzumab (Herceptin) has resulted in improved survival for breast cancer patients. Although organ-confined prostate cancer is highly curable, more than 32,000 U.S. men are expected to die of metastatic prostate cancer in 2010 (1). Multiple approved therapies (and newer agents in late-stage development) target the androgen signaling axis in metastatic disease; however, additional targeted therapies are lacking.

We previously used a bioinformatics approach, cancer outlier profile analysis (COPA), to systematically prioritize genes with marked overexpression in a subset of cancers (outlier expression). This strategy identified outlier expression of the ETS (erythroblastosis virus E26 transformation-specific) family members *ERG* and *ETV1* in a subset of prostate cancers across multiple gene expression profiling studies. It also led to the discovery of recurrent gene fusions involving the 5' untranslated region of the androgen-regulated gene *TMPRSS2* with ETS transcription factors (*ERG*, *ETV1*, *ETV4*, or *ETV5*) (2–5).

Subsequent in vitro and in vivo studies have demonstrated a driving role for ETS fusions in prostate oncogenesis and cancer progression (6–9).

Subsequently, we used a “meta-outlier approach,” which used COPA to prioritize genes that consistently showed high-ranking outlier expression across multiple profiling studies. This approach identified *SPINK1* (serine peptidase inhibitor, Kazal type 1) as a high-ranking meta-outlier in a subset of prostate cancer with mutually exclusive outlier expression of *ERG* and *ETV1* across multiple prostate cancer profiling studies (10). *SPINK1*, also known as *pancreatic secretory trypsin inhibitor* (*PSTI*) or *tumor-associated trypsin inhibitor* (*TATT*), encodes a 56-amino acid peptide thought to protect the pancreas from autodigestion by preventing premature activation of pancreatic proteases (11). Apart from its normal expression in pancreatic acinar cells, *SPINK1* mRNA has been reported to be expressed in various human cancers (12–18), and increased serum SPINK1 concentration has been correlated with poor prognosis in some studies (12, 13, 17). The prostate gland also secretes a variety of serine proteases, most notably the kallikrein enzyme PSA (prostate-specific antigen), but also trypsin (19). Thus, SPINK1 may have a role in modulating the activity of cancer-related proteases in other tissues besides the pancreas.

We confirmed the mutually exclusive overexpression of SPINK1 and *ETS* gene fusions using a combined immunohistochemistry (for SPINK1) and fluorescence in situ hybridization (FISH) (for *ETS* fusions) approach across multiple independent cohorts, and demonstrated that *SPINK1* outlier expression is associated with an aggressive subset of prostate cancers (10). We also demonstrated that *SPINK1* outlier expression can be detected noninvasively in urine and con-

¹Michigan Center for Translational Pathology, Ann Arbor, MI 48109, USA. ²Department of Pathology, University of Michigan, Ann Arbor, MI 48109, USA. ³Howard Hughes Medical Institute, University of Michigan Medical School, Ann Arbor, MI 48109, USA. ⁴Department of Radiation Oncology, University of Michigan, Ann Arbor, MI 48109, USA. ⁵Comprehensive Cancer Center, University of Michigan Medical School, Ann Arbor, MI 48109, USA. ⁶Department of Medicine, University of Michigan, Ann Arbor, MI 48109, USA. ⁷Department of Urology, University of Michigan, Ann Arbor, MI 48109, USA.

*To whom correspondence should be addressed: E-mail: arul@umich.edu

tributes to a multiplexed panel of biomarkers, which outperforms serum PSA for prostate cancer diagnosis in patients presenting for needle biopsy (10, 20). Our combined analyses of more than 1500 prostate cancer cases demonstrated *SPINK1* outlier expression in ~10% of all PSA-screened prostate cancers, which were invariably negative for *ETS* gene fusions (*SPINK1*⁺/*ETS*⁻) (10). Furthermore, *SPINK1*⁺ tumors show shorter PSA recurrence-free survival in prostatectomy-treated patients (10) and shorter progression-free survival in endocrine-treated patients (21).

Unlike *ETS* gene fusions that lead to the overexpression of a transcription factor (which are difficult to target therapeutically), *SPINK1* encodes an extracellular secreted protein and thus is potentially more amenable to therapeutic targeting. Here, we qualify *SPINK1* as a therapeutic target in *SPINK1*⁺/*ETS*⁻ prostate cancer and demonstrate the therapeutic potential of a mAb to *SPINK1* in preclinical models. Addition-

ally, we demonstrate that *SPINK1* mediates its oncogenic effects in part through epidermal growth factor receptor (EGFR) and that a mAb to EGFR shows in vitro and in vivo activity in *SPINK1*⁺ prostate cancer.

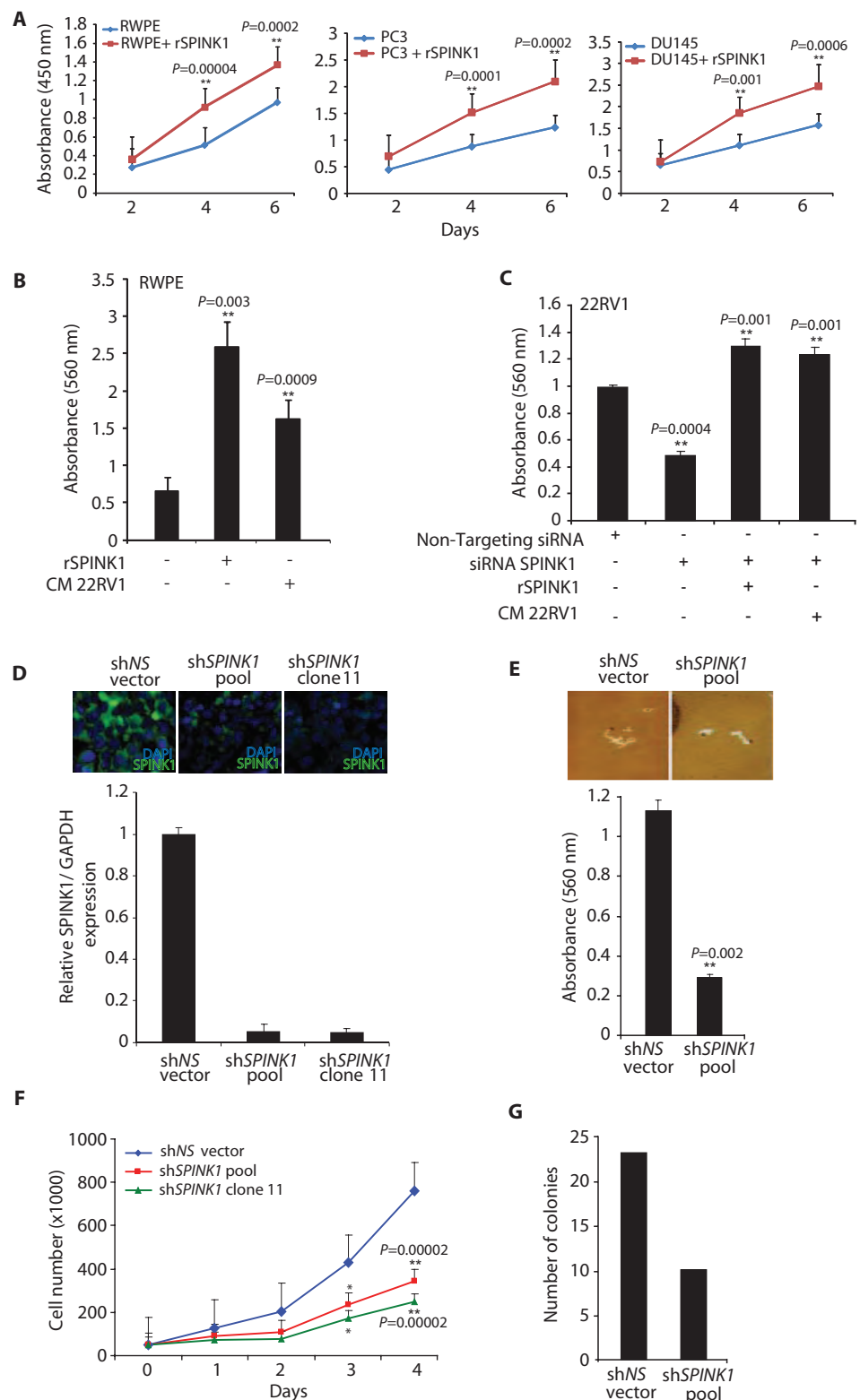


Fig. 1. *SPINK1* has oncogenic effects in prostate cells in vitro. (A) *SPINK1* stimulated cell proliferation in *SPINK1*⁺/*ETS*⁻ cell lines. Benign immortalized prostate cell line RWPE and prostate cancer cell lines DU145 and PC3 (all *SPINK1*⁺/*ETS*⁻) were untreated or treated with rSPINK1 (10 ng/ml). Cell proliferation was measured by a WST-1 colorimetric assay at the indicated time points. (B) *SPINK1* mediates invasion of RWPE cells as measured by Boyden chamber Matrigel invasion assay. RWPE cells were treated with rSPINK1 (10 ng/ml) or conditioned media (CM) from 22RV1 cells (*SPINK1*⁺/*ETS*⁻). (C) As in (B), except using 22RV1 cells transfected with siRNA against *SPINK1*. *SPINK1*-silenced 22RV1 cells were further treated with rSPINK1 (10 ng/ml) or CM from 22RV1 cells. (D) *SPINK1* expression in *SPINK1* knockdown 22RV1 cells (stable pooled shSPINK1 or stable shSPINK1 clone 11) compared to nontargeting pooled stable control (shNS vector) cells by qPCR (transcript) or immunofluorescence using an antibody against *SPINK1* (protein, upper inset; 600× magnification). (E) Invasion assay using shSPINK1 and shNS cells. Representative photomicrographs (400× magnification) showing cell motility assay (top inset) are shown. shNS vector cells exhibit longer cell motility tracks compared to shSPINK1 knockdown cells. (F) Cell proliferation assay using pooled shSPINK1, shSPINK1 clone 11, or shNS cells at the indicated time points. (G) Soft agar colony assay using pooled shSPINK1 and shNS cells. All experiments were independently performed in triplicate. Data represent means ± SEM. *P* values from significant two-sided Student's *t* tests are given (**P* < 0.05; ***P* < 0.001).

RESULTS

SPINK1 as an autocrine factor in prostate cancer

To further investigate the role of *SPINK1* in prostate cancer, we determined the effects of exogenous *SPINK1* on invasion and proliferation using recombinant hexahistidine (6XHis)-tagged *SPINK1* protein (rSPINK1) (fig. S1A) or conditioned media (CM) collected from 22RV1 prostate cancer cells (*SPINK1*^{+/ETS}) (fig. S1B) (10). We treated benign immortalized RWPE prostate epithelial cells and DU145 and PC3 prostate cancer cells (both of which are *SPINK1*^{-/ETS}) with rSPINK1 (10 ng/ml), which resulted in a significant increase in cell proliferation (Fig. 1A). We next characterized the effect of rSPINK1 or 22RV1 CM on cell invasion using a Boyden chamber Matrigel invasion assay. As shown in Fig. 1B, addition of rSPINK1 or 22RV1 CM to RWPE cells significantly increased invasion ($P = 0.003$ and 0.0009 , respectively). Similar effects were observed when MCF7 breast cancer cells were treated with rSPINK1 or 22RV1 CM (fig. S1C). Multiple recombinant 6XHis-tagged control proteins or CM collected from RWPE or LNCaP prostate cancer cells did not induce invasion in RWPE cells (figs. S1D and S2).

We previously showed that transient small interfering RNA (siRNA)-mediated knockdown of *SPINK1* in 22RV1 cells decreased cell invasion (10). Here, we extended these results by demonstrating that the addition of rSPINK1 or 22RV1 CM rescued the invasive phenotype of 22RV1 cells in which *SPINK1* was knocked down (Fig. 1C; $P = 0.001$ for both rSPINK1 and 22RV1 CM).

We next investigated whether the exogenous effect of *SPINK1* on cell proliferation and invasion was dependent on protease inhibitory activity of trypsin [which has been shown to be simultaneously expressed with *SPINK1* in different tumor types (17, 22)] or PSA. Initial experiments demonstrated that *PRSS1* (trypsinogen) mRNA expression in 22RV1 cells is relatively low compared with the CAPAN-1 pancreatic cancer cell line (fig. S3A), although a significant increase in *PRSS1* transcript was observed in siRNA-mediated *SPINK1* knockdown 22RV1 cells (fig. S3B). However, as shown in fig. S3C, stimulation of 22RV1 cells with rSPINK1 or EGF did not affect trypsin expression. siRNA-mediated knockdown of *PRSS1* in 22RV1 cells also had no effect on invasion (fig. S3, D and E). Similarly, stimulation of 22RV1 cells with rSPINK1 or EGF did not significantly affect PSA expression (fig. S4A). Finally, blocking PSA with a mAb did not significantly inhibit 22RV1 cell invasion (fig. S4B). Together, these findings demonstrate that extracellular *SPINK1* induces prostate cancer cell proliferation and invasion independent of protease inhibitory activity of trypsin or PSA. Although effects on other proteases cannot be excluded, our results suggest that *SPINK1* is an autocrine pro-proliferative and proinvasive factor with effects independent of trypsin and PSA activity.

The role of SPINK1 in cell proliferation and invasion

To further investigate the role of *SPINK1* in cell proliferation and invasion, we generated short hairpin RNA (shRNA) against *SPINK1* and established stable 22RV1 cells where *SPINK1* was silenced (shSPINK1). Knockdown of *SPINK1* in both pooled and clonal shSPINK1 cells compared to non-targeting control cells (shNS cells) was confirmed at the RNA level by quantitative polymerase chain reaction (qPCR) (more than 80% in both), as well as at the protein level by immunofluorescence staining with an antibody against *SPINK1* (Fig. 1D). Next, we investigated the role of *SPINK1* in cell invasion and motility using shSPINK1 cells. As anticipated, shSPINK1 cells showed decreased cell invasion by more than 75% in a Boyden chamber Matrigel assay compared to non-specific vector control (shNS) cells (Fig. 1E; $P = 0.002$). Reduction of cell motility in a bead motility assay was also observed in shSPINK1 cells compared to shNS cells (Fig. 1E, top panel).

To investigate the role of *SPINK1* in cell proliferation, we carried out assays using pooled shSPINK1, the clone with the greatest *SPINK1* knockdown (shSPINK1 clone 11), and shNS cells. Both pooled (55% reduction) and clonal shSPINK1 cells (66% reduction) showed significantly decreased proliferation compared to shNS cells (Fig. 1F; $P = 0.00002$ in both cases). Further, shSPINK1 cells showed decreased soft agar colony formation when compared to shNS cells (Fig. 1G).

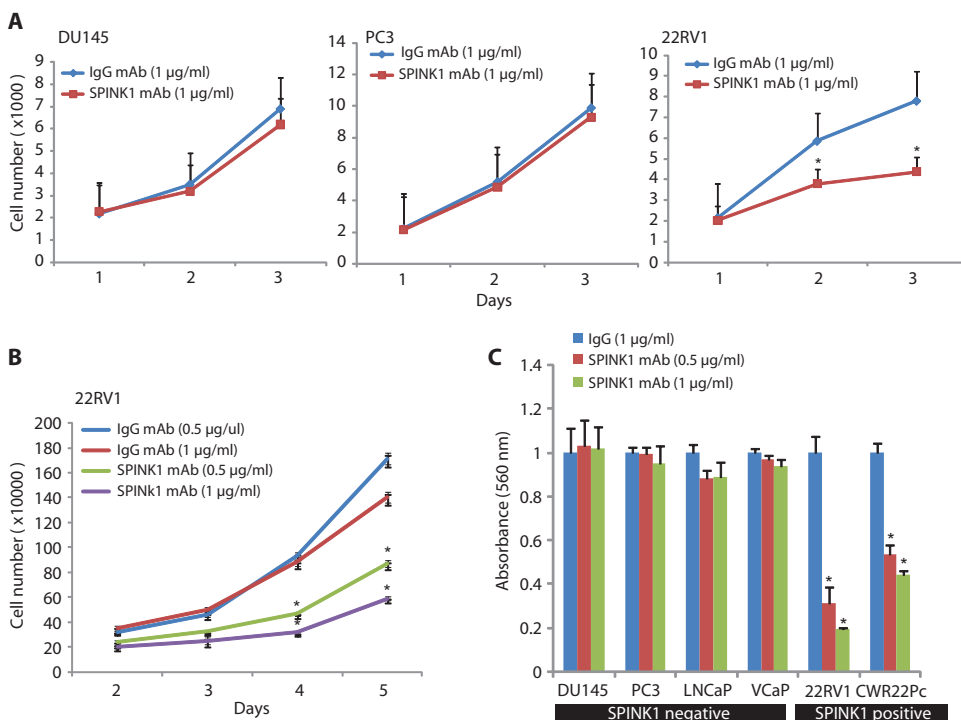


Fig. 2. An antibody to *SPINK1* attenuates in vitro proliferation and invasion exclusively in *SPINK1*^{+/ETS} prostate cancer cells. (A) Cell proliferation of DU145, PC3, and 22RV1 cells was assessed in the presence of *SPINK1* mAb or IgG mAb (1 µg/ml). (B) As in (A), except using 22RV1 cells and *SPINK1* mAb or IgG mAb (0.5 to 1 µg/ml). (C) Effect of *SPINK1* mAb or IgG mAb on invasion of *SPINK1*^{+/ETS} cells (22RV1 and CWR22Pc) and *SPINK1*^{-/ETS} cells (DU145, PC3, LNCaP, and VCaP). All experiments were independently performed in triplicates. Data represent means ± SEM. P values from significant two-sided Student's t tests are given (* $P < 0.05$; ** $P < 0.001$).

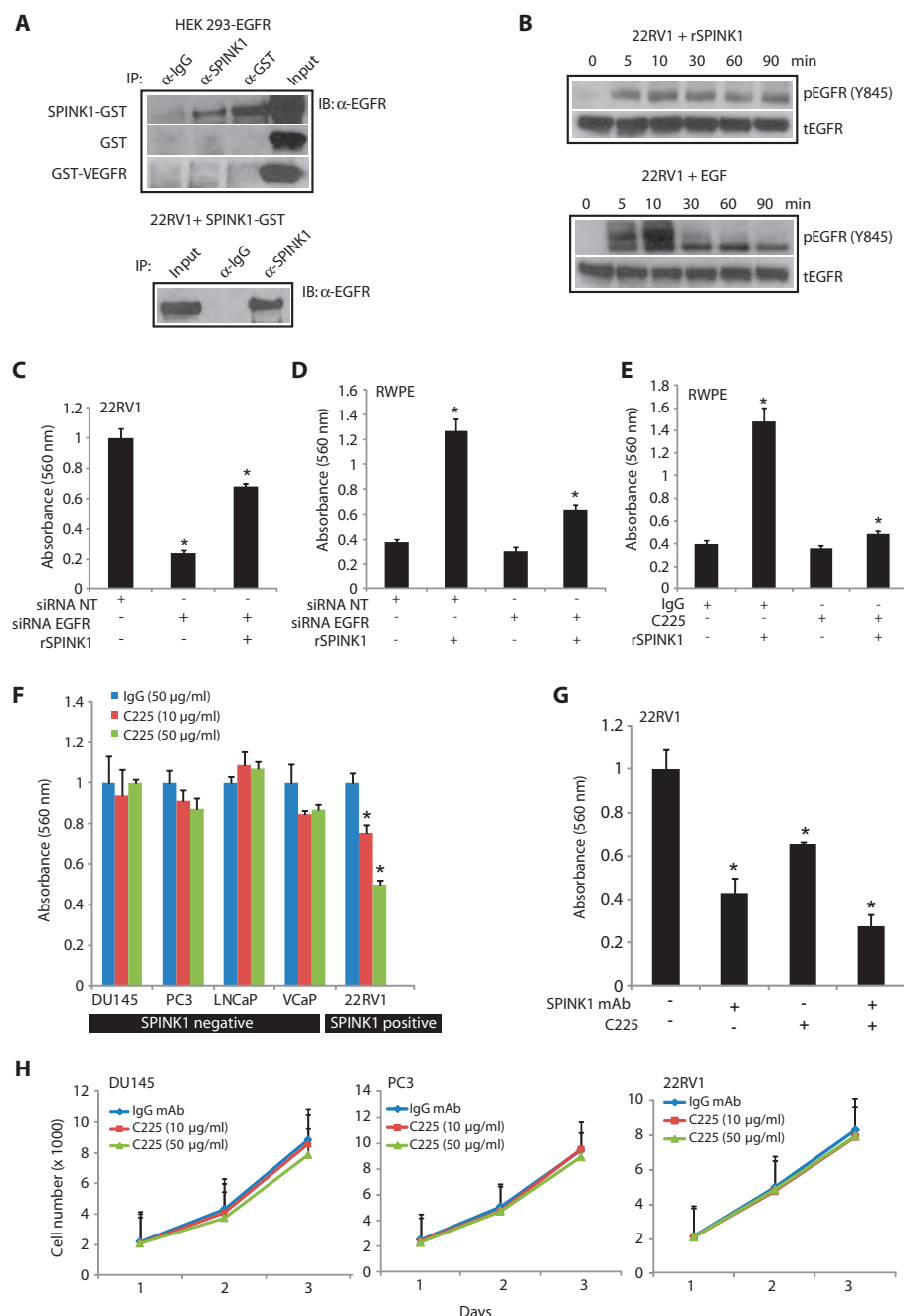


Fig. 3. SPINK1 mediates its oncogenic effects in part through EGFR. **(A)** Immunoprecipitation using antibodies to IgG, SPINK1, or GST of exogenous SPINK1-GST, GST, or GST-VEGFR added to HEK 293 cells transfected with EGFR and immunoblotted with an antibody to EGFR (top panel), and immunoprecipitation using antibodies to IgG or SPINK1 of exogenous SPINK1-GST added to 22RV1 cells and immunoblotted with an antibody to EGFR (bottom panel). **(B)** Western blot showing EGFR phosphorylation in response to rSPINK1 (100 ng/ml) or EGF (10 ng/ml) stimulation. **(C)** Invasion assay showing siRNA-mediated *EGFR* knockdown 22RV1 cells treated with rSPINK1 (10 ng/ml). **(D)** Same as in (C), except with RWPE cells. **(E)** Invasion assay showing rSPINK1 (10 ng/ml)-stimulated RWPE cells in the presence or absence of C225 [cetuximab (50 μ g/ml)] or IgG mAb (50 μ g/ml). **(F)** Invasion assay showing the effect of IgG or C225 antibody on *SPINK1*⁺ and *SPINK1*⁻ cancer cells. **(G)** As in (F), except 22RV1 cells were treated with a combination of antibodies to SPINK1 (1 μ g/ml) and/or C225 (50 μ g/ml). **(H)** Cell proliferation assay using the indicated cells in the presence of IgG mAb or C225. All experiments were independently performed in triplicates. Data represent means \pm SEM. *P* values from significant two-sided Student's *t* tests are given (**P* < 0.05; ***P* < 0.001).

In vitro targeting of SPINK1 using a mAb

Because our results above demonstrate a role for *SPINK1* in invasion and proliferation, and *SPINK1* is an extracellular secreted protein, we hypothesized that a mAb against *SPINK1* may be able to directly target *SPINK1*⁺/*ETS*⁻ prostate cancer cells. Thus, we tested the effects of an antibody to *SPINK1* on 22RV1 cell proliferation and invasion. The *SPINK1* mAb (0.5 and 1 μ g/ml) significantly inhibited 22RV1 cell proliferation by 40 and 50%, respectively, compared to a control monoclonal immunoglobulin G (IgG) antibody (Fig. 2, A and B; *P* = 0.0001 and *P* = 0.0007, respectively). However, the antibody to *SPINK1* had no effect on DU145 and PC3 cell proliferation.

In addition to inhibiting proliferation, the mAb to *SPINK1* (0.5 and 1 μ g/ml) significantly attenuated cell invasion by 69 and 81%, respectively, compared to a control IgG mAb in 22RV1 cells (Fig. 2C; *P* = 0.002 and *P* = 0.007, respectively). Similar to 22RV1, which is an androgen signaling-independent derivative of primary CWR22 human prostate xenograft tumors, we also investigated CWR22Pc cells, an androgen signaling-dependent derivative of CWR22 (23), which also express high amounts of *SPINK1*. As expected, CWR22Pc cell invasion was blocked by 47 and 54% by the mAb to *SPINK1* at 0.5 and 1 μ g/ml of *SPINK1* mAb concentration (Fig. 2C; *P* = 0.003 and *P* = 0.002, respectively). The mAb to *SPINK1* had no significant effect on invasion of *SPINK1*⁻ prostate cancer cell lines including PC3, DU145, LNCaP, or VCaP (Fig. 2C). Finally, the mAb to *SPINK1* attenuated 22RV1 cell motility compared to IgG control, but had no effect on PC3 (*SPINK1*⁻/*ETS*⁻) cell motility (fig. S5A).

Oncogenic effects of SPINK1 in part through interaction with EGFR

SPINK1 has a similar structure as EGF, with ~50% sequence homology and three intrachain disulfide bridges (24, 25). To characterize potential *SPINK1* and EGFR interaction, we overexpressed EGFR in human embryonic kidney (HEK) 293 cells and incubated the lysates with *SPINK1*-GST (glutathione *S*-transferase), GST, or GST-VEGF (vascular endothelial growth factor) receptor 2 (GST-VEGFR) recom-

binant proteins. We observed a strong interaction between SPINK1-GST and EGFR but not with GST alone or GST-VEGFR recombinant protein (Fig. 3A, top panel). Endogenous SPINK1 and EGFR interaction was not detected by immunoprecipitation and immunoblotting in 22RV1 cells, because of the secretory nature of the SPINK1 protein. However, addition of GST-SPINK1 to 22RV1 cells followed by immunoprecipitation and immunoblotting confirmed the interaction of SPINK1 and endogenous EGFR in 22RV1 cells (Fig. 3A, bottom panel).

To further delineate the role of EGFR mediation of SPINK1 in prostate cancer, we next assessed whether exogenous SPINK1 was capable of inducing EGFR phosphorylation (similar to the cognate ligand EGF). Stimulating 22RV1 cells with rSPINK1 resulted in EGFR phosphorylation, although weaker than that observed with EGF (Fig. 3B). rSPINK1 stimulation resulted in sustained EGFR phosphorylation over a 90-min time course, whereas EGF resulted in strong EGFR phosphorylation, which diminished after only 10 min. Similarly, stable shSPINK1 knockdown 22RV1 cells (pooled and clonal) showed decreased phosphorylated EGFR (pEGFR), with slightly decreased total EGFR (possibly because of EGFR degradation) (fig. S6A). Finally, we demonstrate that rSPINK1 is able to induce dimerization of EGFR, although more weakly than EGF (fig. S6B).

We next examined the functional consequences of SPINK1-EGFR interaction in the context of *SPINK1*⁺ prostate cancer using 22RV1 cells. Transient knockdown of EGFR (fig. S5B) blocked 22RV1 cell invasion by 75% (Fig. 3C; $P = 0.004$), which was partially rescued by addition of exogenous SPINK1. A similar effect of EGFR knockdown was observed in RWPE cells treated with rSPINK1 (Fig. 3D; $P = 0.014$ and $P = 0.021$, respectively). These results suggest that some but not all of SPINK1's effects are mediated by EGFR.

Because mAbs to EGFR are Food and Drug Administration (FDA)-approved for certain cancers, we sought to determine whether EGFR blockade could inhibit the oncogenic effects of SPINK1. We first demonstrated that mAb to EGFR (cetuximab, C225) blocked the cell-invasive effects of rSPINK1 in RWPE cells (Fig. 3E). C225 also blocked cell invasion of *SPINK1*⁺ 22RV1 cells but not in *SPINK1*⁻ cell lines DU145, PC3, LNCaP, or VCaP (Fig. 3F). Combining mAbs to SPINK1 and EGFR had an additive effect in the inhibition of 22RV1 cell invasion (Fig. 3G; $P = 0.001$). In contrast to mAb to SPINK1 (Fig. 2A), C225 had no effect on 22RV1 cell proliferation or PC3 and DU145 cell proliferation (Fig. 3H). Together, these experiments suggest that SPINK1 has both EGFR-dependent and EGFR-independent functions in prostate cancer.

As a preliminary exploration of the downstream signaling pathways involved in the SPINK1-EGFR axis, we studied the mitogen-activated protein kinase (MAPK) and protein kinase B/AKT pathways in stable *SPINK1* knockdown 22RV1 cells (shSPINK1 clone 11). We observed decreased pMEK (phosphorylated mitogen-activated or extracellular signal-regulated protein kinase), pERK (phosphorylated extracellular signal-regulated kinase), and pAKT (phosphorylated AKT) in stable shSPINK1 cells compared to control shNS cells (fig. S5C). Likewise, 22RV1 cells treated with SPINK1 mAb antibody showed decreased pERK (fig. S5D). These observations provide the foundation for further studies of the SPINK1-EGFR axis.

The role of SPINK1 in vivo and as a therapeutic target

Our in vitro studies demonstrated that SPINK1 mediates cell proliferation and invasion in *SPINK1*⁺ prostate cancer cells, and suggested that

a mAb can target extracellular SPINK1. To investigate the role of *SPINK1* in intravasation, a key step involved in the process of metastasis, we used a chick chorioallantoic membrane (CAM) model system (26) and demonstrate that rSPINK1 induced intravasation of benign RWPE cells (Fig. 4A). Similarly, SPINK1 mAb and C225 significantly inhibited 22RV1 cell intravasation ($P = 0.01$ and $P = 0.03$, respectively), but did not significantly inhibit PC3 cell intravasation (Fig. 4, B and C).

To qualify SPINK1 as a potential therapeutic target in vivo, we implanted pooled shSPINK1-luciferase (luc) and shNS-luc 22RV1 cells in nude male mice. At both 4 and 5 weeks after implantation, 22RV1-shSPINK1-luc cells formed significantly smaller tumors (55% reduction at week 4, $P = 0.008$, and 63% reduction at week 5, $P = 0.013$) compared to shNS-luc cells (Fig. 4, D and H).

To demonstrate preclinical efficacy of the mAb to SPINK1, we treated nude mice implanted with 22RV1-luc cells with either the mAb to SPINK1 or an isotype-matched monoclonal IgG (10 mg/kg) twice a week. As shown in Fig. 4, E and I, administration of SPINK1 mAb monotherapy resulted in a 61% reduction of tumor burden at week 4 ($P = 0.015$) and 58% reduction at week 5 ($P = 0.015$). A significant decrease in Ki-67-positive immunostained nuclei was observed in the SPINK1 mAb-treated group compared to the control group (fig. S7).

Because SPINK1 mediates its oncogenic effects in part through EGFR, we similarly assessed the mAb to EGFR (C225) using the same dosage schedule. C225 treatment resulted in a 41% reduction at week 4 ($P = 0.04$) and 37% reduction at week 5 ($P = 0.02$) (Fig. 4, E and I). By combining mAbs to SPINK1 and EGFR, we observed an additive effect in vivo showing a 74 and 73% reduction in the growth of 22RV1 xenografts at weeks 4 ($P = 0.01$) and 5 ($P = 0.003$), respectively (Fig. 4, F and I).

To confirm our in vitro results, which suggested no effect of SPINK1 or EGFR inhibition on *SPINK1*⁻ prostate cancer, we performed a similar xenograft study using PC3 cells. As expected, neither SPINK1 mAb nor C225 significantly inhibited tumor growth in PC3 xenografted mice (Fig. 4, G and I). Finally, to investigate the potential toxicity of SPINK1 mAb therapy, we investigated whether the mAb to SPINK1 interacts with SPINK3, the murine homolog of SPINK1. The mAb to SPINK1 used in our studies does not recognize murine SPINK3, thus explaining the lack of observed toxicity in SPINK1 mAb-treated mice (fig. S8, A to C).

DISCUSSION

Previous studies demonstrated that *SPINK1* outlier expression identified a subset of *ETS*-negative prostate cancers (~10% of all PSA-screened prostate cancers), although the mechanism for SPINK1 outlier expression remains unknown (10). *SPINK1* defines a distinct molecular subtype of prostate cancer characterized by lack of *ETS* gene fusions as well as a more aggressive phenotype as corroborated by independent groups across distinct cohorts of prostate cancer patients (10, 21). Thus, our working hypothesis is that *SPINK1*⁺ prostate cancer represents an aggressive form of prostate cancer that may respond to different therapies than *ETS* gene fusion-positive prostate cancers.

Here, we show that *SPINK1* promotes prostate cancer proliferation and invasion through autocrine and paracrine signaling. We also demonstrate an in vivo role for SPINK1 in intravasation and tumor xeno-

graft growth. At present, the precise mechanism and signaling pathways responsible for these effects in *SPINK1*⁺ prostate cancer are unclear. A recent study showed that mutation of *SPINK1* at leucine 18 (L18) in the trypsin interaction site reduced tumor growth, angiogenesis, and lung metastases in HT-29 5M21 human colon carcinoma tumor xenografts, suggesting that the cancer-related phenotypes of *SPINK1* may be related to its anti-proteinase activity (27). Moreover, the invasive behavior of these HT-29 5M21 colon cancer cells was abolished with an antibody to *SPINK1* (27). However, in our study, we did not observe any effect of *SPINK1* on trypsin or PSA, two candidate proteases in prostate cancer.

Recent studies also indicate that *SPINK1* may be an apoptosis inhibitor prevent-

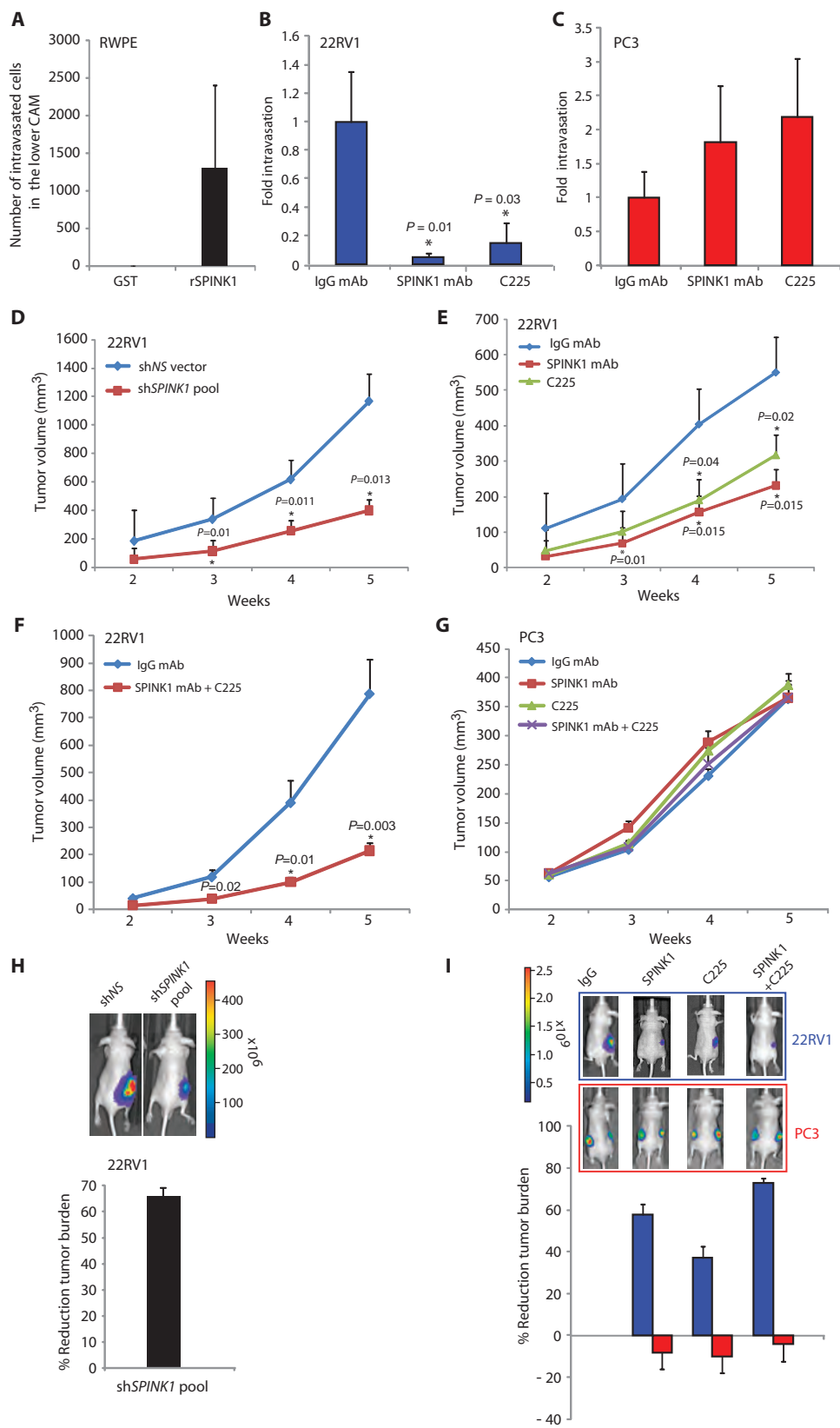


Fig. 4. *SPINK1* is a therapeutic target in *SPINK1*⁺ prostate cancer. (A) Chick chorioallantoic membrane (CAM) assay quantifying intravasated RWPE cells upon stimulation with rSPINK1 ($n = 6$ in each group). (B) CAM assay using 22RV1 cells in the presence of IgG mAb, SPINK1 mAb, or C225 ($n = 5$ in each group), with fold change of intravasated cells compared to IgG mAb plotted. (C) As in (B), except using PC3 cells. (D) Subcutaneous xenograft growth of shNS-luciferase (luc) or shSPINK1-luc 22RV1 cells implanted in male BALB/c nu/nu mice ($n = 10$ in each group). (E) As in (D), except using 22RV1-luc cell xenografts treated with control IgG mAb ($n = 8$), SPINK1 mAb ($n = 6$), or C225 ($n = 8$) (10 mg/kg) twice a week. (F) Same as in (E), except mice ($n = 7$ per group) were treated with a combination of SPINK1 and C225 mAb (10 mg/kg for both). (G) As in (E) and (F), except using PC3-luc xenografts treated with control IgG mAb, SPINK1 mAb, or C225 ($n = 8$ per group) (10 mg/kg) alone or in combination twice a week. (H) Representative bioluminescence images from mice in (D) bearing pooled shNS-luc or shSPINK1-luc xenografts and percent reduction in tumor volume at week 5. (I) Same as (H), except bioluminescence images from mice bearing 22RV1-luc xenografts (red, top panel) or PC3-luc (blue, lower panel) mice treated with IgG mAb, SPINK1 mAb, or C225 mAb alone or in combination, with comparative percent reduction plot in tumor volume at week 5. Data represent means \pm SEM. P values from significant two-sided Student's t tests are given (* $P < 0.05$; ** $P < 0.001$).

ing serine protease-dependent cell death (28). Here, we show that SPINK1, which has structural similarities with EGF (29), binds to EGFR, and inhibiting SPINK1 attenuates key downstream mediators of the EGFR pathway including MEK, ERK, and AKT. Furthermore, we also show that SPINK1 dimerizes EGFR and induces sustained phosphorylation of EGFR, which have been shown to be critical for downstream signaling activation after ligand binding (30). However, in contrast to SPINK1 mAb, EGFR mAb only partially inhibited the cell-invasive effects of 22RV1 cells and had no effect on cell proliferation, suggesting that SPINK1 engages both EGFR-dependent and EGFR-independent pathways to mediate its oncogenic effects. SPINK1 has also been shown to engage the EGFR/MAPK cascade in NIH 3T3 fibroblasts and pancreatic cancer cells (31).

This study provides compelling evidence that *SPINK1* overexpression is oncogenic in prostate cancer and that inhibition of *SPINK1* via RNA interference or blocking antibodies may have therapeutic potential. Our preclinical models suggest that this therapeutic effect would only be effective in patients with *SPINK1*⁺ prostate cancer, suggesting that such therapies would need to be evaluated in a molecularly guided fashion. Because the area of antibody-based therapeutics for extracellular targets is well developed, based on examples such as trastuzumab in breast cancers with ERBB2 overexpression, we postulate that a SPINK1-blocking antibody may have similar efficacy on a molecularly defined subset of prostate cancers. We have previously demonstrated that patients with the subset of *SPINK1*⁺/*ETS*[−] prostate cancers can be reliably identified by immunohistochemistry (10, 20), as would be required for a molecularly defined clinical trial. Although humanized SPINK1 mAbs are not yet available for clinical testing, our studies show that SPINK1 partially mediates its oncogenic effects through EGFR.

This finding prompted us to evaluate the utility of the FDA-approved EGFR mAb cetuximab, which showed in vitro and in vivo activity only against *SPINK1*⁺ prostate cancer cells (although less effective than SPINK1 mAb). Phase I/II clinical trials of cetuximab (32) and EGFR small molecules have been largely disappointing in metastatic prostate cancer (33, 34); however, a small subset of patients have had responses, including 3 of 36 (8%) patients who showed >50% PSA decline in a Phase Ib/IIa clinical trial of cetuximab in combination with docetaxel in castrate-resistant metastatic prostate cancer patients (32). Results from our study provide a plausible mechanism for why only the limited subset of patients with positive cancers (~10% of all cases) may benefit from EGFR inhibition. This hypothesis can be assessed retrospectively and in biomarker-informed clinical trials of patients with *SPINK1*⁺ prostate cancer. Because the mAb to SPINK1 used in our studies did not interact with murine SPINK3 (the homolog of SPINK1), our study does not inform on the potential toxicity of SPINK1 mAb therapy. However, an FDA-approved mAb to EGFR has specific in vivo activity against *SPINK1*⁺ prostate cancer, providing an immediately translatable strategy for targeting *SPINK1*⁺ cancers that can be clinically investigated while toxicity of humanized SPINK1 antibody therapy is explored.

In summary, our results support *SPINK1* as an oncogene in a subset of prostate cancers that can be molecularly identified, and provide the rationale to develop humanized SPINK1 antibodies for human clinical trials. Our work also reinforces the molecular subclassification of prostate cancer in clinical trials (whether through *SPINK/ETS* status or other relevant biomarkers), which has lagged behind other common epithelial cancers (that is, breast, lung, and colon).

MATERIALS AND METHODS

Cell lines and *SPINK1* knockdown

The benign immortalized prostate cell line RWPE as well as prostate cancer cell lines DU145, PC3, and 22RV1 were obtained from the American Type Culture Collection (ATCC) and were grown according to ATCC guidelines. For stable knockdown of *SPINK1*, human lentiviral shRNA^{mir} individual clone (ID V2LHS_153419) targeting against *SPINK1* or nonsilencing lentiviral shRNA^{mir} in GIPZ vectors was purchased from Open Biosystems (Thermo Scientific Open Biosystems). Details are available in Supplementary Materials and Methods.

Quantitative PCR

Total RNA was isolated with a miRNeasy mini kit following the manufacturer's instruction (Qiagen). Complementary DNA was synthesized from 1 µg of total RNA with SuperScript III (Invitrogen) in the presence of random primers. qPCR was performed with the StepOne Real-Time PCR system (Applied Biosystems). Details and primer information are available in Supplementary Materials and Methods.

Cell proliferation assay

Proliferation for control and experimental cells was measured by a colorimetric assay based on the cleavage of the tetrazolium salt WST-1 by mitochondrial dehydrogenases (cell proliferation reagent WST-1; Roche Diagnostics) at the indicated time points in triplicate. Cell counts for shNS vector and sh*SPINK1* cells were estimated by trypsinizing cells and analysis by Coulter counter (Beckman Coulter) at different time points in triplicates.

Basement membrane matrix invasion assay

For invasion assays, shNS vector- or sh*SPINK1*-transduced cells, as well as RWPE, PC3, and 22RV1 cells were used. Equal numbers of the indicated cells were seeded onto the basement membrane matrix (BD Biosciences) present in the insert of a 24-well culture plate. RPMI media supplemented with 10% fetal bovine serum were added to the lower chamber as a chemoattractant. After 48 hours, noninvading cells and extracellular matrix were removed with a cotton swab. Invaded cells were stained with crystal violet and photographed. The inserts were treated with 10% acetic acid, and absorbance was measured at 560 nm.

CAM assay

The assay was performed essentially as described (26). Two million RWPE cells were mixed with either 200 ng of multiple tag control protein or 200 ng of rSPINK1 protein and applied to the CAM of 11-day-old chicken embryo. Similarly, 2 million 22RV1 or PC3 cells were mixed with either monoclonal IgG or antibodies to SPINK1 or C225 (1 µg/ml) and applied onto the upper CAM of a fertilized chicken embryo. Three days after implantation, the relative number of cells that intravasate into the vasculature of the lower CAM was analyzed by extracting genomic DNA with the Puregene DNA purification system. Quantification of the human cells in the extracted DNA was done as described (35).

22RV1 and PC3 xenograft models

Four-week-old male BALB/c nu/nu mice were purchased from Charles River Inc. (Charles River Laboratory). Stable 22RV1 shNS-luc and 22RV1

shSPINK1-luc cells (5×10^5), or 22RV1-luc (2×10^5) or PC3-luc (5×10^5) cells were resuspended in 100 μ l of saline with 20% Matrigel (BD Biosciences) and were implanted subcutaneously into the left flank regions of the mice. Details are available in Supplementary Materials and Methods.

Statistical analysis

All values presented in the study were expressed as means \pm SEM. The significant differences between the groups were analyzed by a Student's *t* test, and a *P* value of <0.05 or <0.001 was considered significant.

SUPPLEMENTARY MATERIAL

www.sciencetranslationalmedicine.org/cgi/content/full/3/72/72ra17/DC1

Materials and Methods

Fig. S1. rSPINK1 or CM collected from 22RV1 cells induces invasion in benign or cancer cells.
Fig. S2. CM collected from 22RV1 cells induces cell invasion, but not CM, from LNCaP cells.
Fig. S3. PRSS1 (trypsin1) knockdown in 22RV1 cells has no effect on SPINK1-mediated cell invasion.
Fig. S4. Exogenous rSPINK1 has no effect on PSA in 22RV1 cells.
Fig. S5. SPINK1 mAb reduces SPINK1⁺ cell motility and SPINK1 knockdown alters MAPK pathway.
Fig. S6. Exogenous SPINK1 induces EGFR dimerization and phosphorylation.
Fig. S7. SPINK1 mAb induces decrease in tumor proliferation index.
Fig. S8. Anti-SPINK1 mAb, which does not recognize the murine homolog of SPINK1 (SPINK3), has no observed toxic effect in treated mice.

Reference

REFERENCES AND NOTES

1. A. Jemal, R. Siegel, J. Xu, E. Ward, Cancer statistics, 2010. *CA Cancer J. Clin.* **60**, 277–300 (2010).
2. B. E. Helgeson, S. A. Tomlins, N. Shah, B. Laxman, Q. Cao, J. R. Prensner, X. Cao, N. Singla, J. E. Montie, S. Varambally, R. Mehra, A. M. Chinnaiyan, Characterization of TMPRSS2:ETV5 and SLC45A3:ETV5 gene fusions in prostate cancer. *Cancer Res.* **68**, 73–80 (2008).
3. S. A. Tomlins, D. R. Rhodes, S. Perner, S. M. Dhanasekaran, R. Mehra, X. W. Sun, S. Varambally, X. Cao, J. Tchinda, R. Kuefer, C. Lee, J. E. Montie, R. B. Shah, K. J. Pienta, M. A. Rubin, A. M. Chinnaiyan, Recurrent fusion of TMPRSS2 and ETS transcription factor genes in prostate cancer. *Science* **310**, 644–648 (2005).
4. S. A. Tomlins, R. Mehra, D. R. Rhodes, L. R. Smith, D. Roulston, B. E. Helgeson, X. Cao, J. T. Wei, M. A. Rubin, R. B. Shah, A. M. Chinnaiyan, TMPRSS2:ETV4 gene fusions define a third molecular subtype of prostate cancer. *Cancer Res.* **66**, 3396–3400 (2006).
5. S. A. Tomlins, B. Laxman, S. M. Dhanasekaran, B. E. Helgeson, X. Cao, D. S. Morris, A. Menon, X. Jing, Q. Cao, B. Han, J. Yu, L. Wang, J. E. Montie, M. A. Rubin, K. J. Pienta, D. Roulston, R. B. Shah, S. Varambally, R. Mehra, A. M. Chinnaiyan, Distinct classes of chromosomal rearrangements create oncogenic ETS gene fusions in prostate cancer. *Nature* **448**, 595–599 (2007).
6. S. A. Tomlins, A. Bjartell, A. M. Chinnaiyan, G. Jenster, R. K. Nam, M. A. Rubin, J. A. Schalken, ETS gene fusions in prostate cancer: From discovery to daily clinical practice. *Eur. Urol.* **56**, 275–286 (2009).
7. Y. Zong, L. Xin, A. S. Goldstein, D. A. Lawson, M. A. Teitell, O. N. Witte, ETS family transcription factors collaborate with alternative signaling pathways to induce carcinoma from adult murine prostate cells. *Proc. Natl. Acad. Sci. U.S.A.* **106**, 12465–12470 (2009).
8. J. C. King, J. Xu, J. Wongvipat, H. Hieronymus, B. S. Carver, D. H. Leung, B. S. Taylor, C. Sander, R. D. Cardiff, S. S. Couto, W. L. Gerald, C. L. Sawyers, Cooperativity of TMPRSS2-ERG with PI3-kinase pathway activation in prostate oncogenesis. *Nat. Genet.* **41**, 524–526 (2009).
9. B. S. Carver, J. Tran, A. Gopalan, Z. Chen, S. Shaikh, A. Carracedo, A. Alimonti, C. Nardella, S. Varmeh, P. T. Scardino, C. Cordon-Cardo, W. Gerald, P. P. Pandolfi, Aberrant ERG expression cooperates with loss of PTEN to promote cancer progression in the prostate. *Nat. Genet.* **41**, 619–624 (2009).
10. S. A. Tomlins, D. R. Rhodes, J. Yu, S. Varambally, R. Mehra, S. Perner, F. Demichelis, B. E. Helgeson, B. Laxman, D. S. Morris, Q. Cao, X. Cao, O. Andr n, K. Fall, L. Johnson, J. T. Wei, R. B. Shah, H. Al-Ahmadie, J. A. Eastham, S. E. Eggeger, S. W. Fine, K. Hotakainen, U. H. Stenman, A. Tsodikov, W. L. Gerald, H. Lilja, V. E. Reuter, P. W. Kantoff, P. T. Scardino, M. A. Rubin, A. S. Bjartell, A. M. Chinnaiyan, The role of SPINK1 in ETS rearrangement-negative prostate cancers. *Cancer Cell* **13**, 519–528 (2008).
11. L. A. Kazal, D. S. Spicer, R. A. Brahinsky, Isolation of a crystalline trypsin inhibitor-anticoagulant protein from pancreas. *J. Am. Chem. Soc.* **70**, 3034–3040 (1948).
12. E. Kelloniemi, E. Rintala, P. Finne, U. H. Stenman; Finnbladder Group, Tumor-associated trypsin inhibitor as a prognostic factor during follow-up of bladder cancer. *Urology* **62**, 249–253 (2003).
13. A. Lukkonen, S. Lintula, K. von Boguslawski, O. Carpen, B. Ljungberg, G. Landberg, U. H. Stenman, Tumor-associated trypsin inhibitor in normal and malignant renal tissue and in serum of renal-cell carcinoma patients. *Int. J. Cancer* **83**, 486–490 (1999).
14. C. Haglund, M. L. Huhtala, H. Halila, S. Nordling, P. J. Roberts, T. M. Scheinin, U. H. Stenman, Tumour-associated trypsin inhibitor, TATI, in patients with pancreatic cancer, pancreatitis and benign biliary diseases. *Br. J. Cancer* **54**, 297–303 (1986).
15. M. Higashiyama, T. Monden, N. Tomita, M. Murotani, Y. Kawasaki, H. Morimoto, A. Murata, T. Shimano, M. Ogawa, T. Mori, Expression of pancreatic secretory trypsin inhibitor (PSTI) in colorectal cancer. *Br. J. Cancer* **62**, 954–958 (1990).
16. M. L. Huhtala, K. Kahanp  , M. Sepp  , H. Halila, U. H. Stenman, Excretion of a tumor-associated trypsin inhibitor (TATI) in urine of patients with gynecological malignancy. *Int. J. Cancer* **31**, 711–714 (1983).
17. A. Paju, J. Vartiainen, C. Haglund, O. Itkonen, K. von Boguslawski, A. Leminen, T. Wahlstr m, U. H. Stenman, Expression of trypsinogen-1, trypsinogen-2, and tumor-associated trypsin inhibitor in ovarian cancer: Prognostic study on tissue and serum. *Clin. Cancer Res.* **10**, 4761–4768 (2004).
18. Y. Ohmachi, A. Murata, N. Matsuura, T. Yasuda, T. Yasuda, M. Monden, T. Mori, M. Ogawa, K. Matsubara, Specific expression of the pancreatic-secretory-trypsin-inhibitor (PSTI) gene in hepatocellular carcinoma. *Int. J. Cancer* **55**, 728–734 (1993).
19. A. Bjartell, A. Paju, W. M. Zhang, V. Gadaleanu, J. Hansson, G. Landberg, U. H. Stenman, Expression of tumor-associated trypsinogens (TAT-1 and TAT-2) in prostate cancer. *Prostate* **64**, 29–39 (2005).
20. B. Laxman, D. S. Morris, J. Yu, J. Siddiqui, J. Cao, R. Mehra, R. J. Lonigro, A. Tsodikov, J. T. Wei, S. A. Tomlins, A. M. Chinnaiyan, A first-generation multiplex biomarker analysis of urine for the early detection of prostate cancer. *Cancer Res.* **68**, 645–649 (2008).
21. K. A. Leinonen, T. T. Tolonen, H. Bracken, U. H. Stenman, T. L. Tammela, O. R. Saram ki, T. Visakorpi, Association of SPINK1 expression and TMPRSS2:ERG fusion with prognosis in endocrine-treated prostate cancer. *Clin. Cancer Res.* **16**, 2845–2851 (2010).
22. K. Hotakainen, A. Bjartell, A. Sankila, R. J rvinen, A. Paju, E. Rintala, C. Haglund, U. H. Stenman, Differential expression of trypsinogen and tumor-associated trypsin inhibitor (TATI) in bladder cancer. *Int. J. Oncol.* **28**, 95–101 (2006).
23. A. Dagvadorj, S. H. Tan, Z. Liao, L. R. Cavalli, B. R. Haddad, M. T. Nevalainen, Androgen-regulated and highly tumorigenic human prostate cancer cell line established from a transplantable primary CWR22 tumor. *Clin. Cancer Res.* **14**, 6062–6072 (2008).
24. L. T. Hunt, W. C. Barker, M. O. Dayhoff, Epidermal growth factor: Internal duplication and probable relationship to pancreatic secretory trypsin inhibitor. *Biochem. Biophys. Res. Commun.* **60**, 1020–1028 (1974).
25. D. C. Bartlett, R. Shapanka, L. J. Greene, The primary structure of the human pancreatic secretory trypsin inhibitor. Amino acid sequence of the reduced S-aminoethylated protein. *Arch. Biochem. Biophys.* **179**, 189–199 (1977).
26. A. Zijlstra, R. Mellor, G. Panzarella, R. T. Aimes, J. D. Hooper, N. D. Marchenko, J. P. Quigley, A quantitative analysis of rate-limiting steps in the metastatic cascade using human-specific real-time polymerase chain reaction. *Cancer Res.* **62**, 7083–7092 (2002).
27. V. Gouyer, D. Fontaine, P. Dumont, O. de Wever, H. Fontayne-Devaud, E. L teurtre, S. Truant, D. Del cour, H. Drob cq, J. P. Kerckaert, Y. de Launoit, M. Bracke, C. Gespach, J. L. Desseyn, G. Huet, Autocrine induction of invasion and metastasis by tumor-associated trypsin inhibitor in human colon cancer cells. *Oncogene* **27**, 4024–4033 (2008).
28. X. Lu, J. Lamontagne, F. Lu, T. M. Block, Tumor-associated protein SPIK/TATI suppresses serine protease dependent cell apoptosis. *Apoptosis* **13**, 483–494 (2008).
29. L. A. Scheving, Primary amino acid sequence similarity between human epidermal growth factor-urogastrone, human pancreatic secretory trypsin inhibitor, and members of porcine secretin family. *Arch. Biochem. Biophys.* **226**, 411–413 (1983).
30. J. Mendelsohn, J. Baselga, The EGF receptor family as targets for cancer therapy. *Oncogene* **19**, 6550–6565 (2000).
31. N. Ozaki, M. Ohmuraya, M. Hirota, S. Ida, J. Wang, H. Takamori, S. Higashiyama, H. Baba, K. Yamamura, Serine protease inhibitor Kazal type 1 promotes proliferation of pancreatic cancer cells through the epidermal growth factor receptor. *Mol. Cancer Res.* **7**, 1572–1581 (2009).
32. S. F. Slovin, W. K. Kelly, A. Wilton, M. Kattan, P. Myskowski, J. Mendelsohn, H. I. Scher, Anti-epidermal growth factor receptor monoclonal antibody cetuximab plus doxorubicin in the treatment of metastatic castration-resistant prostate cancer. *Clin. Genitourin. Cancer* **7**, E77–E82 (2009).
33. C. Nabhan, T. M. Lestingi, A. Galvez, K. Tolzien, S. K. Kelby, D. Tsarwhas, S. Newman, J. D. Bitran, Erlotinib has moderate single-agent activity in chemotherapy-na ve castration-resistant prostate cancer: Final results of a phase II trial. *Urology* **74**, 665–671 (2009).

34. C. Pezaro, M. A. Rosenthal, H. Gurney, I. D. Davis, C. Underhill, M. J. Boyer, D. Kotasek, B. Solomon, G. C. Toner, An open-label, single-arm phase two trial of gefitinib in patients with advanced or metastatic castration-resistant prostate cancer. *Am. J. Clin. Oncol.* **32**, 338–341 (2009).
35. E. H. van der Horst, J. H. Leupold, R. Schubbert, A. Ullrich, H. Allgayer, TaqMan-based quantification of invasive cells in the chick embryo metastasis assay. *Biotechniques* **37**, 940–942, 944, 946 (2004).
36. **Acknowledgments:** We thank X. Jiang, X. Jing, A. Yocum, J. Siddiqui, K. Suleman, R. Mehra, and C. A. Maher for the technical assistance; M. Dhanasekaran and C. Brenner for discussions; and J. Granger for critically reading the manuscript. **Funding:** This work is supported in part by the Department of Defense W81XWH-08-1-0031, Early Detection Research Network UO1 CA111275, Prostate SPORE P50CA69568, and NIH (R01CA132874). A.M.C. is supported by the Doris Duke Charitable Foundation Clinical Scientist Award, Burroughs Wellcome Foundation Award in Clinical Translational Research, and the Prostate Cancer Foundation (PCF). A.M.C. is an American Cancer Society research professor. B.A. is supported by the Genentech Foundation Postdoctoral Fellowship and Young Investigator Award from the Expedition Inspiration Fund for Breast Cancer Research. S.A.T. is supported by a Young Investigator Award from the PCF. Q.C. is supported by U.S. Department of Defense (PC094725). S.V. is supported by a Prostate Cancer SPORE

Career Development award. **Author contributions:** B.A., S.A.T., and A.M.C. designed the research plan and wrote the manuscript; B.A., B.L., Q.C., and X.C. performed the in vitro experiments; I.A.A. performed CAM assays; B.A. performed in vivo xenograft experiments; B.A., B.L., I.A.A., S.A.T., F.Y.F., K.J.P., S.V., and A.M.C. analyzed the data. **Competing interests:** The University of Michigan has filed for patents on SPINK1, on which A.M.C., B.A., and S.A.T. are named as inventors. A.M.C. is a consultant for Gen-Probe Inc. S.A.T. has consulted for Cougar Biotechnology, AstraZeneca, and Compendia Biosciences. The diagnostic field of use has been licensed to Gen-Probe Inc. Gen-Probe was not involved in the design or funding of these studies. The other authors declare that they have no competing interests.

Submitted 14 July 2010

Accepted 10 February 2011

Published 2 March 2011

10.1126/scitranslmed.3001498

Citation: B. Ateeq, S. A. Tomlins, B. Laxman, I. A. Asangani, Q. Cao, X. Cao, Y. Li, X. Wang, F. Y. Feng, K. J. Pienta, S. Varambally, A. M. Chinnaiyan, Therapeutic targeting of SPINK1-positive prostate cancer. *Sci. Transl. Med.* **3**, 72ra17 (2011).

BIOGRAPHICAL SKETCH

Provide the following information for the Senior/key personnel and other significant contributors in the order listed on Form Page 2.
Follow this format for each person. **DO NOT EXCEED FOUR PAGES.**

NAME Qi Cao		POSITION TITLE Post-doctoral Research Associate	
eRA COMMONS USER NAME (credential, e.g., agency login) qicao1			
EDUCATION/TRAINING <i>(Begin with baccalaureate or other initial professional education, such as nursing, include postdoctoral training and residency training if applicable.)</i>			
INSTITUTION AND LOCATION	DEGREE <i>(if applicable)</i>	MM/YY	FIELD OF STUDY
Peking University, Beijing, China	B.S.	07/98	Cell Biology and Genetics
Peking University, Beijing, China	M.S.	07/01	Cell Biology
University of Michigan, Ann Arbor, MI	Ph.D.	03/08	Pathology

Please refer to the application instructions in order to complete sections A, B, C, and D of the Biographical Sketch.

A. Personal Statement

The goal of this study is to explore the functional and regulatory network between Polycomb Repressive Complexes (PRCs, including PRC1 and PRC2) and Androgen Receptor (AR) in prostate cancer (PCa), and their role in the development of castration-resistant prostate cancer (CRPC). In addition, we will examine the synergistic efficiency of PRCs and AR inhibitors in the treatment of CRPC. I have been dedicated to study the role of PRCs in prostate cancer over the past nine years, and have extensive experience, outstanding publication record and leadership to successfully accomplish the proposed aims. I was a co-investigator of a GSK-funded project on "The Role of AVODART in Pre-Clinical Models of Gene Fusion Positive Prostate Cancer", and have participated in many NIH, NCI and DOD PCRP-funded projects. Currently I am supported by a Department of Defense Prostate Cancer Research Program postdoctoral training award. In summary, I have a demonstrated exceptional record in the field of epigenetics and prostate cancer research, and through the successful execution of this project, help further the research missions of PCF.

B. Positions and Honors**Positions and Employment**

2002-2008 Graduate Student Research Assistant, Department of Pathology, University of Michigan, Ann Arbor, MI
2008- Post-doctoral Research Associate, Michigan Center for Translational Pathology, Department of Pathology, University of Michigan, Ann Arbor, MI

Other Experience and Professional Memberships

2008- Associate member, American Association for Cancer Research

Honors

1994-1995 Outstanding Freshmen Scholarship, Peking University, Beijing, China
1994-1996 Fellowship of Honor Science Program, Peking University, Beijing, China
1995-1996 Young Eagle Scholarship, Peking University, Beijing, China
2010-2012 Department of Defense Prostate Cancer Research Program Post-Doctoral Traineeship Award
2011 American Association for Cancer Research 102nd Annual Meeting AACR-Aflac Scholar-in-Training Award

C. Selected Peer-reviewed Publications (Selected from 26 peer-reviewed publication)

First and co-first authored papers:

1. **Cao Q**, Mani RS, Ateeq B, Dhanasekaran SM, Asangani IA, Prensner JR, Kim JH, Brenner JC, Jing X, Cao X, Wang R, Li Y, Dahiya A, Wang L, Pandhi M, Lonigro RJ, Wu Y-M, Tomlins SA, Palanisamy N, Qin Z, Yu J, Maher CA, Varambally S, Chinnaiyan AM. Coordinated regulation of Polycomb group complexes through microRNAs in cancer. **Cancer Cell**. Aug. 2011 (In press)

2. Rhodes DR*, Ateeq B*, **Cao Q***, Tomlins SA*, Mehra R, Laxman B, Kalyana-Sundaram S, Lonigro RJ, Helgeson BE, Bhojani MS, Rehemtulla A, Kleer CG, Hayes DS, Lucas PC, Varambally S, Chinnaiyan AM. AGTR1 Over-Expression Defines a Subset of Breast Cancer and Confers Sensitivity to Losartan, an AGTR1 Antagonist. **Proc Natl Acad Sci USA**. 2009, Jun 23;106(25):10284-9. PMID: 19487683 (***Co-first authors with equal contribution.**)

Contribution: designed and performed *in vitro* experiments.

3. Varambally S*, **Cao Q***, Mani RS, Shankar S, Wang X, Ateeq B, Laxman B, Cao X, Jing X, Ramnarayanan K, Brenner JC, Yu J, Kim JH, Han B, Tan P, Kumar-Sinha C, Lonigro RJ, Palanisamy N, Maher CA, Chinnaiyan AM. Genomic Loss of miR-101 Leads to Overexpression of EZH2 in Cancer. **Science**. 2008 Dec 12;322(5908):1695-9. PMID: 19008416 (***Co-first authors with equal contribution**)

Contribution: conceived the idea and designed the experiments; performed most experiments.

4. **Cao Q**, Yu J, Dhanasekaran SM, Kim JH, Mani RS, Tomlins SA, Mehra R, Laxman B, Cao X, Yu J, Kleer CG, Varambally S, Chinnaiyan AM. Repression of E-cadherin by the Polycomb Group Protein EZH2 in Cancer. **Oncogene**. 2008 Dec 11;27(58):7274-84. **Featured Article**. PMID: 18806826

5. Kleer CG*, **Cao Q***, Varambally S*, Shen R, Ota I, Tomlins SA, Ghosh D, Sewalt RG, Otte AP, Hayes DF, Sabel MS, Livant D, Weiss SJ, Rubin MA, Chinnaiyan AM. EZH2 is a marker of aggressive breast cancer and promotes neoplastic transformation of breast epithelial cells. **Proc Natl Acad Sci USA**. 2003, 100(20):11606-11. (***Co-first authors with equal contribution**)

Contribution: conceived the idea and designed the experiments; performed most experiments.

Additional recent publications related to current application

6. Prensner JR, Iyer MK, Balbin OA, Dhanasekaran SM, **Cao Q**, Brenner JC, Laxman B, Asangani IA, Grasso C, Kominsky HD, Cao X, Jing X, Wang X, Siddiqui J, Wei JT, Robinson D, Iyer HK, Palanisamy N, Maher CA, Chinnaiyan AM. Transcriptome Sequencing Identifies PCAT-1, a Novel lincRNA Implicated in Prostate Cancer Progression. **Nat. Biotechnol**. Aug. 2011 (In press)

7. Mani RS, Iyer MK, **Cao Q**, Brenner JC, Wang L, Ghosh A, Cao X, Lonigro RJ, Tomlins SA, Varambally S, Chinnaiyan AM. TMPRSS2-ERG-mediated feed-forward regulation of wild-type ERG in human prostate cancers. **Cancer Res**. 2011 Jun 15. [Epub ahead of print]. PMID: 21676887

8. Brenner JC, Ateeq B, Li Y, Yocum AK, **Cao Q**, Asangani IA, Patel S, Wang X, Liang H, Yu J, Palanisamy N, Siddiqui J, Yan W, Cao X, Mehra R, Sabolch A, Basrur V, Lonigro RJ, Yang J, Tomlins SA, Maher CA, Elenitoba-Johnson KS, Hussain M, Navone NM, Pienta KJ, Varambally S, Feng FY, Chinnaiyan AM. Mechanistic Rationale for Inhibition of Poly(ADP-Ribose) Polymerase in ETS Gene Fusion-Positive Prostate Cancer. **Cancer Cell**. 2011 May 17;19(5):664-78. **Featured Cover Article**. PMID: 21575865

9. Sun Y, Varambally S, Maher CA, **Cao Q**, Chockley P, Toubai T, Malter C, Nieves E, Tawara I, Wang Y, Ward PA, Chinnaiyan AM, Reddy P. Targeting of microRNA-142-3p in dendritic cells regulates endotoxin induced mortality. **Blood**. 2011 Jun 9;117(23):6172-83. Epub 2011 Apr 7. PMID: 21474672

10. Yu J, **Cao Q**, Yu J, Wu L, Dallol A, Li J, Chen G, Grasso C, Cao X, Lonigro RJ, Varambally S, Mehra R, Palanisamy N, Wu JY, Latif F, Chinnaiyan AM. The neuronal repellent SLIT2 is a target for repression by EZH2 in prostate cancer. **Oncogene**. 2010 Sep 30;29(39):5370-80. PMID: 20622896
11. Yu J, Yu J, Mani RS, **Cao Q**, Brenner CJ, Cao X, Wang X, Wu L, Li J, Hu M, Gong Y, Cheng H, Laxman B, Vellaichamy A, Shankar S, Li Y, Dhanasekaran SM, Morey R, Barrette T, Lonigro RJ, Tomlins SA, Varambally S, Qin ZS, Chinnaiyan AM. An Integrated Network of Androgen Receptor, Polycomb, and TMPRSS2-ERG Gene Fusions in Prostate Cancer Progression. **Cancer Cell**, 2010, 17:443-454. **Featured Cover Article**. PMID: 20478527
12. Wang XS, Prensner JR, Chen G, **Cao Q**, Han B, Dhanasekaran SM, Ponnala R, Cao X, Varambally S, Thomas DG, Giordano TJ, Beer DG, Palanisamy N, Sartor MA, Omenn GS, Chinnaiyan AM. An integrative approach to reveal driver gene fusions from paired-end sequencing data in cancer. **Nat. Biotechnol.** 2009, 27(11):1005-11. PMID: 19881495
13. Sreekumar A, Poisson LM, Rajendiran TM, Khan AP, **Cao Q**, Yu J, Laxman B, Mehra R, Lonigro RJ, Li Y, Nyati MK, Ahsan A, Kalyana-Sundaram S, Han B, Cao X, Byun J, Omenn GS, Ghosh D, Pennathur S, Alexander DC, Berger A, Shuster JR, Wei JT, Varambally S, Beecher C, Chinnaiyan AM. Integrative Metabolomic Analysis of Prostate Cancer Progression. **Nature**. 2009 Feb 12;457(7231):910-4. PMID: 19212411
14. Yu J, **Cao Q**, Mehra R, Laxman B, Yu J, Tomlins SA, Creighton CJ, Dhanasekaran SM, Shen R, Chen G, Morris DS, Marquez VE, Shah RB, Ghosh D, Varambally S, Chinnaiyan AM. Integrative genomics analysis reveals silencing of beta-adrenergic signaling by polycomb in prostate cancer. **Cancer Cell**. 2007 Nov;12(5):419-31. **Featured Article**. PMID: 17996646
15. Tomlins SA, Dhanasekaran SM, Laxman B, Helgeson BE, Cao X, Morris DS, Menon A, Jing X, **Cao Q**, Han B, Montie JE, Rubin MA, Pienta KJ, Roulston D, Shah RB, Varambally S, Mehra R, Chinnaiyan AM. Distinct Classes of Chromosomal Rearrangements Create Oncogenic ETS Gene Fusions in Prostate Cancer, **Nature**, 2007 Aug 2;448(7153):595-9.

D. Research Support

The role of microRNA miR-101 in prostate cancer progression

PC094290 Cao (PI) 09/01/2010-09/30/2012

Department of Defense Prostate Cancer Research Program Post-Doctoral Traineeship Award

The major goal of this project is characterize miR-101 as a biomarker of metastatic prostate cancer, and the role of miR-101 in prostate cancer progression and identify the mechanism by which miR-101 is dysregulated in prostate cancer.

The Role of AVODART in Pre-Clinical Models of Gene Fusion Positive Prostate Cancer

Varambally (PI) 07/01/08 – 06/30/09

GlaxoSmithKline (GSK)

The major goal of this project is to analyze of the effect of AVODART on fusion positive prostate cancer cell proliferation, invasion, and gene expression and evaluate the effect of AVODART on tumor growth in a TMPRSS2-ERG xenograft model of prostate cancer.